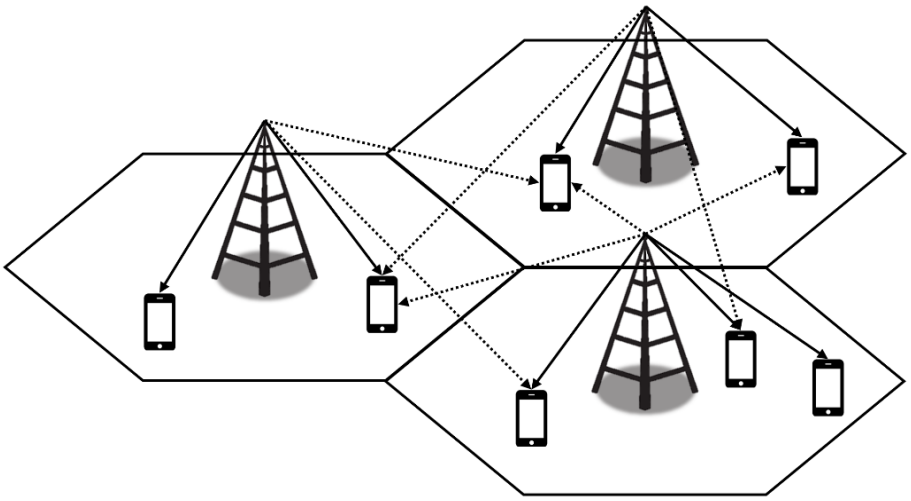

User Equipment Throughput Enhancement using Base Station Cooperation with Particle Swarm Optimisation in 5G

NUNO MIGUEL JUZARTE BRAGANÇA

(Licenciado em Engenharia Informática, Redes e Telecomunicações)

Dissertação para obtenção do grau de Mestre
em Engenharia de Eletrónica e Telecomunicações

Orientadores:

Doutor António João Nunes Serrador
Doutor Nuno Miguel Soares Datia

Júri:

Presidente: Doutor Vitor Manuel de Oliveira Fialho
Vogais:
Doutor António João Nunes Serrador
Mestre Nuno António Fraga Juliano Cota

Novembro, 2024

User Equipment Throughput Enhancement using Base Station Cooperation with Particle Swarm Optimisation in 5G

NUNO MIGUEL JUZARTE BRAGANÇA
(Licenciado em Engenharia Informática, Redes e Telecomunicações)

Dissertação para obtenção do grau de Mestre
em Engenharia de Eletrónica e Telecomunicações

Orientadores:
Doutor António João Nunes Serrador, ISEL
Doutor Nuno Miguel Soares Datia, ISEL

Júri:
Presidente: Doutor Vitor Manuel de Oliveira Fialho, ISEL
Vogais:
Doutor António João Nunes Serrador, ISEL
Mestre Nuno António Fraga Juliano Cota, ISEL

Novembro, 2024

AGRADECIMENTOS

No desenvolvimento desta dissertação contei com o apoio de diversas pessoas, às quais estarei sempre grato.

Gostaria de agradecer aos meus orientadores, Doutor António Serrador e Doutor Nuno Datia, cuja orientação foi essencial na formulação das questões e metodologia de investigação corretas. Ambos os vossos comentários perspicazes fizeram-me pensar e progredir na direção certa e tornaram o resultado final ainda melhor.

Por fim, gostaria de agradecer à minha família e amigos pelo apoio incondicional ao longo do meu percurso académico e por todo o incentivo, paciência e ajuda constante.

ACKNOWLEDGEMENTS

Throughout the development of this dissertation, I had the support of several people, for which I am grateful.

I would like to thank my advisors, Doctor António Serrador and Doctor Nuno Datia, whose guidance was essential in formulating the right research questions and methodology. Both of your insightful feedback made me think and progress in the right direction and made the end result even better.

I would also like to thank my family and friends for their unwavering support throughout my academic journey and for all their encouragement, patience and constant help.

STATEMENT OF INTEGRITY

I declare that this dissertation / project work / internship report is the result of my personal and independent research. Its content is original, and all sources listed in the bibliographic references were consulted and are duly mentioned in the text. I further declare that all scientific and technical references relevant to the development of the work are duly cited and included in the bibliographic references.

The author

Assinado por: **Nuno Miguel Juzarte Bragança**
Num. de Identificação: 30285885
Data: 2024.11.27 11:26:40+00'00'

Lisbon, ……., ……

RESUMO

Em redes móveis celulares, a taxa de transferência de dados dos utilizadores deve ser sempre melhorada para que possam realizar as suas ações pretendidas na rede. Isto pode ocorrer por várias razões, seja um utilizador estar numa localização de difícil acesso para a rede, ter altos níveis de interferência, ou até mesmo um caso especial em que um utilizador específico necessite dessa melhoria. Qualquer uma destas circunstâncias pode resultar em queda de chamadas em curso, redução da taxa de bits da ligação ou alguma troca de dados que não pode ser completada, o que pode impactar negativamente a experiência do utilizador. Para prevenir ou minimizar estas situações, existem várias técnicas de gestão de feixes e coordenação de interferência, que requerem comunicação entre estações base, ou seja, cooperação entre estações base, e algum tipo de algoritmo para a tomada de decisões. Esta tese propõe uma solução de IA para melhorar a taxa de transferência de dados do utilizador utilizando um algoritmo de otimização por enxame de partículas para fazer os ajustes e decisões necessárias. A cooperação fará uso da capacidade das antenas de se moverem tanto horizontal como verticalmente, numa tentativa de diminuir a interferência entre sectores e melhorar a relação sinal-ruído recebida por qualquer utilizador, enquanto mantém níveis de serviço satisfatórios para os restantes utilizadores.

Para configurar o algoritmo, as estações base afetadas devem ter um indicador-chave de desempenho (KPI) que represente a qualidade média da rede e/ou os requisitos mínimos da rede. De vários parâmetros de rede possíveis, a relação sinal-interferência-mais-ruído (SINR) foi escolhida por representar uma métrica abrangente que reflete aspetos cruciais para o desempenho da rede. Considera tanto a potência do sinal recebido desejado como os fatores de interferência, e não só quantifica a qualidade dos sinais recebidos, mas também oferece perceções importantes para avaliar a qualidade de serviço (QoS), resultando numa experiência de utilizador melhorada. Além disso, um valor mais alto de SINR permite que os utilizadores alcancem taxas de dados mais altas, o que maximiza a capacidade da rede e contribui diretamente para o objetivo geral de melhorar a taxa de transferência média dos utilizadores. Portanto, através do uso de um algoritmo de otimização por enxame de partículas e dos dados fornecidos pelas estações base, será possível melhorar a taxa de transferência de dados dos utilizadores enquanto preserva a qualidade geral da rede. Os resultados obtidos mostraram melhorias na SINR de até 28.9 % e, consequentemente, um aumento na taxa de transferência de 25.6 %.

Palavras-Chave: Melhoria da Taxa de Transferência, Cooperação entre Estações Base, Inteligência Artificial, Otimização por Enxame de Partículas

ABSTRACT

In cellular mobile networks, user's throughput should always be improved in order to perform their intended actions on the network. This can arise from multiple reasons, whether a user is in a location that is hard to reach by the radio network, has high levels of interference, or even a special case in which a specific user needs this improvement. Any of these circumstances may result in an undergoing call dropping, data connection bit rate reduction, or some data exchange that can't be completed, which could negatively impact the user experience. To prevent or minimize these situations, there are several beam management and interference coordination techniques, which require communication between base stations, meaning base station cooperation, and some kind of decision-making algorithms. This thesis proposes an AI solution to enhance user throughput using a particle swarm optimisation algorithm to make the necessary adjustments and decisions. The cooperation will make use of the antenna's ability to move both horizontally and vertically, in an attempt to decrease cross-sector interference and enhance the signal to noise ratio received by any given user, while maintaining satisfactory service levels for the other remaining users.

To setup the algorithm, the affected base stations must have a key performance indicator (KPI) that represents the average network quality and/or minimum network requirements. From several possible network parameters, the signal-to-interference-plus-noise ratio (SINR) was chosen as it represents a comprehensive metric reflecting key aspects crucial for network performance. It considers both the desired received signal strength and interfering factors, and not only quantifies the quality of received signals, but also offers important insights into evaluating quality of service (QoS), resulting in an improved user experience. Furthermore, a higher SINR value allows users to achieve higher data rates, which maximizes network capacity and directly contributes to the overarching objective of improving average user throughput. Therefore, using a particle swarm optimisation algorithm and the data provided by base stations, it will be feasible to enhance UE throughput while preserving the overall network quality. The results obtained showed SINR improvements up to 28.9 % and, consequently, a throughput enhancement of 25.6 %.

Keywords: Throughput Enhancement, Base Station Cooperation, Artificial Intelligence, Particle Swarm Optimisation

INDEX

FIGURE INDEX

TABLE INDEX

ACRONYMS INDEX

UE	User Equipment. 2, 43, 44, 46, 47, 50, 51, 53, 56, 58-61, 63, 65, 67, 69, 70, 73

1. INTRODUCTION

The evolution of wireless communication technologies in recent years has been marked by an unrelenting quest for increased connectivity, faster speeds, higher capacity, and lower latency. Prominent within this paradigm shift of technology is the fifth generation of wireless networks, more commonly known as 5th Generation (5G). Expanding upon the groundwork established by its predecessors, 5G, as a new generation, represents a substantial progression within the telecommunications industry, holding the potential to fundamentally transform not only interpersonal connections but also the interactions among machines, devices, and entire industries in the era of digitalisation.

Nevertheless, during the enthusiasm surrounding the implementation of 5G networks, it is critical to acknowledge and confront the complex challenges that arise with this technological achievement. To maximise the overall network performance, reliability, and efficiency of 5G systems, network operators are confronted with a list of optimisation challenges as the demand for ubiquitous connectivity and high-speed data continues to soar.

An inherent obstacle in the optimisation of 5G networks is the effective interference management. This challenge is complex due to: proliferation of various communication technologies, dense network deployments, and the constrained availability of spectrum resources. Ensuring dependable and consistent connectivity, reducing packet loss, and improving the overall quality of service (QoS) for end-users are all dependent on interference mitigation.

In prior iterations of wireless networks, conventional methods of interference management, such as power regulation, frequency reuse, and antenna sectorization, proved to be essential in reducing interference. Nevertheless, the ever evolving and diverse characteristics of 5G systems present novel intricacies, which call for enhanced interference management methods capable of adjusting to evolving network circumstances, reducing co-channel interference, and optimising real-time resource allocation.

In recent times, Artificial Intelligence (AI) and evolutionary algorithms have surfaced as powerful tools for addressing optimisation challenges in wireless communication networks. AI algorithms have the capability to optimise network parameters and

configurations in real-time using machine learning (ML) and optimisation techniques. This results in an overall improvement in network performance and efficiency.

Particle Swarm Optimisation (PSO), one of several types of AI methods, has received significant interest due to its effectiveness in tackling optimisation obstacles within 5G networks. Driven by the swarming behaviour observed in natural ecosystems, PSO presents an iterative and decentralised technique for the optimisation of intricate, non-linear problems. Through the implementation of PSO algorithms, network operators can improve throughput and QoS metrics, resulting in enhanced user experiences and optimal utilisation of network resources.

1.1. OBJECTIVES

This thesis explores the application of an AI solution to tackle optimisation challenges in 5G networks, with a particular focus on radio interface throughput optimisation, QoS improvement, and interference management. Figure 1.1 depicts the cross-sector interference that will be addressed.

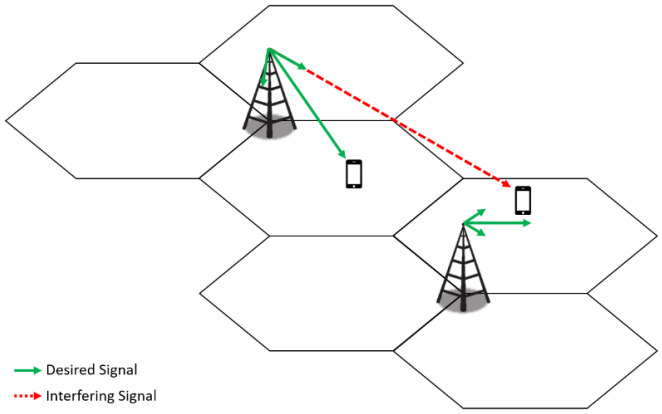

Figure 1.1 - Interference between sectors

To tackle these objectives, the cooperation between base stations (BSs) and their shared feedback is used to enhance average user throughput, using a PSO algorithm to make the necessary adjustments and decisions. Through the antenna's capability of horizontal and vertical movement, the cooperation will reduce cross-sector interference and improve the signal received by a specific user equipment (UE). Although it's attempting to optimise a given user performance, the algorithm will simultaneously seek to ensure acceptable service levels for the remaining users on the network.

So, the primary goal is to design and implement a PSO algorithm that incorporates a 5G network simulation as its fitness function, with the goal of optimising the throughput for a particular user and ensuring a satisfactory level for all other users. However, by

adjusting the evaluation process of the fitness function outcomes, it is also feasible to attempt to optimise the remainder of the network while maintaining its main purpose of maximising performance for a specific user. Figure 1.2 illustrates the objective of managing cross-sector interference, as well as directing the antenna signal towards a specific user.

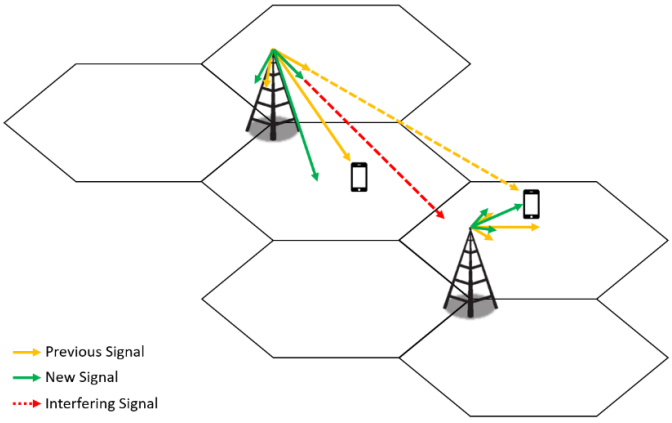

Figure 1.2 - Intended interference management between sectors

1.2. THESIS OUTLINE

To effectively illustrate the complete sequence of events from initial research to implementation of the proposed architecture, it was determined that the report should be structured into four main chapters.

Chapter 2 provides an analysis of the distinct components used and different alternatives. It begins with a 5G overview, then proceeds to examine the specific theme of BS cooperation, the application of AI in 5G, the implementation of a PSO algorithm, the network simulators that are currently available, and concludes with a selection of relevant works and papers.

In Chapter 3, a methodology and architecture are proposed, along with a breakdown and explanation of the architectural components, their respective functions, and the ways in which they interact.

Chapter 4 defines the test scenarios that were developed, considering the intended evaluations, the architecture employed, challenges that emerged, and the decisions that were made. In addition to providing examples of the architecture operation and delineating certain aspects of its implementation, it also includes results and conclusions derived from the testing process.

At last, in Chapter 5, a comprehensive reflection is made regarding the progress made and some future work ideas, encompassing the difficulties encountered during the thesis development.

2. STATE OF THE ART

Mobile cellular systems have been in use for some time, currently several 5G networks are already in commercial operation. This generation represents a significant advancement in mobile technology, offering an extremely flexible and scalable network infrastructure. 5G networks are designed to support high data speeds and very low latency, making them ideal for a wide range of applications, from enhanced mobile broadband to critical communications. The development of 5G technology is guided by the 3rd Generation Partnership Project (3GPP), a collaborative effort among telecommunications standards organizations to define the specifications for cellular networks. Since its inception, 3GPP has released several iterations of 5G standards, each bringing new capabilities and enhancements to the network infrastructure [1]. Release 15 introduced the first 5G mobile communications standard, laying the groundwork for commercial 5G deployments globally. Since then, 3GPP has continued to work on its development in Releases 16 through 18, which represents the beginning of 5G Advanced Evolution, to significantly enhance performance and accommodate new use cases [2].

In the following chapters, all the significant subjects that influenced the development of this thesis will be introduced and explained. These include a synopsis of each 3GPP 5G release, the concept of BS cooperation, AI in 5G networks, the base optimisation algorithm that was adopted, the network simulators that were considered, and additional research papers and works that pertain to the optimisation of network resources.

2.1. STANDARDS EVOLUTION

This chapter will cover the progression of 3GPP 5G releases, from Release 15 to 18. Figure 2.1 depicts the overall 3GPP's progression of 5G towards 5G Advanced.

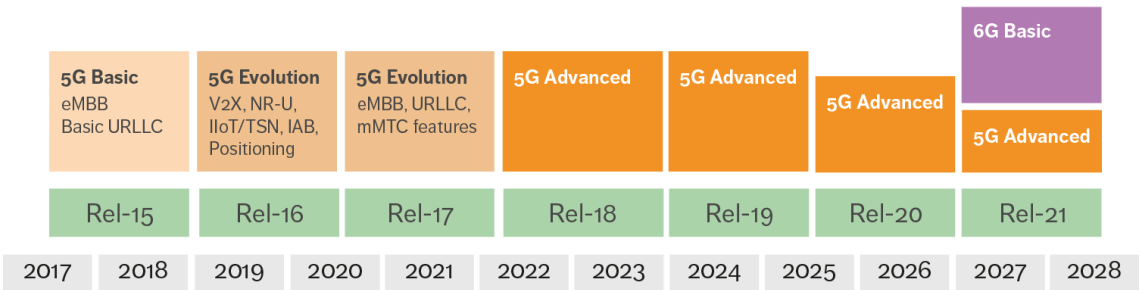

Figure 2.1 - 3GPP's 5G evolution timeline [29]

2.1.1. 3GPP Release 15

3GPP Release 15 represents a significant milestone in the development of wireless communication networks, as it introduces the first set of specifications for the deployment of 5G technology. The release detailed the introduction of a new 5G air interface designed for catering a variety of different use cases.

Enhanced Mobile Broadband

This release brings improved mobile broadband capabilities, known as enhanced mobile broadband (eMBB). The eMBB capabilities provide substantially higher data rates and enhanced network capacity in comparison to previous generations. Users can benefit from rapid internet connectivity, high-quality video streaming, and engaging multimedia experiences on their devices equipped with 5G technology.

Massive Machine-Type Communications

Release 15 not only focuses on eMBB, but also caters to the growing demand for connectivity in the Internet of Things (IoT) era, by incorporating support for massive machine-type communications. This enables the efficient management of a massive number of IoT devices, sensors, and applications by networks, thereby enabling the implementation of smart cities, smart homes, and industrial automation systems.

Ultra-Reliable Low-Latency Communications

Ultra-reliable low-latency communications is also brought to the 5G capabilities, supporting the transmission of critical data with minimal delay and high reliability. Real-time responsiveness is a crucial requirement for various applications, including autonomous vehicles, remote surgery, and industrial control systems [3].

New Radio Interface

To support these advanced features, this release defined the New Radio (NR) interface, which serves as the foundation for 5G air interface technology, supporting both standalone (SA) and non-standalone (NSA) deployment modes. NSA refers to a deployment option that relies on the control plane of an existing 4G Long Term Evolution (LTE) network for initial access, mobility management, and control operations, while 5G NR focuses only on the user plane. On the other hand, the SA operation alludes to the use of 5G for both signalling and data transmission, enabling the deployment of 5G without depending on LTE signalling.

The NR interface is designed to deliver higher throughput, lower latency, and increased spectral efficiency compared to previous generations, ensuring optimal performance in diverse deployment scenarios.

In its entirety, 3GPP Release 15 establishes the foundation for the global commercial deployment of 5G networks, empowering service providers to deliver consumers, businesses, and industries with ultra-reliable communication services and massive IoT and high-speed connectivity.

2.1.2. 3GPP Release 16

Release 16 further develops and expands the functionalities of 5G technology to accommodate evolving use cases and requirements, building upon the groundwork laid by Release 15.

Network Slicing

This release introduces network slicing, a crucial architectural concept that allows operators to split a single physical network infrastructure into multiple virtual networks, each of them customised for specific use cases or service requirements. This enables the efficient allocation of network resources, segregation of network traffic, and tailoring of services to accommodate a wide range of applications with distinct performance goals [4].

Enhanced Vehicle-to-Everything Communications

Vehicle-to-everything communication capabilities are also improved in Release 16, building upon the automotive industry's overarching goal of connected and autonomous vehicles. This advancement allows vehicles to exchange information with one another, roadside infrastructures, and other road users. This development supports enhanced traffic management, autonomous driving functionalities, and vehicle safety, thereby establishing a foundation for transportation systems that are both secure and efficient [4].

Industrial IoT Support

Release 16 grants the deployment of predictive maintenance systems, remote monitoring, and smart factories, by supporting the integration of 5G networks into industrial environments. These developments give industries the capacity of increasing operational flexibility, efficiency, and productivity through advancements in industrial IoT connectivity, low-latency communication, and reliability [4].

BASE STATION COOPERATION

Another key feature introduced in Release 16 is BS cooperation, which allows multiple BSs to collaborate and coordinate their operations and opens new optimisation possibilities for network enhancement. By working together, BSs can mitigate interference, enhance coverage, and maximize spectral efficiency, ultimately providing a better user experience and improving the overall network performance. Being this the relevant feature addressed by this thesis.

CONTINUED OPTIMISATION AND EFFICIENCY

In addition to introducing new features, this release also includes optimisations and enhancements to improve the efficiency and performance of 5G networks. This includes areas such as spectral efficiency, coverage extension, and energy efficiency, ensuring optimal utilization of network resources and delivering a seamless and reliable user experience.

EVOLVING STANDARDS AND SPECIFICATIONS

In response to feedback from operators and industry stakeholders, Release 16 strengthens and broadens the specifications and standards established in Release 15. To ensure scalability, compatibility, and interoperability throughout the 5G ecosystem, these modifications involve revisions to the radio access network, NR interface, and core network architecture.

In all aspects, 3GPP Release 16 represents a substantial growth in the development of 5G technology, emphasising the introduction of new use cases, enhancement of network efficiency, and delivering improved connectivity and services to both end users and industries. This release, through its persistent innovation and evolution, sets up a foundation for the global implementation and acceptance of 5G networks, which in turn, stimulates economic expansion and innovation, while propelling digital transformation.

2.1.3. 3GPP RELEASE 17

Release 17 expands 5G technology by consistently prioritising enhancements in efficiency, performance, and compatibility with emerging use cases.

Network Reliability and Resilience

This release improves network reliability, robustness, and resilience, ensuring uninterrupted connectivity and service availability even in challenging environments or during network failures. This involves enhancements in areas such as redundancy,

failover mechanisms, and disaster recovery, enabling operators to deliver reliable communication services to users and businesses [5].

Coverage and Capacity Optimisation

In order to address the growing demand for high-speed connectivity and seamless coverage, Release 17 introduces optimisations to improve network coverage, capacity, and spectral efficiency. These developments include progress in antenna technologies, beamforming techniques, and interference reduction strategies, providing users with consistent and superior service experiences in various deployment scenarios.

Integrated Access and Backhaul

This release also focuses on enhancing the integration of access and backhaul networks, making deploy cost-effective and scalable solutions possible for extending coverage and capacity in underserved or remote areas. This involves the deployment of integrated access and backhaul nodes, leveraging advanced radio technologies and protocols to simplify network deployment and management [5].

Non-Terrestrial Networks

Building upon the vision of ubiquitous connectivity, Release 17 explores the integration of non-terrestrial networks into the 5G ecosystem, providing smooth connectivity in remote or hard-to-reach areas. It involves the deployment of satellite, airborne, or high-altitude platforms to complement terrestrial networks, and provide extended coverage and capacity where traditional infrastructures are limited or unavailable [5].

Public Safety Communications

Release 17 also improves support for public safety applications and mission-critical communications, in order to meet the needs of emergency responders and public safety agencies. These enhancements encompass areas like priority access, multicast/broadcast services, and interoperability with legacy systems. As a result, communication during emergency situations and disaster scenarios becomes reliable, as well as resilient [5].

In general, 3GPP Release 17 contributes to the progression of 5G technology by introducing additional functionalities and capabilities that improve connectivity, performance, and reliability. Moreover, it advances the goal of creating a society that is entirely connected and digitised.

2.1.4. 3GPP Release 18

3GPP Release 18 represents the most recent advancement in the ongoing development of 5G technology, expanding the functionalities and capabilities of 5G networks by building upon the groundwork established by its prior releases.

eMBB Improvements

Release 18 aims to enhance the performance and efficiency of eMBB services, catering to the increasing demand for high-speed data transmission and multimedia applications. This includes optimisations in areas such as spectral efficiency, coverage extension, and throughput enhancements, ensuring a seamless and immersive user experience for bandwidth-intensive applications [6].

Massive IoT Connectivity

Release 18 emphasises the expansion of support for massive IoT connectivity because of the proliferation of IoT devices and applications. This enhancement allows for the implementation of large-scale IoT deployments that exhibit improved reliability, scalability, and energy efficiency. These improvements encompass features such as device management enhancements, power-saving mechanisms, and assistance for low-power wide-area technologies [6].

Mission-Critical Services and Public Safety Communications

Following its predecessor, this release ensures that emergency responders, public safety agencies, and critical infrastructures have access to more robust and resilient connectivity, by addressing the new requirements for mission-critical services and public safety communications. This entails improvements in network dependability, priority access, and compatibility with legacy systems, thereby facilitating reliable communication in demanding environments and critical circumstances.

Network Efficiency and Optimisation

To improve the performance and efficiency of 5G networks, Release 18 incorporates enhancements and optimisations into the protocols, management mechanisms, and network architecture. These technological advancements include edge computing, network slicing, and self-organizing networks, which support efficient resource allocation, optimising network operations, and deliver customised services to meet specific requirements and use cases.

VERTICAL INDUSTRY INTEGRATION AND USE CASE SUPPORT

Release 18 prioritises the incorporation of 5G technology across multiple vertical industries and diverse use cases, thereby allowing the digital transformation in several sectors, including transportation, healthcare, entertainment, and manufacturing. This process entails the creation of frameworks, standards, and solutions that are specific to each industry, to tackle the distinct challenges and needs of various sectors. By doing so, it creates prospects for increased productivity, innovation, and economic expansion.

2.2. BASE STATION COOPERATION

As stated in the section 2.1.2, BS cooperation represents a pivotal advancement in the optimisation of 5G networks, offering a paradigm shift in how multiple BSs collaborate to enhance network performance and efficiency.

In traditional cellular networks, BSs operate independently, providing coverage to their designated areas without engaging in direct coordination with adjacent cells. However, the exponential growth in mobile data traffic, the proliferation of connected devices, and the diverse requirements of emerging applications have required a more collaborative approach to network management and resource allocation.

BS cooperation entails the intelligent coordination and collaboration of multiple BSs within a network, leveraging spatial diversity and collective resources to overcome challenges such as interference, coverage gaps, and capacity limitations. By working together seamlessly, BSs can enhance spectral efficiency, improve coverage and capacity, and mitigate interference, ultimately delivering a better QoS to end-users.

This chapter provides a detailed review of the principles, techniques, implementation challenges, and future directions of BS cooperation in 5G networks. The main topics to be covered include the fundamental concepts behind BS cooperation, the key objectives and benefits it offers, the techniques and mechanisms employed to achieve collaboration, and the considerations and challenges associated with its implementation. Moreover, this work will examine the evolving role of BS cooperation in shaping the trajectory of wireless communication networks, as well as the opportunities it offers for enhancing connectivity, performance, and user experience.

2.2.1. Concept and Principles

BS cooperation involves the coordination and collaboration of multiple BSs (neighbours) within a network to enhance the overall system performance. As cellular networks need to deliver higher data rate services to a large number of UEs, they require a high spectral efficiency over the whole cell area. Therefore, it is essential that the radio interface minimises interference. A crucial component of mobile radio networks is spatial reuse. It refers to the reuse of resource elements, such as timeslots or frequency bands, across a geographical distance where signal strength is compromised due to path loss or other forms of interference. Modern technologies often rely on frequency reuse, which inevitably leads to inter-cell interference (ICI), as shown in Figure 2.2. ICI particularly manifests when different cells reuse the same radio resource in an uncoordinated way. ICI reduces more significantly the performance of UEs at the cell edge, than at the inner-cell, thereby creating a performance gap between them.

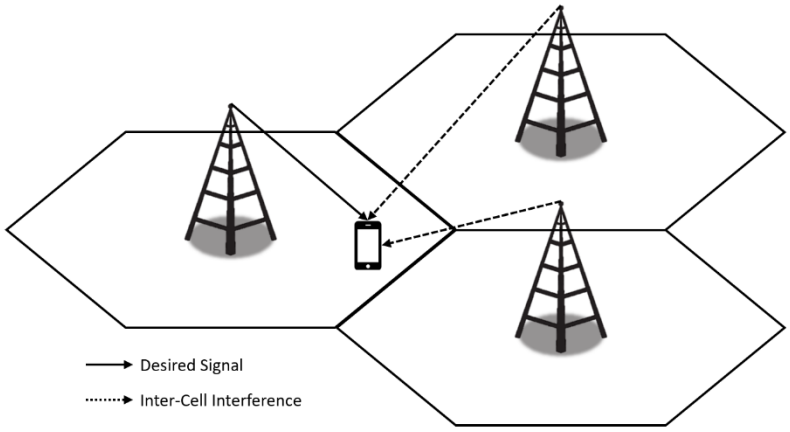

Figure 2.2 - Inter-cell interference scheme

Interference management, coordinated scheduling, and joint transmission are examples of the collaboration techniques that can be implemented to reduce these types of interference and ultimately delivering a better QoS to end-users.

2.2.2. Key Objectives and Benefits

The primary objectives of BS cooperation in 5G networks are to enhance spectral efficiency, improve coverage and capacity, and mitigate interference. BSs can optimise the use of their resources, reduce signal degradation, and ensure users have access to more consistent and dependable connectivity by coordinating their operations. This results in increased data rates, decreased latency, and enhanced network performance, which ultimately improves the QoS for users. Furthermore, this approach helps the streamlining of resource allocation, the mitigation of operational expenses, the

integration of emerging applications and the increasing need for high-speed data services.

2.2.3. TECHNIQUES AND MECHANISMS

To accomplish its goals efficiently, BS cooperation employs a diverse array of mechanisms and techniques. These include coordinated beamforming, joint transmission and reception, coordinated scheduling, and interference cancellation.

COORDINATED BEAMFORMING

Coordinated beamforming is a technique wherein multiple BSs coordinate their transmit beamforming vectors to focus energy towards specific users or areas in the coverage sector [7], illustrated in Figure 2.3. By aligning transmission beams, BSs can enhance signal strength and quality for targeted users, mitigate interference, and improve overall spectral efficiency. Coordinated beamforming involves the following sub-techniques and considerations:

- Beamforming Vector Coordination: BSs exchange information and coordinate their beamforming vectors to ensure coherent transmission towards intended users or areas.
- User Selection and Precoding: BSs select appropriate users or groups of users for coordinated beamforming and apply precoding techniques to optimize signal transmission.
- Interference Coordination: BSs collaborate to mitigate inter-cell interference by coordinating beamforming patterns and power allocation strategies.

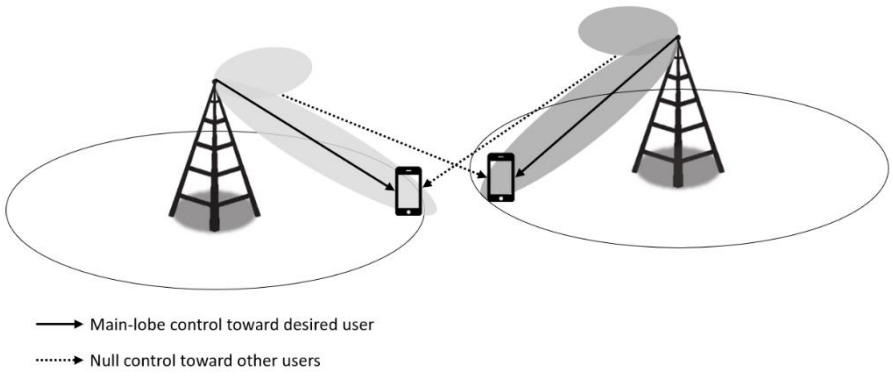

Figure 2.3 - Coordinated beamforming example scheme

JOINT TRANSMISSION AND RECEPTION

Joint transmission and reception involve the collaborative transmission and reception of data between multiple BSs and/or user devices [7], depicted in Figure 2.4. This technique enables BSs to exploit spatial diversity, multipath propagation, and interference cancellation to improve spectral efficiency and enhance user experience. Joint transmission and reception encompass the following aspects:

- Cooperative Multiple-Input Multiple-Output Transmission: BSs coordinate their transmission strategies to exploit multi-antenna diversity and achieve spatial multiplexing gains.
- Coordinated Reception and Signal Combining: BSs coordinate their reception strategies to combine received signals from multiple antennas or BSs, enhancing signal quality and reliability.
- Distributed Antenna Systems: BSs deploy distributed antenna systems to facilitate joint transmission and reception, leveraging distributed antenna elements to enhance coverage and capacity.

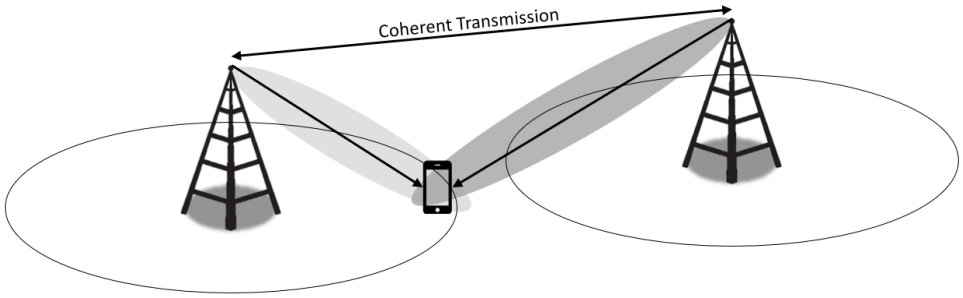

Figure 2.4 - Joint transmission/reception example scheme

COORDINATED SCHEDULING

Coordinated scheduling involves the joint optimisation of resource allocation and scheduling decisions across multiple BSs to maximize network throughput, fairness, and efficiency [7]. This technique enables BSs to coordinate the allocation of time, frequency, and power resources to users dynamically. Coordinated scheduling encompasses the following aspects:

- Resource Allocation Optimisation: BSs optimize resource allocation decisions, such as time slot assignment, frequency channel allocation, and transmit power control to maximize network throughput and fairness.

- QoS-Aware Scheduling: BSs prioritize users and applications based on QoS requirements, ensuring equitable access to network resources and meeting diverse service-level agreements.
- Load Balancing and Congestion Management: BSs coordinate scheduling decisions to balance network load, mitigate congestion, and optimize resource utilization across cells and sectors.

INTERFERENCE CANCELLATION

Interference cancellation techniques aim to mitigate interference caused by simultaneous transmissions from multiple BSs or users [7]. By cancelling interference at the receiver side, BSs can improve signal-to-interference-plus-noise ratio (SINR), enhance spectral efficiency, and increase network capacity. Interference cancellation techniques include:

- Spatial Interference Cancellation: BSs exploit spatial diversity and multipath propagation to cancel interference at the receiver side, using techniques such as successive interference cancellation and spatial filtering.
- Interference Coordination and Mitigation: BSs coordinate their transmission strategies to minimize mutual interference, employing techniques such as interference alignment, interference-aware precoding, and interference cancellation coding.

2.2.4. IMPLEMENTATION CHALLENGES AND CONSIDERATIONS

While BS cooperation offers significant benefits, its implementation presents various challenges and considerations. These include synchronization requirements, backhaul constraints, and overhead associated with coordination. Ensuring accurate synchronization among cooperating BSs is essential to avoid interference and maximize the effectiveness of collaborative efforts. Additionally, backhaul capacity and latency play a crucial role in supporting coordination and exchange of information between BSs. Addressing these challenges requires careful planning, optimisation, and integration of BS cooperation mechanisms into existing network architectures. Furthermore, interoperability issues, standardization efforts, and vendor-specific implementations may also impact the deployment and scalability of BS cooperation solutions.

2.2.5. Future Directions and Opportunities

BS cooperation is expected to play an increasingly important role in future 5G networks and beyond. As network architectures evolve towards more dynamic and flexible deployments, the demand for efficient coordination and collaboration among BSs will continue to grow. Future research and development efforts are likely to focus on advanced coordination algorithms, distributed optimisation techniques, and dynamic resource allocation strategies to further enhance the performance and efficiency of BS cooperation in 5G networks. Moreover, the integration of AI and ML techniques may enable autonomous decision-making and adaptive optimisation in BS cooperation, unlocking new opportunities for innovation and optimisation in wireless communication networks.

In summary, BS cooperation represents a fundamental technology that significantly contributes to the optimisation of 5G networks by providing a revolutionary method for managing networks and allocating resources. The incorporation of AI into 5G networks has the potential to considerably widen prospects for automation, optimisation, and intelligent decision-making. Moreover, the convergence of AI and BS cooperation offers promising prospects for collaborative intelligence, wherein BSs not only engage in cooperative operations but also acquire knowledge and adjust accordingly in response to user activity and network dynamics. The amalgamation of these technologies presents new opportunities for advancement in domains like personalised services, network slicing, throughput enhancement, and edge computing.

2.3. Artificial Intelligence and 5G

The convergence of AI and 5G wireless networks broadcasts a new era of connectivity, characterized by intelligent automation, adaptive optimisation, and personalized services. AI technologies, such as ML, deep learning, and natural language processing, are fundamentally transforming the design, deployment, and operation of 5G networks.

The heterogeneous nature of wireless networks today, poses difficulties in terms of network design and implementation, as it consists of numerous access networks, frequency bands, and cells with overlapping coverage regions. In the context of 5G networks, AI algorithms use historical data, technical characteristics, and geographic information to extract valuable insights and optimise network performance, predict user behaviour, and automate network management tasks. AI, as a result, comprises an extensive range of technologies and techniques that empower machines performance.

The following sections will delve into the wide-ranging impact of AI on 5G networks, examining its different algorithms, applications, advantages, challenges, and potential future directions.

2.3.1. MACHINE LEARNING

The subfield of AI, known as ML, is comprised into three different categories: supervised, unsupervised, and reinforced learning. By analysing historical data, identifying patterns and trends, and making well-informed decisions, these algorithms optimise network performance by dynamically adapting to changing network conditions and user demands.

The primary distinctions between the above categories tie into their operational mechanisms and training processes. Supervised learning is the primary and most common type of ML. During training, the model is provided with properly labelled data and employs it to learn and enhance itself by predicting outcomes for other data samples. Unsupervised learning algorithms, on the other hand, receive unlabelled data. The algorithm can then use the acquired data to construct models and analyse the correlations between different data points, thereby providing a deeper knowledge of the data. Reinforcement learning, the last type of ML, acquires knowledge by collecting feedback from the outcomes of its actions, frequently in the form of a reward. In general, reinforcement algorithms comprise two essential components: an action-executing agent and the environment in which the action is carried out.

In the three ML categories, there are hundreds of distinct algorithms, and each can be utilised to optimise 5G networks in a different way. Supervised learning algorithms, including support vector machines and decision trees, can predict network traffic patterns and resource demands, enabling proactive resource allocation and capacity planning. Unsupervised learning algorithms, like clustering and anomaly detection, have the capacity to identify network anomalies, detect security threats, and optimize network configuration parameters. As for reinforcement learning algorithms, such as Q-learning and deep Q-networks, can adaptively optimize network policies and configurations based on feedback from the environment, enabling autonomous network management and optimisation.

In recent research, ML-based approaches have been implemented to many research fields to address issues such as energy efficiency [8][9], user association and resource allocation [10][11], cell sleeping control [12] and error propagation [13].

2.3.2. DEEP LEARNING

Deep learning algorithms, including convolutional neural networks, recurrent neural networks, and deep reinforcement learning, offer advanced capabilities for radio resource management and optimisation in 5G networks. Convolutional neural networks can extract spatial features from radio signals, enabling accurate channel estimation and beamforming optimisation. Recurrent neural networks have the capacity to capture temporal dependencies in network traffic patterns, facilitating dynamic resource allocation and traffic prediction. As for deep reinforcement learning algorithms, such as deep Q-networks and deep deterministic policy gradients (DDPG), they can learn optimal policies for radio resource allocation, power control, and interference management in dynamic and complex network environments.

To achieve these advanced functionalities, it is imperative to have access to large quantities of high-quality and properly tagged data. The collection and curation of such data poses significant challenges. The data must be comprehensive and accurately labelled to train deep learning models effectively. However, acquiring and maintaining this level of data quality can be difficult due to the complexity of 5G networks and the variability of radio environments. Data scarcity and the labour-intensive nature of data annotation further complicate this process, highlighting the need for robust data management strategies and advanced data augmentation techniques to support deep learning applications in 5G networks.

2.3.3. EVOLUTIONARY ALGORITHMS

Evolutionary algorithms, including PSO, Genetic Algorithms (GA), and Ant Colony Optimisation (ACO), offer efficient and scalable solutions for network optimisation problems and optimizing network parameters in 5G networks. The operation of these algorithms resembles natural selection, where the most viable and robust solutions are re-evaluated and reassessed in subsequent iterations, with the objective of determining the most optimal solution to achieve the intended results.

Popularised as an optimisation technique for addressing dynamic and complex optimisation problems in 5G networks, PSO is a population-based optimisation algorithm that emulates the social behaviour of flocking birds or schooling fish to find optimal solutions to optimisation problems. PSO algorithms leverage the principles of swarm intelligence to iteratively update the positions of particles in a search space, guided by their own best-known position and the global best-known position found by the swarm. This algorithm was chosen for the optimization problem due to its main qualities:

- Simplicity and Implementation: It's relatively simple to understand and implement when comparing to other optimization algorithms, making it suitable for complex problems without requiring extensive computational resources [30].
- Efficiency: Is particularly effective when solving non-linear, multi-dimensional optimization problems [31], which is required in 5G network scenarios.
- Flexibility and Adaptability: PSO can be adapted to a wide range of optimization challenges [32], such as interference management and resource allocation, by adjusting parameters or combining with other software.
- Convergence Speed: PSO tends to converge faster towards a good solution when compared to traditional methods [33], which is valuable for real-time applications where quick decision-making is crucial.
- Scalability: The algorithm is scalable with problem sizes [34], making it useful for 5G networks with numerous variables and constraints.
- Robustness: PSO demonstrates robustness in finding optimal solutions even in dynamic and uncertain environments [35], which are characteristic of wireless networks.
- Global Optimization: Its ability to escape local optima and explore a global search space ensures high-quality solutions for optimizing network performance [36].
- Historical Success: PSO has been successfully applied in various optimization problems in 5G networks, including resource allocation [14], BS clustering and beamforming [15] and energy consumption [16].

2.3.4. Implications and Future Directions

In expectation of the future, AI in 5G networks will likely continue to grow and advance. The primary objectives of research will be the advancement of AI algorithm complexity, the improvement of interoperability and scalability, and the investigation of novel use cases and applications, made possible by AI-powered insights and automation. On top of that, the amalgamation of AI and nascent technologies including edge computing, the IoT, and distributed ledger technology (DLT) presents tremendous possibilities for transforming 5G networks and introducing new opportunities for innovation and connectivity.

In summary, the incorporation of AI into 5G networks signifies a fundamental change in the conceptualization, implementation, and management of wireless communication networks. Operators can optimise network performance, elevate the user experience, and unlock new potential for expansion and innovation by leveraging the versatility of AI algorithms.

2.4. PARTICLE SWARM OPTIMISATION

As previously mentioned, PSO is an optimisation approach inspired by the social behaviour of animals such as swarms of insects, flocks of birds, or schools of fish. In PSO, a population of potential solutions, known as particles, start at random locations scattered along the space, and are iteratively updated to find the best solution to the given issue.

Three variables are associated with each particle: position, velocity, and personal best position. The position is restricted to a specified range and signifies a possible solution to the problem at hand. On the other hand, the velocity indicates the trajectory in which the particle is going to move. Regarding the personal best position, it stores the particle position that generated the best solution.

In every iteration, the algorithm analyses the efficiency of each particle position using a fitness function that converts the position of the particle to a scalar value, representing its objective value or key performance indicator (KPI). This objective function is determined and guided by the optimisation problem, meaning every problem will have a different function.

Iteration by iteration, each particle adjusts its position and velocity depending on its best-known position and the best-known position of the swarm. This behaviour is analogous to birds in a flock altering their flight direction depending on the location and movements of other birds nearby.

Upon the achievement of a stopping condition, such as a specified maximum number of iterations, the algorithm ends and returns the best-known location discovered. Figure 2.5 illustrates the behaviour of a base PSO algorithm which reflects this entire logic.

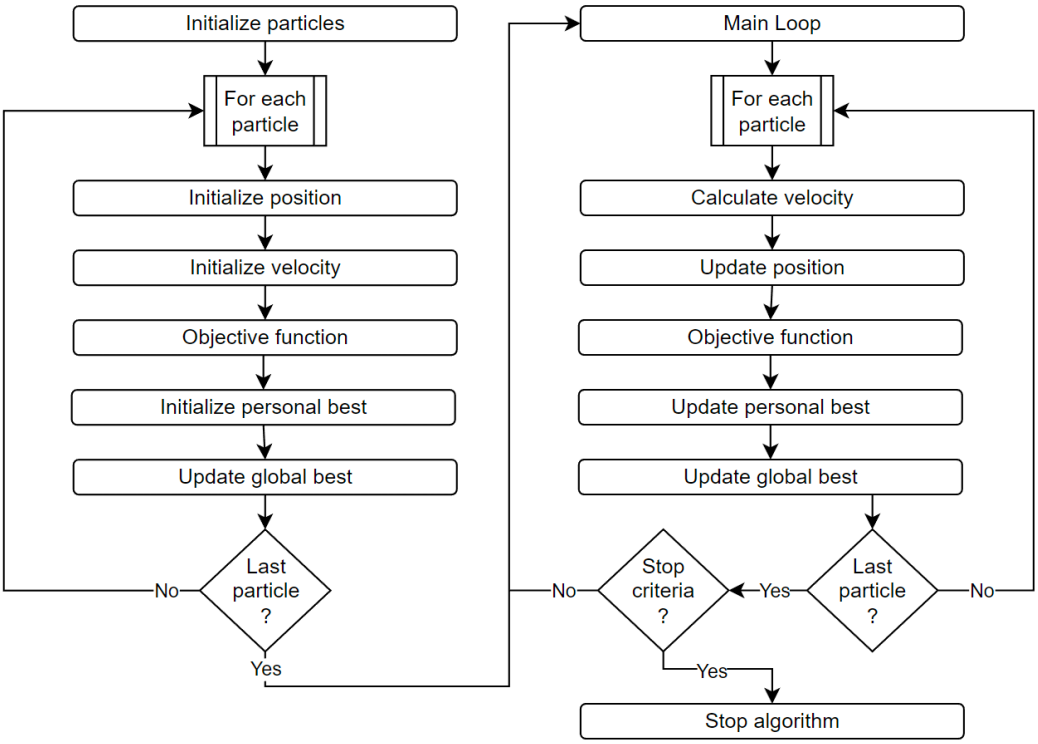

Figure 2.5 - Base PSO algorithm diagram

The following subchapters will provide an in-depth explanation of each parameter comprised in a PSO algorithm, in addition to the particle initialisation and main loop, which are the two main sections of the diagram.

2.4.1. BASE PARAMETERS

In short, a PSO algorithm is a swarm containing a certain number of particles, with each component being associated with several parameters. As stated before, a particle has three variables, described in Table 2.1

Table 2.1 - Base PSO particle parameters

Parameter	Description
$\boldsymbol{P_i}$	Position of particle i
$\boldsymbol{V_i}$	Velocity of particle i
$\boldsymbol{P_{bi}}$	Personal best position of particle i

In terms of the swarm, it consists of eight parameters displayed in Table 2.2.

Table 2.2 - Base PSO swarm parameters

Parameter	Description
$\boldsymbol{F(P_i)}$	Objective/fitness function
$\boldsymbol{n}$	Number of particles
$\boldsymbol{G_b}$	Global best position
$\boldsymbol{t}$	Current iteration
$\boldsymbol{W}$	Inertia weight
$\boldsymbol{C_1}$	Cognitive/personal constant
$\boldsymbol{C_2}$	Social constant
$\boldsymbol{U_1, U_2}$	Random numbers

The objective function, $F(P_i)$, is responsible for converting the particles current position to a scalar value, known as fitness value, to allow the comparison between all the different particles possible solutions. The swarm global best position, G_b, is similar to the particle personal best position, P_{b_i}, in the sense that it retains the position from which the best solution was generated after every iteration involving all particles. As suggested by its description, t retains the current swarm iteration number. Regarding the last five parameters, each one represents a different weight in the velocity calculation and, consequently, the position update. A more in-depth description of these parameters will be provided in the section 2.4.3.

2.4.2. PARTICLE INITIALISATION

To help with the explanation, an example function will be employed into a base PSO algorithm. The subsequent figures will employ function (1), which the algorithm will try to minimize.

$$F(x, y) = (x - \pi)^2 + (y - \pi)^2 \quad (1)$$

Here, x and y represent the particles position, as they will be the values changed in each iteration to generate new results. The function generates the solution space shown in Figure 2.6 , delimited between 0 and 5 in both axis, with the optimal solution denoted by a white cross in the lowest value, since the objective is to minimise (1). The colour bar represents the range of achievable values of function (1), with the x and y axis limitations previously mentioned.

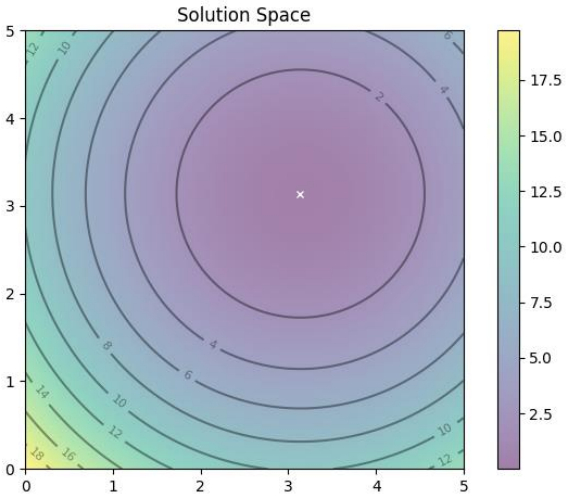

Figure 2.6 - Example fitness function solution space

So, the particle initialisation, as shown in Figure 2.5, begins by iterating over all particles and generating random initial positions, and velocities. Here, the objective function is provided with the positions of the particles as input. In this example, the value indicated in the colour bar serves as the returned numeric result, fitness value.

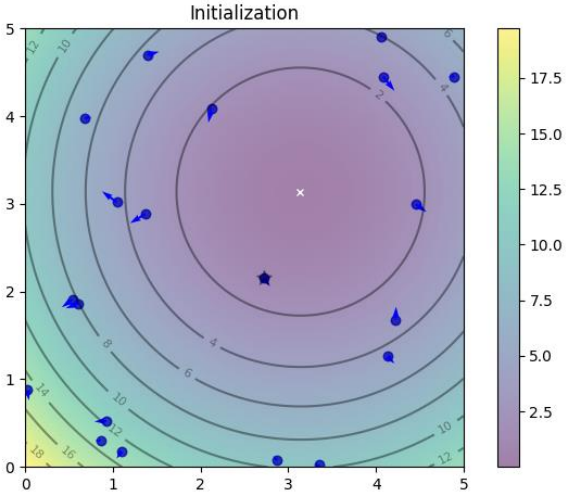

Figure 2.7 - Example fitness function initial positions

Figure 2.7 plot visually represents the position of each particle as a blue circle, its velocity as a blue arrow, and the global best position, G_b, as a grey star. It is worth noting that the personal best positions, P_b, are first set with their particle's initial positions, which appears as such on the graph. However, as the subsequent figures will demonstrate, this position is depicted by a grey circle. As a last detail in the initialisation, the global best position is updated if a lower value is discovered after each particle computing its objective value via the fitness function.

2.4.3. MAIN LOOP

The main loop will consist of iterations that sequentially traverse every particle until an established stopping criteria is met. The particle's velocity, V_i, is updated at the start of each iteration, incorporating the constants specified in Table 2.1 and Table 2.2. This results in equation (2) [27].

$$V_i^{t+1} = W \times V_i^t + C_1 U_1^t \left(P_{b_i}^t - P_i^t\right) + C_2 U_2^t \left(G_b^t - P_i^t\right) \quad (2)$$

Each particle's velocity is updated using three components: inertia, which is responsible for looking for new solutions, the cognitive component, which is based on the particle's best-known location, and the social component, which is based on the best-known position of the swarm. These factors are weighted and summed to determine the new velocity of the particle.

The first component from (2), $W \times V_i^t$, is responsible for seeking alternative solutions and identifying locations with the greatest potential solutions. In this instance, the inertia, W, causes the particle to proceed in the same direction, but with a slight difference based on its weight. This parameter is a positive constant that is essential for balancing the global and local search, which is referred to as exploration when higher values are set, and exploitation when lower values are set. If W is set to 1, the particle's motion is completely determined by its prior motion, therefore it may continue in the same direction. Alternatively, if W is set between 0 and 1, this impact is diminished, and the particle will move to other locations of the search area.

As for the second part, $C_1 U_1^t \left(P_{b_i}^t - P_i^t\right)$, it analyses the previous personal best position and determines a new direction based on it. The cognitive influence supervises the individual improvement of each particle, causing it to revert to a prior position, P_b, if the present one is not better. In the term $P_{b_i}^t - P_i^t$, the difference must rise as the particle moves farther away from its known personal best position, P_b. So, when this term increases, the particle is drawn to its current optimal location. The parameter C_1 is a positive constant and an individual cognition parameter, since it measures the significance of a particle's own prior experiences. The second hyper-parameter that makes up the product of the first term, U_1^t, is a random value parameter between zero and one. This random parameter is critical for preventing premature convergences, hence improving the likelihood of a global optimum solution.

Regarding the social impact, $C_2 U_2^t \left(G_b^t - P_i^t\right)$, it causes the particle to move toward the best location attained by the swarm, G_b. This happens because the difference $G_b^t - P_i^t$ increases as the particle moves farther away from the global best position, G_b. Similarly to the previous, C_2 is a social learning metric that measures the significance of the swarm's global learning, and U_2^t performs the same function as U_1^t.

When balancing the constants C_1 and C_2, their sum must be equal to 1, indicating a dependency in that regard. This condition was implemented so that, if C_1 is increased and C_2 is subsequently decreased, the particles tend towards their own best position, P_b, while drawing less attention to the global best location, G_b. Alternatively, if C_1 is lower than C_2, the particles will disregard their own personal best and gravitate more towards the global best. This way, a balance is created between pulling the particles in either direction, without altering the velocity to extreme values.

Once the velocity has been updated, the particle's current location is added to the newly adjusted velocity to determine its new location (3) [27].

$$P_i^{t+1} = P_i^t + V_i^{t+1} \tag{3}$$

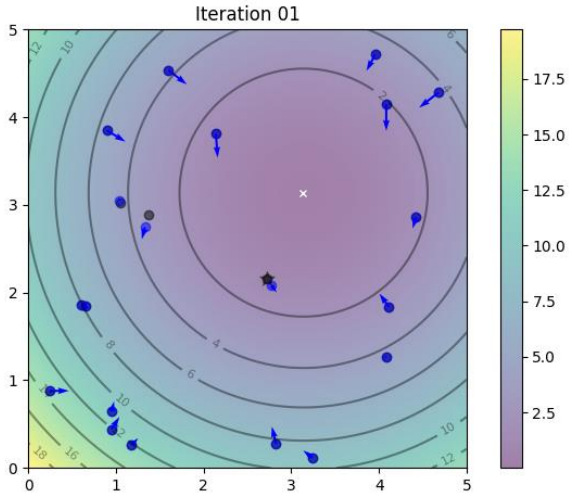

Figure 2.8 - Example fitness function first iteration

In the first iteration, shown in Figure 2.8, the majority of particles adjust their velocities in the direction of the optimal region (purple). Additionally, a small number of particles that deviated from the optimal area exhibit their personal best positions as grey circles.

As the iteration nears its conclusion, revisions are made to both the personal and global best positions. Firstly, in the given example, should the particle attain a lower value, it is updated to its personal best position; otherwise, no update is made.

Furthermore, this method is extended to the update of the global best position; however, in this case, the comparison is made between the newly acquired position of the particle and the optimal position of the swarm.

In the end, each iteration concludes with a verification of the stopping conditions; if any of them are met, the algorithm stops. Figure 2.9 displays the algorithms final iteration with function (1).

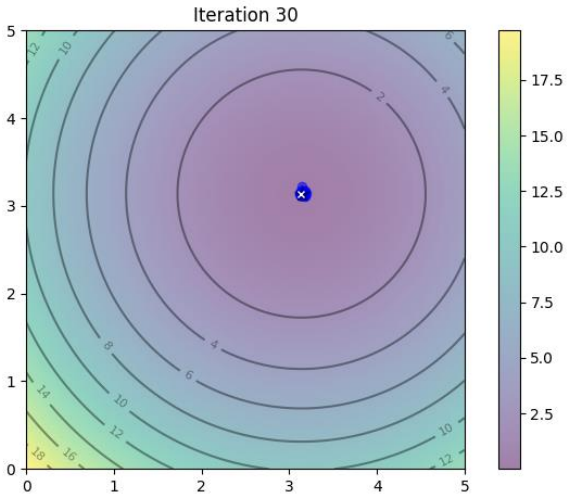

Figure 2.9 - Example fitness function final iteration

2.5. 5G NETWORK SIMULATORS

After conducting research on the selected algorithm, it becomes essential to select a network simulator to evaluate the performance and behaviour of 5G networks across different scenarios. By offering a simulated environment, network simulators enable the evaluation of the potential consequences of implementing various network configurations, protocols, and algorithms prior to their actual deployment. NS-3, OMNeT++, and MATLAB-based simulations are simulators used for 5G networks. Each of these simulators provides distinct functionalities and capabilities that facilitate the modelling and analysis of networks.

2.5.1. NS3

NS3 is an open-source discrete-event network simulator widely used for modelling and simulating communication networks, including an extension to simulate 5G networks. It provides a comprehensive framework for simulating various network protocols, traffic models, and mobility patterns, making it a popular choice among researchers and developers.

ADVANTAGES

- Open-Source: NS3 is freely available and extensively documented, allowing users to modify and extend its functionalities to suit their requirements.
- Realistic Modelling: NS3 supports detailed modelling of network protocols, physical layer characteristics, and channel models, enabling realistic simulations of 5G networks.
- Modularity: The modular architecture of NS3 facilitates easy integration of new modules and protocols, promoting flexibility and extensibility.

DISADVANTAGES

- Steep Learning Curve: NS3 has a steep learning curve, especially for users unfamiliar with C++ programming and simulation concepts.
- Performance Overhead: Due to realistic modelling, simulations in NS3 can be computationally intensive, requiring substantial computational resources and time for large-scale scenarios.
- Limited Visualization: NS3 lacks built-in visualization tools, making it challenging to visualize simulation results and analyse network behaviour.

2.5.2. OMNET++

OMNet++ is a modular, component-based simulation framework designed for modelling and simulating communication networks and distributed systems. It offers a rich set of features for modelling complex network architectures, protocols, and applications.

ADVANTAGES

- Modularity and Reusability: OMNet++ promotes modularity and reusability through its component-based architecture, facilitating the creation and integration of reusable simulation models.
- Extensive Library: OMNet++ provides an extensive library of pre-built modules and models for simulating various network components and protocols, reducing development effort.
- Visual Simulation Environment: OMNet++ offers a graphical user interface and visualization tools, allowing users to design, debug, and visualize simulations with ease.

- Scalability: OMNet++ is scalable and efficient, capable of simulating large-scale networks with thousands of nodes and complex topologies.

DISADVANTAGES

- Limited Protocol Support: OMNet++ may have limited support for some advanced protocols and features compared to other simulators like NS3.
- Steep Learning Curve: Similar to NS3, OMNet++ has a steep learning curve, especially for users without prior experience with simulation frameworks.
- Resource Intensive: Simulations in OMNet++ can be resource-intensive, particularly for large-scale scenarios, requiring significant computational resources and time.

2.5.3. MATLAB

Matlab-based simulations refer to simulations conducted using the Matlab programming language and its simulation toolbox. It provides a versatile environment for modelling and simulating communication systems, signal processing algorithms, and wireless networks.

ADVANTAGES

- Ease of Use: Matlab offers a user-friendly and interactive environment for developing and simulating communication systems, making it accessible to users with diverse backgrounds.
- Rich Toolbox: Matlab provides a rich set of built-in functions, toolboxes, and libraries for signal processing, communications, and system simulation, enabling rapid prototyping and experimentation.
- Integration with Other Toolboxes: Matlab-based simulations seamlessly integrate with other Matlab toolboxes for data analysis, visualization, and algorithm development, enhancing productivity and workflow efficiency.

DISADVANTAGES

- Limited Scalability: Matlab-based simulations may lack scalability for simulating large-scale networks or complex scenarios compared to dedicated network simulators like NS3 or OMNet++.
- Closed-Source: Matlab is a proprietary software, and access to its advanced features and toolboxes may require purchasing licenses, limiting accessibility for some users.

- Performance Constraints: Simulations in Matlab may suffer from performance constraints, particularly for computationally intensive tasks or simulations involving large datasets.

2.5.4. SIMULATOR COMPARISON

Overall, each 5G network simulator, including NS3, OMNet++ and Matlab, offers unique features, advantages, and disadvantages. The choice of simulator depends on various factors such as the specific research or development objectives, simulation requirements, user expertise and available computational resources.

When evaluating the suitability of a simulator, the primary goals are to identify one that allows for source code modification to accommodate specific needs, supports scalable simulations, requires least computational resources, and has a relatively short learning curve.

Considering this, Matlab has the most favourable learning curve among the three simulators; however, it might not allow simulations to be scaled and customised to the required degree. OMNet++, while featuring a graphical user interface that aids in the development and troubleshooting of simulations, offers a reduced degree of customisation and makes more extensive use of computational resources in comparison to NS-3. So, in comparison to the other simulators, NS-3 is the one that exhibits the greatest potential for successfully performing the intended features.

2.6. RELATED WORK

This section provides an overview of recent developments in the optimisation of 5G networks, with a specific emphasis on the integration of ML and AI algorithms into resource allocation. Resource allocation, spectrum efficiency, interference mitigation, traffic management and energy consumption are some of the critical issues that have been addressed in the selected papers, which represent some research in the field.

While network slicing enables the creation of multiple virtual networks on a shared physical framework, to fully capitalise on its advantages, resource allocation must be optimised. The authors in [20] employ an artificial neural network in combination with a PSO algorithm to calculate the most effective parameters for the network slicing process. The method that has been created is implemented through a two-way functionality that can accommodate a variety of industrial requirements. The process comprises three fundamental stages: data collection, optimisation of the most effective weighted parameters, and finally, slicing classification. By abstaining from imposing optimisation

parameters, this well-established method enables operators to generate the most optimal solution for the given objective.

Moreover, millimetre wave (mmWave) systems are a recurring topic in 5G mobile networks; however, their implementation is significantly obstructed by path loss at higher frequencies. Such systems require a narrow beampattern to minimise the energy path loss of mmWave signals. Two three-dimensional beamforming algorithms were suggested in [21] for the purpose of tracking users in the azimuth and elevation planes. The operation of the beamforming algorithms relies on the singular value decomposition and PSO principles. Moreover, the side lobes of these beam-forming algorithms were intentionally designed to be minimal or non-existent, thereby reducing interference for other users operating within the same cell. Practical results showed that the algorithms performed very well in achieving a substantial capacity and reduced side lobes.

Another emerging domain in wireless networks is cognitive radio networks. Incorporating multimedia and integrated services, this network provides an alternative and more suitable resolution to the present resource demands. The usefulness of this radio network is reliant upon the efficient allocation of these spectrums and resources [22]. Therefore, optimises the resource allocation problems utilising a PSO technique. Unused licenced spectrum is allocated to secondary users (SR) to prevent interference with licenced primary users. Moreover, resource allocation decisions are contingent upon various factors, including SINR, BER, and the power demands of the SR for each channel. It was demonstrated that as the number of particles in the swarm and the number of iterations increased the fitness values obtained improved even further.

The novel methodology presented in [23] integrates genetic algorithms and PSO to tackle issues related to channel allocation, traffic management, and energy consumption. The objective of the study was to devise an advanced power management approach for 5G networks that simultaneously guarantees optimal network performance and energy efficiency. A complex fitness function was developed to precisely gauge the complex correlation between network performance and energy efficiency. By employing the PSO algorithm to optimise network configurations and dynamically adjust traffic patterns in response to fluctuating loads, the GA component facilitates the development of network frameworks that are inherently energy-efficient.

Delay in the initial access mechanism continues to hinder the achievement of the 5G communication performance specification, given that establishing directional links between BSs and UEs may require considerable time to locate suitable beam alignments. An approach for beam refinement, known as Hybrid Genetic Algorithm and

PSO (HGAPSO), was introduced in [24]. This method was constructed by combining both GA and PSO, continuing the theme from the previous research study. As an evaluation metric for performance, the capacity parameter was compared to the number of iterations (delay). Based on the simulation outcomes, HGAPSO demonstrates the second-lowest number of iterations required to attain convergence with the highest capacity when compared to the GA and PSO methods alone. This characteristic makes HGAPSO a viable option for initial access mechanisms in mmWave 5G communication systems.

3. Proposed Algorithm and Implementation

After the review made about the relevant technologies and their current state, the purpose of this chapter is to outline the suggested architectural solution and the main considerations for implementing it, with the intention of accomplishing the objectives outlined in Chapter 1.

To accomplish the primary objectives, the architecture was established around five fundamental steps:

- Initialisation;
- Main loop;
- Network simulation;
- Result evaluation;
- Stop conditions;

The chapter is organized into three distinct sections: an introduction to the proposed solution architecture; descriptions of the network scenario and simulation parameters; and concludes with the algorithm architecture.

3.1. Proposed Solution Overview

The implementation overview of the proposed architecture is depicted in Figure 3.1, which explicitly shows the five steps.

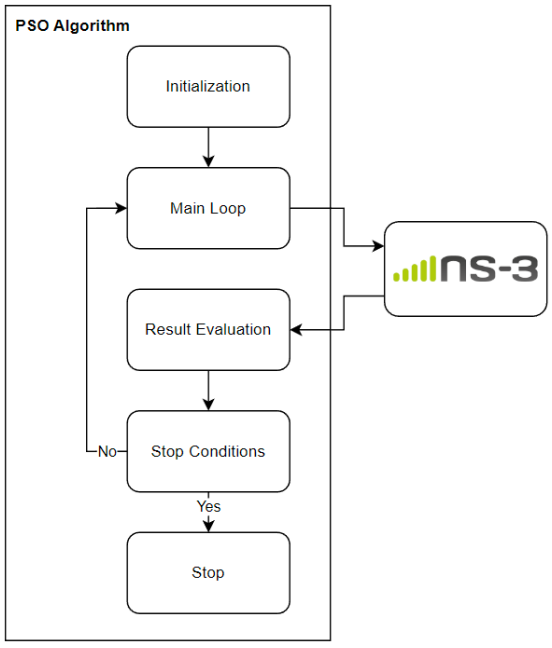

Figure 3.1 - Overall proposed algorithm logic

The **Initialisation** pertains to the phase of the algorithm during which particles are initialized. This component is regarded as a key one given the importance of the modifications made to the base PSO described in Section 2.4. This component is responsible for changing the majority of the base parameters (2.4.1) and removing the randomness inherent in common PSO algorithms. Therefore, as will be elaborated upon in Section 3.4.2, a new logic is developed to accelerate the algorithm convergence and eliminate certain executions that resulted in suboptimal solutions.

Following the initialisation modifications, the **Main Loop** contains the entirety of the implementation logic, making it a second critical element in the architecture. This cycle consists of consecutive iterations until a stopping criterion is met. Here, in each iteration, there will be another loop that courses through every particle, just like in a base PSO.

In the **Network Simulation**, it is regarded as the fitness function since it produces outcomes in accordance with the input provided by the algorithm. Furthermore, as the simulation is responsible for the configuration of each network scenario, it becomes a vital element in the process of developing the solution.

Although the **Result Evaluation** is carried out within the main loop, it is regarded as a crucial aspect as it guides the evolution of the algorithm. After the completion of the network simulation, the returned results are converted to KPIs, and must be analysed and assessed to direct the algorithm appropriately; failure to do so will result in suboptimal outcomes and render the execution wasteful.

At last, the **Stop Conditions** refer to the criteria accessed at the end of each main loop iteration to stop the algorithm. While there are numerous potential features that could be incorporated, only three were ultimately selected for the final solution, as elaborated upon in Section 3.4.4.

To summarise, the algorithm will begin after the definition of the base parameters and advance to the initialisation of the particles. The main algorithm logic then ensues, consisting of numerous iterations until an ending condition is satisfied. Until then, in each iteration, a network simulation will be performed with the algorithms input and returning the main results. So, using these outcomes, the KPIs are computed and evaluated to direct the algorithm towards the optimal resolution.

The following chapters will be explaining each component in-dept, starting with the establishment of the network scenario around which the solution was developed, and explaining the nomenclature used in subsequent chapters.

3.2. Network Scenario and Simulation

The 5G network is characterised by urban macro-cells comprised of tri-sectorized BSs and frequency overlapping. The transmission is evaluated in downlink with a 100 MHz bandwidth and time division duplex (TDD). Since the BSs are tri-sectorized, their antennas are directional and implemented using the parabolic model described in 3GPP TR 38.901 v15.0.0. As for the UEs, they will employ low-latency applications and operate at a moderate traffic load.

In order to streamline the interference analysis between sectors with frequency overlap, the network scenario is simplified into two tri-sectorized BSs. The inter-site distance used is 1732 m, as illustrated in Figure 3.2. Each sector is denoted by a hexagon, and each antenna is represented by an arrow. With the primary objective of enhancing the signal quality for a specific user (referred to as Main User) without compromising service quality for the rest of the network, the optimisation process will be restricted to two sites: the Main Site, which is frequented by the main user, and the Interfering Site, which will interfere with the main site signal and user experience.

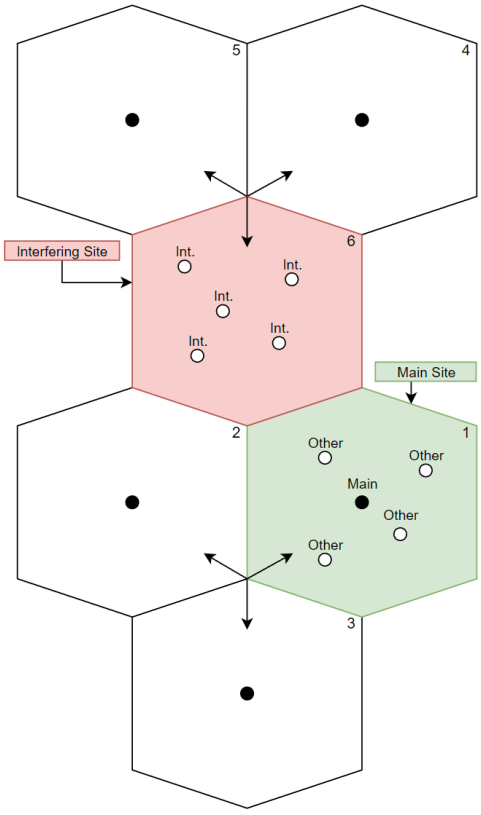

Figure 3.2 - Base network scenario

The two sites, Main and Interfering, will be designated as such; consequently, the users will be referred to as Other Main Site Users and Interfering Users, respectively. In regard to the user's distribution, the positions depicted in Figure 3.2 are purely illustrative. Chapter 4 will present five distinct scenarios, each featuring a particular user placement.

Concerning the network simulation, as previously explained, a network simulation will be executed during each iteration crossing every particle. The input parameters consist of the bearing and downtilt angles of the antenna, which denote its ability to move across both the horizontal and vertical planes. Therefore, a set of parameters containing the bearing and downtilt angles for both the main and interfering sites will be inputted for each simulation. As a result, each antenna is restricted in the bearing to a maximum area of 120 degrees around its designated site and 90 degrees in downtilt, from 0º to -90º. The bearing limits are illustrated in Figure 3.3.

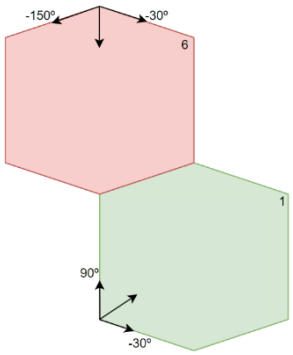

Figure 3.3 - Network bearing angle limits

So, upon completion of the simulation, the SINR values of all users present in the main and interfering sectors are returned. The SINR was selected as the KPI value, as explained in Chapter 1, due to its comprehensive nature and ability to reflect critical network performance aspects. In the subsequent result evaluation process, the SINR values will be incorporated into the algorithms fitness value calculation, enabling comparisons among the various potential solutions.

3.3. Algorithm Architecture

This chapter will be explaining the developed PSO algorithm, describing every decision and change made along its implementation. Figure 3.1 provided a simplified look to the general architecture, highlighting the main components, but the full architecture is in Figure 3.4.

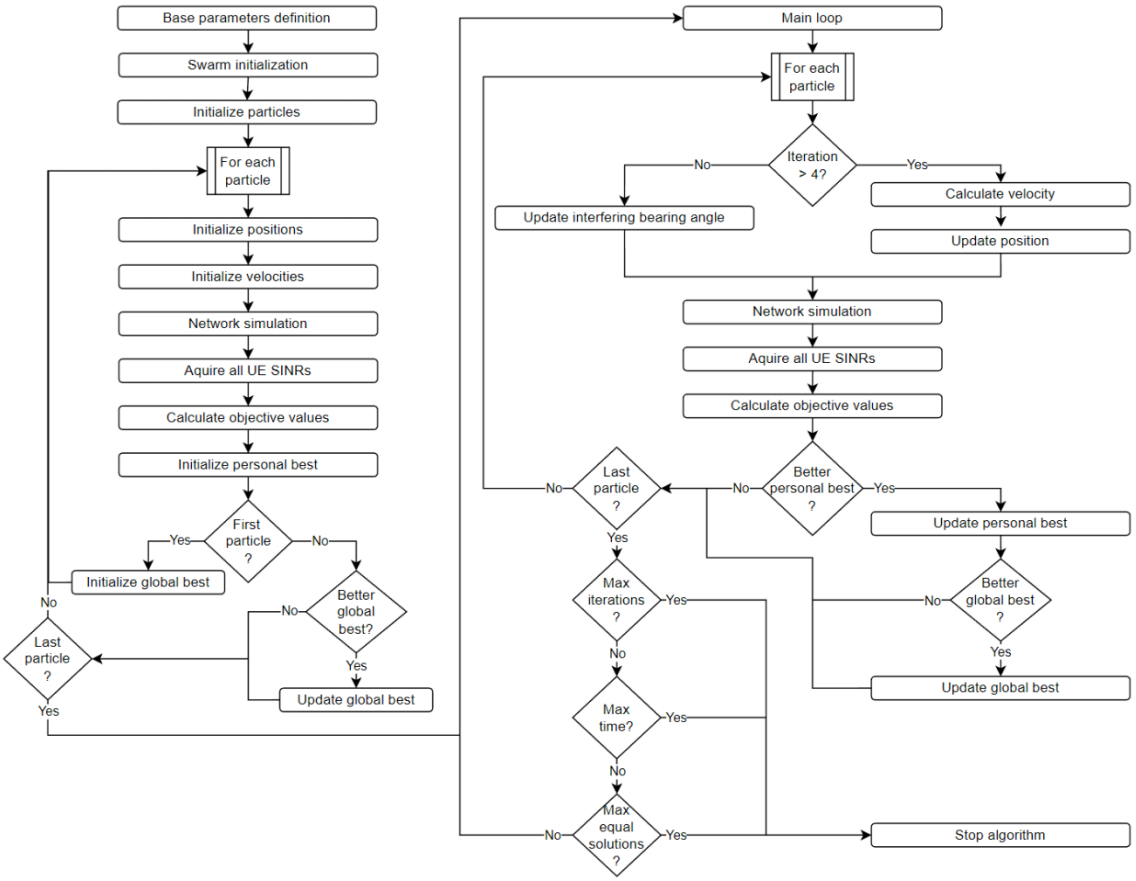

Figure 3.4 - Proposed algorithm architecture

In order to simplify comprehension and presentation, in the subsequent sections the architecture will be subdivided into components as required.

3.4.1. Base Parameters

The developed algorithm follows the basis established in Chapter 2.2, but introduces some changes to optimize the time, search and convergence. Starting with the base parameters, specifically the particle ones (Table 3.1): position, velocity and personal best position. To adapt to the optimisation problem, each previous parameter now as a bigger dimension to include all the bearing and downtilt angles as follows: [Main Bearing, Interfering Bearing, Main Downtilt, Interfering Downtilt]. In addition, a new component was introduced in order to save the simulation results after being translated to their fitness values. This translation will be explained in Section 3.4.3.

Table 3.1 - Developed PSO particle parameters

Parameter	Description	Unit
$\boldsymbol{P_i}$	Position of particle i	Degrees
$\boldsymbol{V_i}$	Velocity of particle i	Degrees/Step
$\boldsymbol{P_{b_i}}$	Personal best position of particle i	Degrees
$\boldsymbol{P_{bF_i}}$	Personal best fitness values of particle i	dB

In terms of the swarm, Table 3.2, a couple new parameters were introduced, and others changed.

Table 3.2 - Developed PSO swarm parameters

Parameter	Description	Unit
$\boldsymbol{F(P_i)}$	Objective/fitness function	dB
$\boldsymbol{n}$	Number of particles	-
$\boldsymbol{G_b}$	Global best position	Degrees
$\boldsymbol{G_{bF}}$	Global best fitness values	Degrees
$\boldsymbol{t}$	Current iteration	-
$\boldsymbol{W}$	Inertia weight	%
$\boldsymbol{C_1}$	Cognitive/personal constant	-
$\boldsymbol{C_2}$	Social constant	-
$\boldsymbol{U_1, U_2}$	Random numbers	-
$\boldsymbol{lwLmts}$	Positions lower limits	Degrees
$\boldsymbol{upLmts}$	Positions upper limits	Degrees
$\boldsymbol{fitThr}$	Fitness values thresholds	dB
$\boldsymbol{a}$	Average constant weight	%
$\boldsymbol{m}$	Median constant weight	%
$\boldsymbol{s}$	Standard deviation constant weight	%
$\boldsymbol{I}$	Maximum number of iterations	-
$\boldsymbol{T}$	Maximum time elapsed	Seconds
$\boldsymbol{S}$	Maximum number of iterations with the same result	-

From the base PSO swarm parameters, Table 2.2, only $F(P_i)$ and G_b where changed. Now the fitness function, $\mathrm{F(P_i)}$, is implemented as the network simulation and the swarms' global best position, G_b, follows the dimension and distribution of P_i: [Main Bearing, Interfering Bearing, Main Downtilt, Interfering Downtilt].

As for the new parameters:

- $\boldsymbol{G_{bF}}$**:** Represents the global best simulation results after being translated to their fitness values;
- $\boldsymbol{lwLmts}$ **and** $\boldsymbol{upLmts}$**:** New swarm input that establishes the lower and upper bearing and downtilt angle limits, respectively;

- $\boldsymbol{fitThr}$**:** This component was introduced in order to enable the definition of a threshold upon which the algorithm will attempt to maintain the other main site and interfering users' fitness values above;
- $\boldsymbol{a}$**,** $\boldsymbol{m}$ **and** $\boldsymbol{s}$**:** These weights are used in the calculation of the fitness values and will be explained in Section 3.4.3;
- $\boldsymbol{I}$**,** $\boldsymbol{T}$ **and** $\boldsymbol{S}$**:** Variables used as the algorithm stopping criteria;

3.4.2. PARTICLE INITIALISATION

Figure 3.5 represents the initialisation component of the proposed architecture, which goes over every particle.

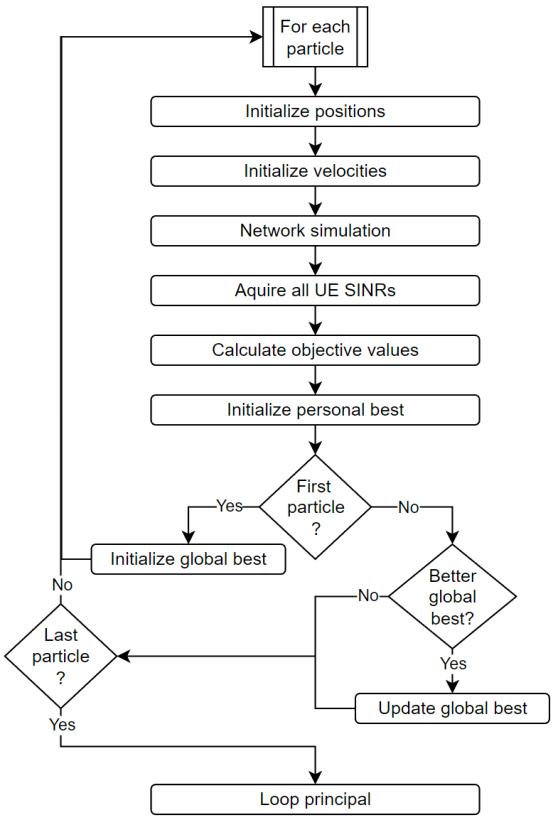

Figure 3.5 - Initialisation architecture

The subsequent section starts the integration of a logic modification into the basic algorithm, which eliminates its stochastic characteristics with regard to particle initialisation and the exploration of potential solutions in space. To clarify, the foundational PSO algorithm begins by specifying random velocities and positions for every particle. Specifically, the interfering sector's range from -150º to -30º and the main sector's range from -30º to 90º. This is done with the goal of distributing the particles' initial space of solutions and subsequently facilitating convergence.

This form of randomised initialisation resulted in different outcomes being generated by each execution, despite the initial parameters remaining unchanged. Furthermore, certain executions ultimately pursued suboptimal solutions due to the concentration of random initial positions in a limited range, such as between -30º and 0º at the main site. In order to eliminate this stochastic nature during the initialisation phase and, by extension, the remainder of the execution, it was determined that the 120º bearing spaces ([-30º, 90º] and [-150º, -30º]) would be partitioned in two distinct manners for the main and interfering sectors during the initial five iterations, including the initialisation.

The division of the main sector's bearing angle is equal to the number of particles; for instance, in the case of five particles, their respective initial angles would be -30º, 0º, 30º, 60º, and 90º, as Figure 3.6 presents. The main site bearing position will be kept by each particle until the conclusion of the fourth iteration.

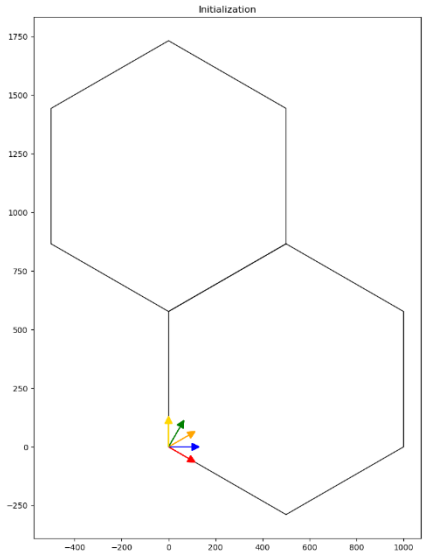

Figure 3.6 - Proposed particle initialisation main bearing division

Concerning the bearing of the interfering sector, it will always be divided by five, that is, regardless of the number of particles, the space will always be subdivided into the angles of -150º, -120º, - 90º, -60º and -30º. In contrast to the main bearing, every particle will have the same interfering bearing position, changing it in each iteration.

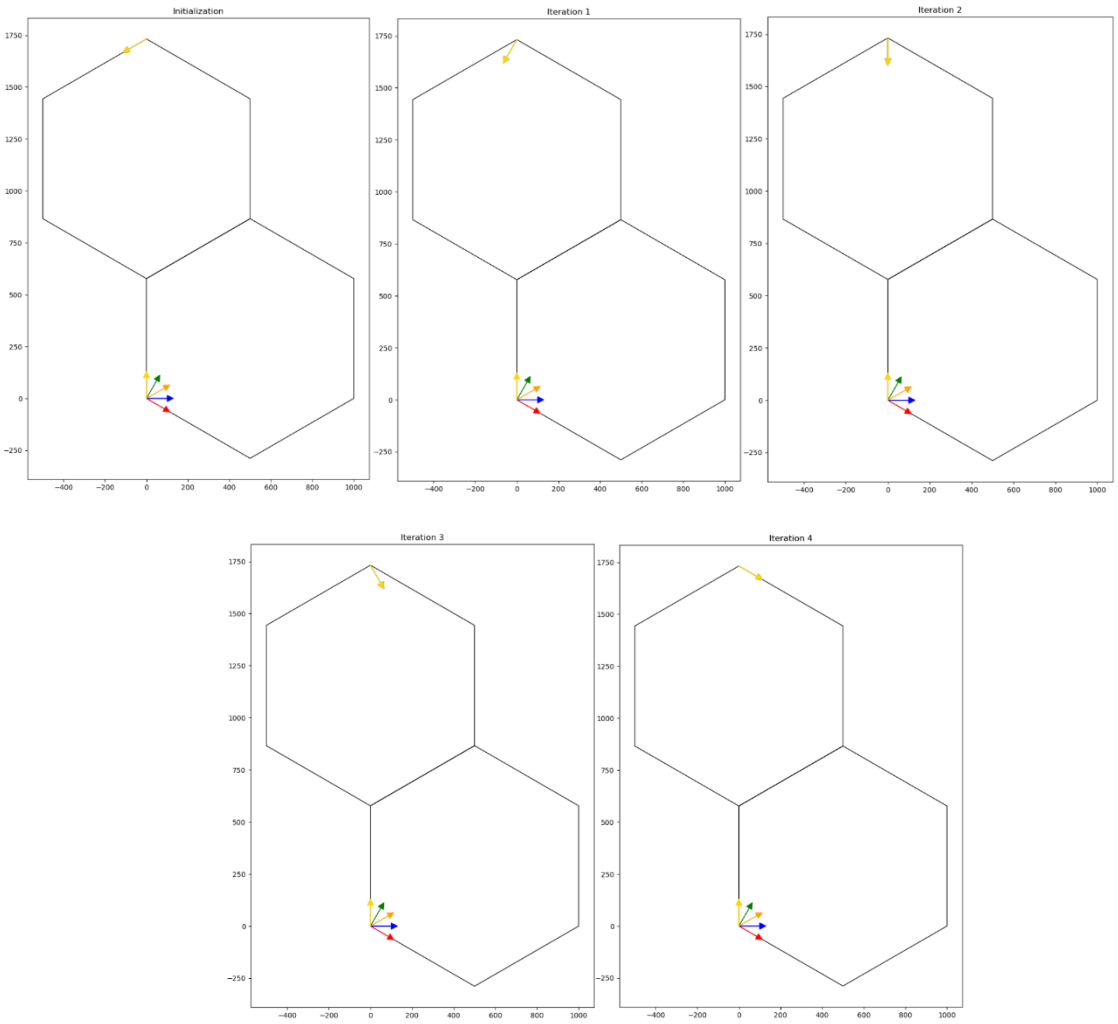

Figure 3.7 - Proposed particle initialisation interfering bearing division

As illustrated in Figure 3.7, during the initial four iterations, the bearing angles of the primary sector will remain unchanged, while the bearing angles of the interfering sector will change. In this way, the algorithm's initial randomness is eliminated, which occasionally produced arbitrary outcomes, and a preliminary correlation and sweep between both sectors is established, thereby facilitating the convergence process that will be elaborated upon in Chapter 4.

In regard to the downtilt positions/angles, they will be set to 0 degrees during the proposed method. This decision was implemented in order to carry out a base correlation sweep, wherein all bearing angles remained constant.

After the positions are initialized, follows the particle velocities initialisation. Since in the proposed initialisation a correlation is made between the two sectors, instead of generating random velocities, the main and interfering are both set to 0 degrees/step. This will mean that in the next iteration, the fifth, each particle position update will only depend on its personal best and global best values acquired after the proposed

initialisation. As for the downtilt velocities, they are initialized with -3 and -6 degrees for the main and interfering sites, respectively.

The network is then simulated and the SINR values from all users are extracted. The objective value calculation that follows will be explained in the main loop (Section 3.4.3).

To finish the initialisation architecture, what remains is the particles personal best initialisation and the swarm's global best initialisation and update. Both the personal best of each particle and swarms global best are initialized with the first result acquired from the simulation. Only after this, in subsequent particles, the global best update method will be used, which will be detailed in the next section.

3.4.3. MAIN LOOP

All of the algorithm's logic will occur at this stage, which will be executed in successive iterations until a stopping criterion is reached. As in a standard PSO, each iteration of this loop will consist of an additional cycle that traverses all the particles.

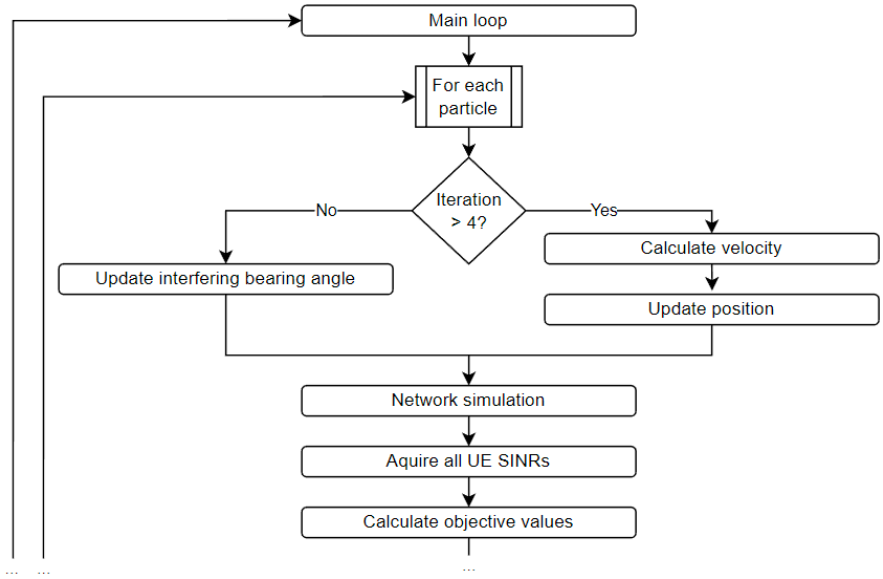

Figure 3.8 - Initial main loop architecture

Starting with this first snippet, Figure 3.8, it refers to the logic explained in the previous section. Thus, during the first four iterations, not counting the initialisation that happened before, only the interfering bearing angles positions will be changed. When iteration five or higher is reached, the new velocity of each particle is then calculated as described in Section 2.4.3.

One point to add regarding the velocities update is the change in the inertia weight logic. This weight refers to the importance of the previous velocity in calculating the new one. This weight is a value that must be decreased with each passing iteration, so that as the algorithm evolves and converges, the new positions depend less and less on the previous speed and more on their personal and global best positions. For this purpose, the inertia weight is now updated after every iteration with an adapted linear decay function in (4), which proved to be more efficient in the algorithm's convergence.

$$W^{t+1} = W_{max} - \frac{t}{I} \times (W_{max} - W_{min}) \tag{4}$$

Where:

- $\boldsymbol{W_{max}}$**:** Represents the maximum value the inertia weight will have;
- $\boldsymbol{W_{min}}$**:** Represents the minimum value the inertia weight will have;

So, after the velocity update, the positions are updated taking into account the defined amplitude limits of the antennas, $lwLmts$ and $upLmts$. If the new position exceeds any of the amplitude limits, it is placed in that limit value, and the velocity direction is reversed and reduced. This method promotes exploration around the limits in order to prevent premature or fixed convergence on the limit.

After this, the simulation is carried out with the new position, the SINR values are returned and now the fitness values are calculated.

FITNESS VALUES

The fitness values calculation is a very important step in the algorithm's development, as it represents the parameters used to progress towards the optimal solution. In other words, these objective values are used to compare different possible solutions and chose the best one. So, if they're not representative of the overall network quality, the solution acquired won't be optimal and won't generate a better network state with the desired improvements.

To tackle this, three objective values were created, $Fitval1$, $Fitval2$ and $Fitval3$, one referring to the main user SINR, another for the SINRs of the remaining users in the main sector and the third one for the interfering users SINRs. The fitness value of the main user is its base SINR value returned from the simulation in dB, (5).

$$FitVal1 = Main\ User\ SINR\ [\mathrm{dB}] \tag{5}$$

As for the objective value of the remaining users in the main sector and interfering one, a new formula was created, (6).

$$FitVal2 = a \times \bar{X}(SINRs) + m \times M(SINRs) + s \times \rho(SINRs)\ [\mathrm{dB}] \quad (6)$$

Where $\bar{X}$ is the average calculation from the set of SINRs, M is the median, and ρ is the standard deviation. The formula applies independently to the remaining two groups of users and is the sum of three parts, each with its associated weight.

- SINRs Average: The average SINR provides a measure of the average signal quality experienced by users in the network. It considers both the strength of the desired signal and the level of interference and noise. Calculating the average SINR gives insights into the overall QoS experienced by users across the network.
- SINRs Median: The median represents the middle value in a sorted list of SINRs. It is less sensitive to outliers compared to the mean (average) and provides a robust measure of central tendency. The median can be particularly useful if there are extreme values or outliers in the SINR distribution that might skew the average SINR.
- SINRs Standard Deviation: Analysing the distribution of SINR values provides insights into the variability and dispersion of signal quality across users. The standard deviation quantifies the spread of SINR values around the mean or median, indicating the level of variability in signal quality. A higher standard deviation suggests greater variability in SINR values, which may impact user experience and network performance consistency.

The mathematical formulas for the average, median (odd and even) and standard deviation are in equations (7), (8.1) and (8.2) and (9), respectively.

$$\bar{X} = \frac{\sum_{i=1}^{n} x_i}{n} \quad (7)$$

Where:

- x_i: Represents each individual value in the dataset;
- n: Represents the total number of values in the dataset;

$$M\ (odd\ n) = x_{\left(\frac{n+1}{2}\right)} \quad (8.1)$$

$$M\ (even\ n) = \frac{x_{\left(\frac{n}{2}\right)} + x_{\left(\frac{n}{2}+1\right)}}{2} \tag{8.2}$$

Where:

- $\boldsymbol{x_{(i)}}$**:** Represents the i^{th} value when the dataset is sorted;
- $\boldsymbol{n}$**:** Represents the total number of values in the dataset;

$$\rho = \sqrt{\frac{\sum_{i=1}^{n}(x_i - \bar{X})^2}{n}} \tag{9}$$

Where:

- $\boldsymbol{x_i}$**:** Represents each individual value in the dataset;
- $\boldsymbol{\bar{X}}$**:** Represents the mean of the dataset;
- $\boldsymbol{n}$**:** Represents the total number of values in the dataset;

These fitness values were created with two purposes: one is evaluating the main users experience directly by its SINR value; and the other to create a parameter capable of reflecting the overall network quality from both the other main sector users and the interfering ones.

When it comes to the weight's distribution, the average and median (a and m) where both attributed with positive values and the standard deviation (s) with negative. The SINRs average weight was set with 60 %, the median with 40 %, and the standard deviation with -20 %.

The average SINR represents the overall signal quality experienced by users in the network. Assigning a relatively high weight to the average SINR reflects its significance in assessing the general performance and throughput of the network. Maximizing the average SINR aligns with the objective of improving the main user's SINR and enhancing overall network quality.

The median complements the mean as it provides a robust measure of central tendency that is less affected by outliers or extreme values. By allocating a substantial weight to the SINRs median, it's ensured that the network's performance is not overly influenced by outlier scenarios or fluctuations in SINR values. Maintaining a satisfactory median SINR contributes to the stability and reliability of user experience across the network.

The negative weight assigned to the standard deviation implies penalizing higher variability among SINR values. A negative weight for the standard deviation reflects the objective of minimizing variability and promoting stability in SINR across users. By subtracting the standard deviation, the optimisation process actively works to mitigate fluctuations in SINR values that may lead to inconsistent user experiences or degraded network performance.

By distributing weights in this manner, improvements in the main user's SINR is prioritized while actively working to minimize variability and ensure consistent SINR levels across the network. The negative weight assigned to the standard deviation reflects a deliberate effort to promote network stability and reliability in the optimisation objectives.

As with any optimisation approach, it is essential to assess the impact of weight distributions on network performance and user experience through simulation experiments and sensitivity analyses. Adjusting these weights based on each particular scenario may be needed to fine-tune the optimisation process and achieve desired network performance outcomes. The established weights of 60 %, 40 % and -20 % where implemented in order to start the algorithm with a good base line, but adjustments may be done to better improve results and algorithm convergence speed.

GLOBAL AND PERSONAL BEST UPDATES

Returning to the architecture, after calculating the objective values, the centre of the algorithm's logic starts, which is the updating of the personal and global best variables, Figure 3.9.

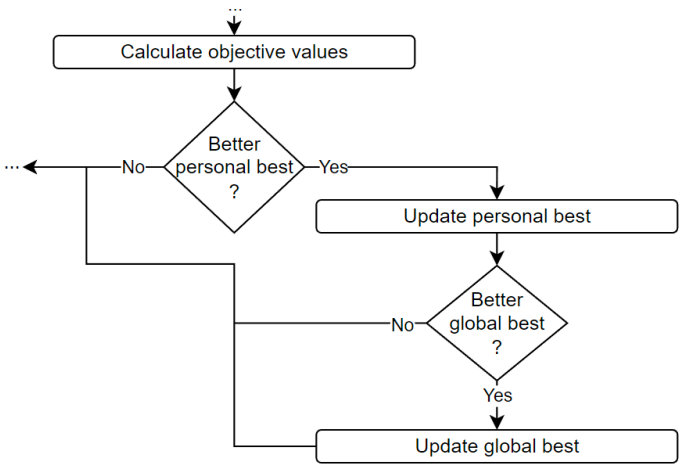

Figure 3.9 - Personal and global best updates from the main loop architecture

Both these updates follow the same logic and are divided into two distinct phases. The first is setting a state where both the other main site users and interfering one's fitness values are above or equal the defined threshold. As for the second, it will try to improve the main user SINR, while keeping the rest above the thresholds, or even try to improve them if possible.

The first phase is further divided into two separate logics. At the outset, achieving the interfering user's fitness value threshold is prioritised; therefore, any solution that produces a higher interfering users fitness value is considered better. However, if the interfering user's objective value does not improve in the current iteration, and only remains the same, an assessment is made to determine whether the objective value of the other main site users has improved. This method promotes faster convergence in the direction where both threshold values are reached, at which point the phase concludes.

In the second stage, it is subdivided into three logics. The first, considers a better solution if the main user fitness value is improved, while the others remain above their respective threshold. The second one, prioritises enhancing the interfering user's fitness value if the following conditions are met: the main user objective value does not improve in the current iteration, and only remains the same; and the other main site user's fitness value is still above the threshold. Regarding the final one, its logic is opposite from the previous: if the main one remains the same, the interfering one is above the threshold and the other main site user's fitness value improves, it is considered a better solution.

As a result, by dividing the updates into these two phases, and giving priority to reaching the minimum thresholds, the entire network converges to a stable state faster. Only after this, it attempts to improve the main user and, if possible, also the remaining ones.

3.4.4. STOP CONDITIONS

In conclusion, the algorithm incorporates three stopping conditions, which are outlined in Table 3.2: the maximum number of iterations, the maximum runtime, and the maximum number of iterations in which the global best result remains unchanged.

4. Definition and Evaluation of Test Scenarios

Once every component of the architecture has been established and implemented, test scenarios are defined and evaluated. The underlying principle is to generate diverse scenarios that validate and assess the functionality and usability of the algorithm across several user distributions.

Five distinct scenarios, each with its own significance and goals, were created in order to evaluate the algorithm capabilities. Starting with a base-line deployment, users are distributed into small groups in a dispersed fashion to replicate a “real” group distribution. The second scenario aims to simulate user groups that are in close proximity to each other in both sectors, such as those found on a train or bus. In a similar fashion, the third one maintains this illustration, but positions users in the interfering site so as to cause interference in the primary sector. In the final two scenarios, a combination of the user distributions from the first and third scenarios will be deployed to generate two distinct variations as a means of evaluating the effects.

As a general rule in all scenarios, the base sector positions will be 0 and 90 degrees for the main and interfering sector bearing, and 0 degrees for both downtilt angles. The base results, from which the comparisons will be made with the algorithms final results, are extracted in conjunction with the SINR radio environment map (REM). Additionally, all tests will be executed with ten users, spread as described above.

Thus, by using the pre-established scenarios, it becomes feasible to examine various user’s distributions, by studying the interference management among sectors it generates, and the effects of each constant and weight defined in Chapter 3. Finally, to ensure that the proposed initialisation establishes a correlation between the two sectors and provides a nearly optimal starting point, as a final comparison and testing step, a final scenario will be executed using a base PSO with random initialisation, similar to the one described in Section 2.4.

4.1. Base-Line Scenario

The first scenario, as mentioned above, will position the users in small groups scattered across the sectors, to create a base-line scenario to test the algorithms interference management. As Figure 4.1 and Figure 4.2 depict, ten users are deployed and the antennas initial positions are 30 º and -90 º for the main and interfering bearing

angles, and 0º for both downtilt angles. In addition, the SINR REM is provided to aid in the verification of the various users' SINRs across the sites.

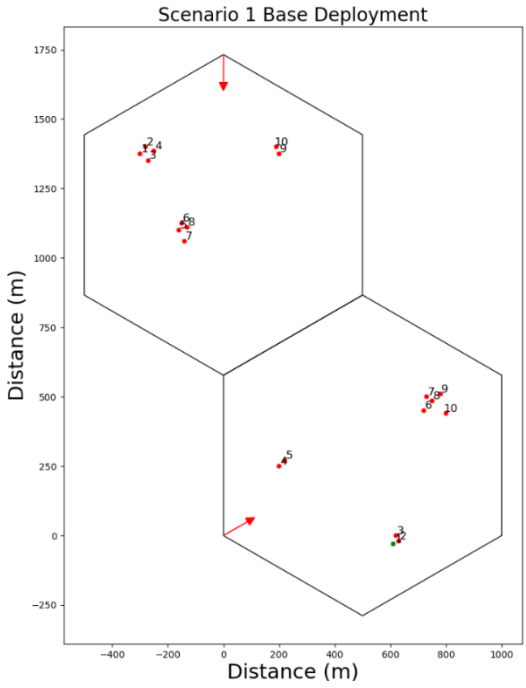

Figure 4.1 - Base-line scenario: Base antennas positions

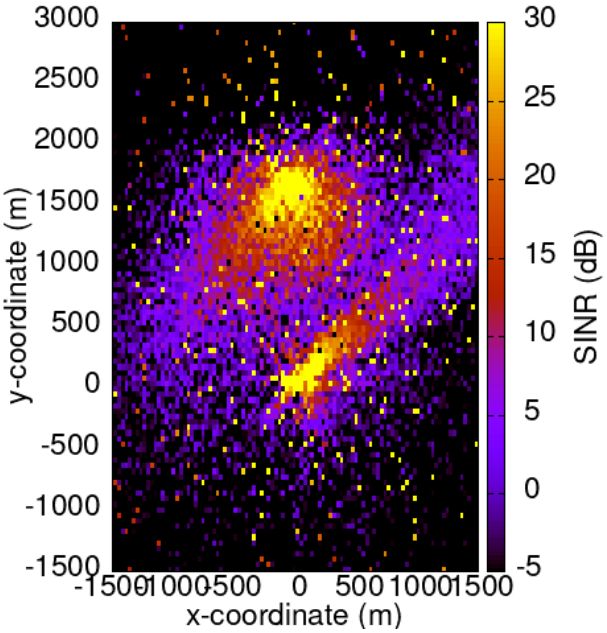

Figure 4.2 - Base antennas REM

Table 4.1 and Table 4.2 show the scenario's base objective values and users SINRs.

Table 4.1 - Base-line scenario: Initial objective values

	Objective Values [dB]
Main UE	10.8
Other UEs	13.2
Interfering UEs	15.2

Table 4.2 - Base-line scenario: Initial UEs SINR values

	SINR values [dB]	
-	**Main Sector**	**Interfering Sector**
UE 1	10.8	18.6
UE 2	1.9	11.1
UE 3	8.4	11.0
UE 4	21.1	12.8
UE 5	20.6	11.8
UE 6	11.7	15.4
UE 7	11.7	23.2
UE 8	15.2	19.5
UE 9	16.9	16.6
UE 10	16.3	21.6

The base scenario results show expected values, when considering the user distribution in conjunction with Figure 4.2 REM, where main site users 2 and 3 have the worst signal quality while the interfering sector presents good SINR values.

First Test

To start the result acquisition and subsequent analysis, the algorithm was initially executed with only five particles and stopping conditions to allow it to run until all the iterations were finished. An important detail in the selected base parameters, are the constants C_1 and C_2, which were given the weights of 0.35 and 0.65, respectively. This wight distribution guides the swarm towards the global best, since the initial correlation made between the two spaces provides a global best position already directed towards the optimum. The base parameters of the algorithm were therefore defined as presented in Table 4.3.

Table 4.3 - Base-line scenario: First test base parameters

Parameter	Value	Unit
n	5	-
W	0.7	%
C_1	0.35	-
C_2	0.65	-
$lwLmts$	[-30, -150, -15, -15]	Degrees
$upLmts$	[90, -30, 0, 0]	Degrees
$fitThr$	[10, 10]	dB
a	0.6	%
m	0.4	%
s	-0.2	%
I	20	-
T	5400	Seconds
S	20	-

After executing the algorithm, the final positions obtained were 45.76 º and -101.19 º for the main and interfering bearing angles, Figure 4.3, and 0 º for both antennas downtilt angles.

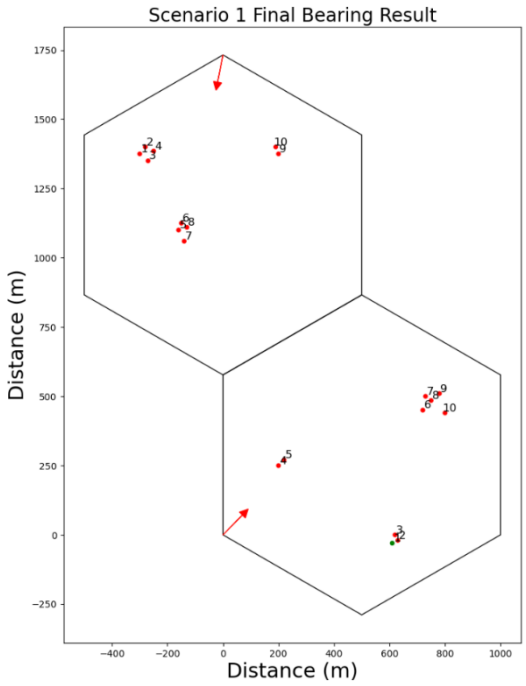

Figure 4.3 - Base-line scenario: First test antennas positions

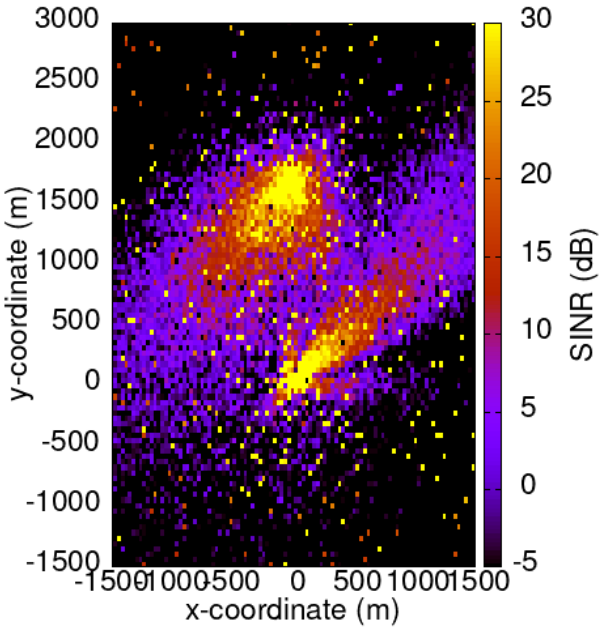

Figure 4.4 - Base-line scenario: First test antennas REM

By analysing the results, the interference between sectors is reduced; as a result, Figure 4.4 depicts a more precise SINR distribution in the map, where the secondary lobes in the primary sector are now visible. In addition, it becomes clear that the interfering sector antenna was relocated towards the outer limits in an attempt to reduce interference, while the primary antenna was repositioned to focus the beam on the region with the largest number of users and uses the side lobe to enhance users 1, 2, and 3.

Table 4.4 - Base-line scenario: First test objective values

	Objective Values [dB]		
-	**Base**	**Result**	**Difference**
Main UE	10.8	12.2	**1.4**
Other UEs	13.2	14.5	**1.3**
Interfering UEs	15.2	14.9	**-0.3**

Table 4.5 - Base-line scenario: First test UEs SINR values

SINR Values [dB]						
	Main Sector			Interfering Sector		
-	Base	Result	Difference	Base	Result	Difference
UE 1	10.8	12.2	1.4	18.6	16.8	-1.8
UE 2	1.9	4.6	2.7	11.1	11.4	0.3
UE 3	8.4	10.7	2.3	11.0	9.9	-1.1
UE 4	21.1	21.8	0.7	12.8	13.7	0.9
UE 5	20.6	20.3	-0.3	11.8	10.6	-1.2
UE 6	11.7	13.3	1.6	15.4	15.6	0.2
UE 7	11.7	13.3	1.6	23.2	22.8	-0.4
UE 8	15.2	16.4	1.2	19.5	18.6	-0.9
UE 9	16.9	16.7	-0.2	16.6	16.0	-0.6
UE 10	16.3	17.5	1.2	21.6	21.1	-0.5
Total	-	-	12.2	-	-	-5.1

Upon initial examination of the objective and SINR values, Table 4.4 and Table 4.5, it becomes apparent that the interfering sector experienced a marginal decrease in value as a result of the emphasis given to improving the primary user. Upon closer inspection, only one interfering user (UE 3) has a SINR value that falls below the specified threshold. Thus, despite the overall decrease in values, 90 % of them remained above the 10 dB threshold, and some even improved.

Now, translating the SINR values acquired to their respective throughput, in this case using the Shannon's capacity formula, (10). It is a fundamental concept in information theory that determines the maximum rate at which information can be reliably transmitted over a communication channel subject to noise. The formula is expressed as [28]:

$$C = B \times \log_2(1 + SINR) \ [bps] \tag{10}$$

Where $\boldsymbol{C}$ is the channel capacity in bps, $\boldsymbol{B}$ is the channels bandwidth in Hz, and $\boldsymbol{SINR}$ the signal-to-noise ratio, in linear value. So, when formula (10) is applied to the values in Table 4.5 over a 100 MHz bandwidth, the result is Table 4.6.

Table 4.6 - Base-line scenario: First test UEs maximum throughput values

Maximum Throughput Values [Mbps]						
	Main Sector			Interfering Sector		
-	Base	Result	Difference	Base	Result	Difference
UE 1	370.3	413.7	**43.4**	619.9	561.1	**-58.8**
UE 2	135.0	195.8	**60.8**	379.5	388.8	**9.3**
UE 3	298.5	367.2	**68.7**	376.4	342.9	**-33.5**
UE 4	701.5	725.1	**23.6**	432.6	461.1	**28.5**
UE 5	686.8	675.7	**-11.2**	401.2	364.2	**-37.0**
UE 6	398.1	448.4	**50.3**	515.7	522.1	**6.5**
UE 7	398.1	448.4	**50.3**	771.4	758.2	**-13.2**
UE 8	509.2	548.1	**38.8**	649.4	619.9	**-29.5**
UE 9	564.3	557.8	**-6.5**	554.6	535.1	**-19.5**
UE 10	544.8	583.9	**39.1**	718.5	702.0	**-16.5**
Total	-	-	**357.4**	-	-	**-163.8**

The estimated maximum throughput values demonstrate substantial enhancements in the main sector, reaching 357 Mbps, whereas the interfering sector experiences a

reduction of almost 164 Mbps. These outcomes represent an equitable allocation of resources that substantially enhances the primary sector while ensuring that the intervening users' values remain above the predetermined threshold.

When evaluating the global best fitness values and positions in each iteration, Figure 4.5 and Figure 4.6, the algorithm's behaviour in each change conforms to the logical principles outlined in Chapter 3.3. The following figures depict these values and their changes along the algorithm's execution.

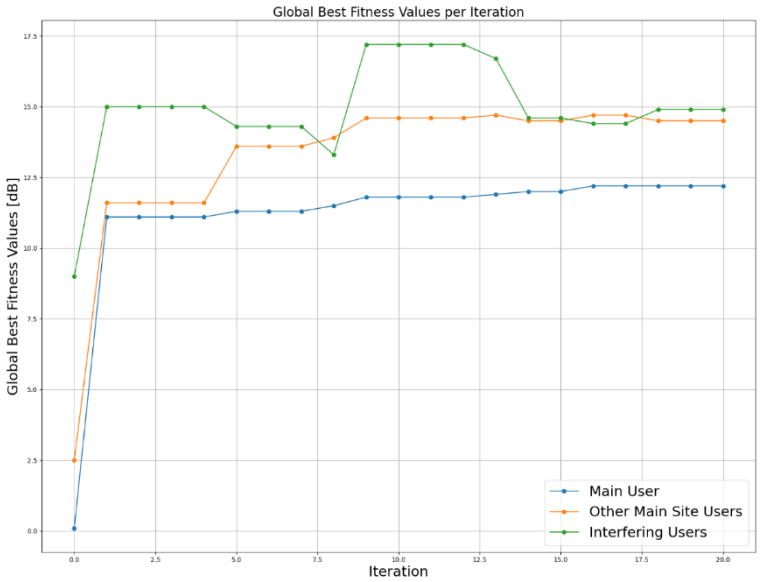

Figure 4.5 - Base-line scenario: First test global best fitness values per iteration

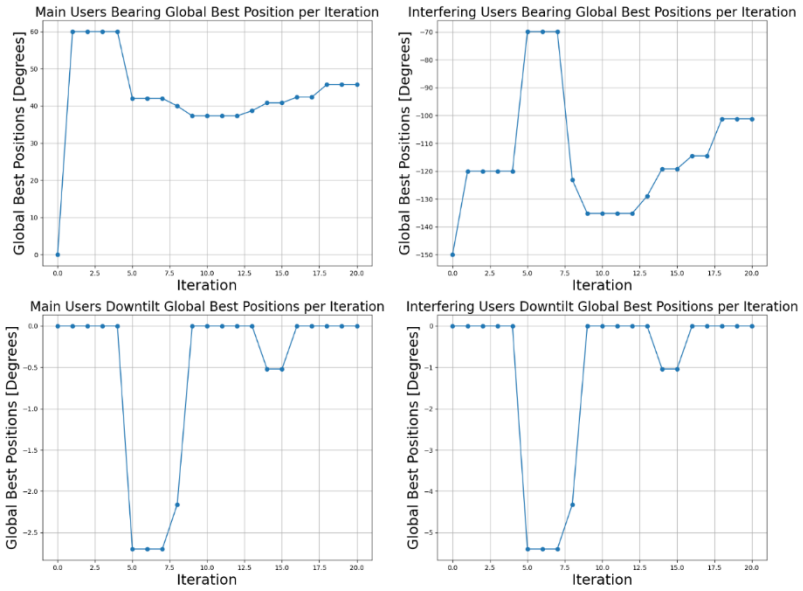

Figure 4.6 - Base-line scenario: First test global best positions per iteration

A state in which the fitness values of both the other main users and the interfering users are above the thresholds of 10 dB is already achieved from initialisation (iteration 0) to iteration 1. This event highlights and reenforces the importance of the proposed initialisation in achieving a good starting point from which the algorithm will find the optimal solution.

The prioritisation of enhancing the primary user, potentially at the cost of the other users, is demonstrated in four points between iterations 4 and 5, 7 and 8, 12 to 13, and 13 to 14. To increase the SINR for the main user, the interfering fitness value was reduced. In contrast, between iterations 8 and 9, a new state was discovered where each fitness value experienced an increase, while the intervening sector also received an enhancement. Ultimately, the final state was attained between iterations 17 and 18, during which the second update phase becomes apparent: while the main user's SINR remained unchanged, the algorithm underwent an update to a new state that featured an improved interfering objective value.

The graphs present in Appendix A display the positions of every particle in each iteration as a concluding representation of the algorithm's path throughout the iterations. Figure A.1 illustrates that, while each particle initially followed an individual path and trajectory, they all ultimately were led towards the same values, which correspond to the optimal solution. In particular, the main bearing position (upper left graph), particle 1 remained in a searching state, separated from the remaining particles.

SECOND TEST

In this second test, the algorithm was executed with ten particles to see and compare the influence that this has in the algorithm progression and final results. Similar to the previous example, the stopping conditions were chosen to let the algorithm run until the final iteration is completed.

Table 4.7 - Base-line scenario: Second test initial parameters

Parameter	Value	Unit
n	10	-
W	0.7	%
C_1	0.35	-
C_2	0.65	-
$lwLmts$	[-30, -150, -15, -15]	Degrees
$upLmts$	[90, -30, 0, 0]	Degrees
$fitThr$	[10, 10]	dB
a	0.6	%
m	0.4	%
s	-0.2	%
I	20	-
T	10000	Seconds
S	20	-

The final positions were 44.15 º and -124.06 º for the main and interfering bearing angles, and 0 º for both the downtilt angles, as shown in Figure 4.7.

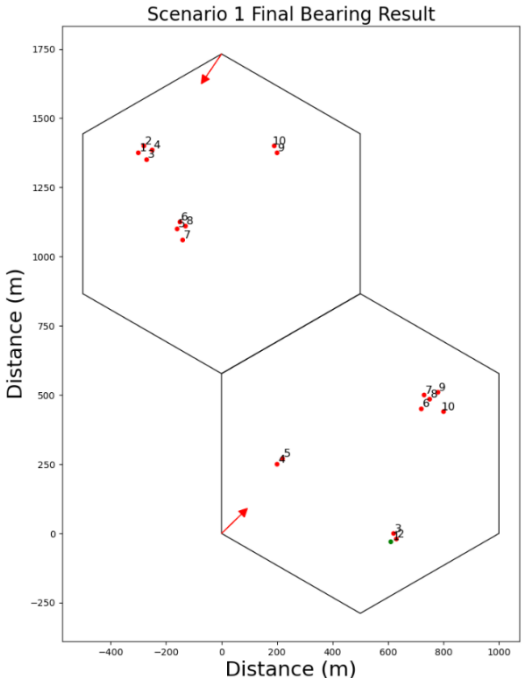

Figure 4.7 - Base-line scenario: Second test antennas positions

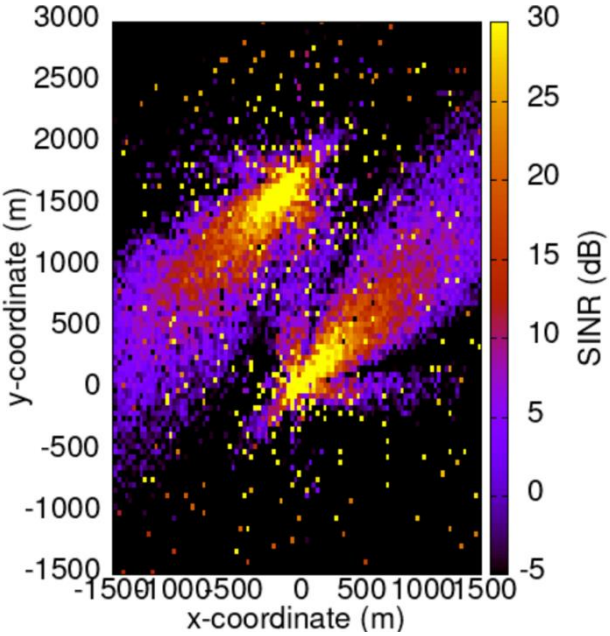

Figure 4.8 - Base-line scenario: Second test antennas REM

The interference between the sectors was further reduced in this execution. Is visible in Figure 4.8 the two secondary lobs from both antennas, as well as a less disturbed interfering antenna SINR dispersion. In a similar way to the previous run, the main antenna was led towards more users to keep the signal quality, while the interfering one was driven away to avoid interference. As for the objective and SINR values, Table 4.8 and Table 4.19 detail the improvements obtained.

Table 4.8 - Base-line scenario: Second test objective values

	Objective Values [dB]		
-	**Base**	**Result**	**Difference**
Main UE	10.8	12.2	**1.4**
Other UEs	13.2	14.7	**1.5**
Interfering UEs	15.2	15.8	**0.6**

Table 4.9 - Base-line scenario: Second test UEs SINR values

SINR Values [dB]						
	Main Sector			Interfering Sector		
-	Base	Result	Difference	Base	Result	Difference
UE 1	10.8	12.2	**1.4**	18.6	19.3	**0.7**
UE 2	1.9	5.0	**3.1**	11.1	12.8	**1.7**
UE 3	8.4	10.6	**2.2**	11.0	12.1	**1.1**
UE 4	21.1	20.4	**-0.7**	12.8	17.1	**4.3**
UE 5	20.6	21.0	**0.4**	11.8	9.0	**-2.8**
UE 6	11.7	13.2	**1.5**	15.4	16.3	**0.9**
UE 7	11.7	13.4	**1.7**	23.2	20.8	**-2.4**
UE 8	15.2	16.7	**1.5**	19.5	16.5	**-3.0**
UE 9	16.9	17.1	**0.2**	16.6	19.5	**2.9**
UE 10	16.3	17.7	**1.4**	21.6	19.4	**-2.2**
Total	**134.6**	**147.3**	**12.7**	**161.6**	**162.8**	**1.2**

The final state acquired shows an overall network improvement with only two users bellow the threshold, main UE 2 and interfering UE 5.

Table 4.10 - Base-line scenario: Second test UEs maximum throughput values

Maximum Throughput Values [Mbps]						
	Main Sector			Interfering Sector		
-	Base	Result	Difference	Base	Result	Difference
UE 1	370.3	413.7	**43.4**	619.9	642.8	**23.0**
UE 2	135.0	205.7	**70.8**	379.5	432.6	**53.1**
UE 3	298.5	364.2	**65.7**	376.4	410.6	**34.1**
UE 4	701.5	679.0	**-22.5**	432.6	570.8	**138.2**
UE 5	686.8	698.7	**11.9**	401.2	316.1	**-85.1**
UE 6	398.1	445.2	**47.1**	515.7	544.8	**29.1**
UE 7	398.1	451.6	**53.5**	771.4	692.2	**-79.2**
UE 8	509.2	557.8	**48.6**	649.4	551.3	**-98.1**
UE 9	564.3	570.8	**6.5**	554.6	649.4	**94.8**
UE 10	544.8	590.4	**45.6**	718.5	646.1	**-72.4**
Total	**4606.7**	**4977.2**	**370.5**	**5419.2**	**5456.7**	**37.5**

Regarding the maximum achievable throughput, Table 4.10, it reflects the aforementioned enhancements, with both sectors exhibiting higher values, with the primary sector being especially notable.

In relation to the global best fitness values and positions in each iteration, the algorithm's behaviour is shown in Figure 4.9 and Figure 4.10.

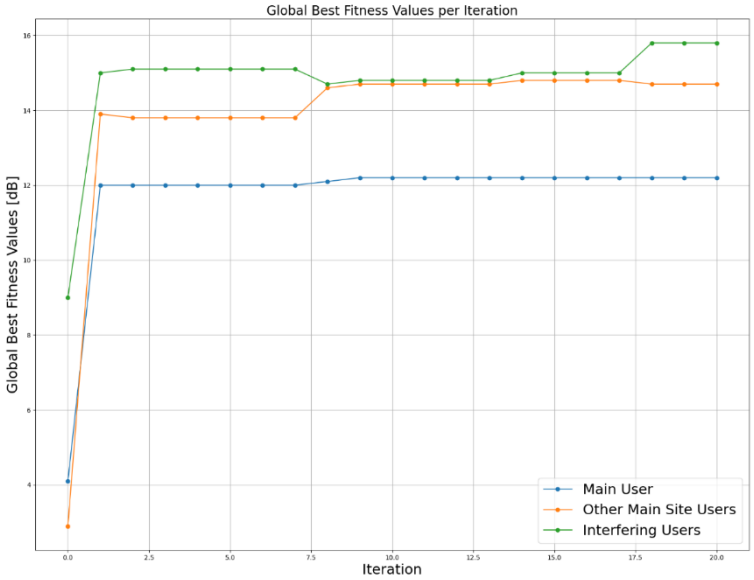

Figure 4.9 - Base-line scenario: Second test global best fitness values per iteration

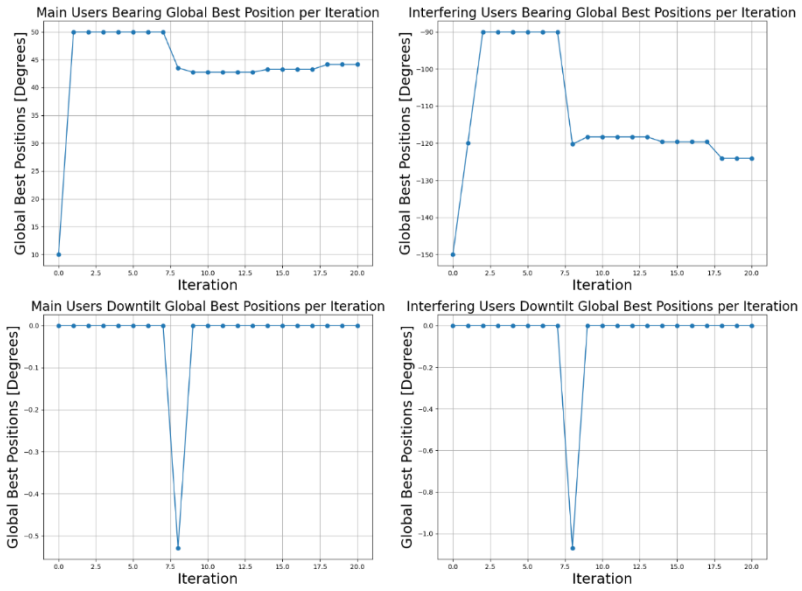

Figure 4.10 - Base-line scenario: Second test global best positions per iteration

Both thresholds are once again satisfied from the initialisation to iteration one, and the swarm subsequently continued to improve. The main user's prioritisation is again noticeable, but only from iteration 6 to 7. In this run the majority of the global best updates were done to improve the other users, as a better main user SINR wasn't found from iteration 10 until the end.

As for the particle's positions in each iteration (Appendix B, Figure B.1), they show a similar behaviour to Figure A.1, where all search the space and ultimately direct towards the optimal solution.

With respect to the variation in the number of particles, increasing this component results in the proposed initialisation achieving an even more optimal position. This will require additional iterations until a better solution is found. Consequently, as the number of particles increases, the positions acquired in the proposed initialisation will be even closer to the optimal. However, it is essential to note that as the number of particles increases, the simulation time increases significantly as well, since a separate simulation is executed for each particle in each iteration. Consequently, these considerations must be incorporated into the process of selecting the base parameters.

In general, the outcomes of the second scenario 1 test demonstrated that the algorithm is effective for this type of deployment, as evidenced by the improved performance and reduced costs of the remaining network devices.

4.2. USERS CLUSTERING SCENARIO

Following with the second scenario, this one will aim to deploy the users in close proximity with each other, simulating a train or bus. Figure 4.11 shows how the ten users are deployed, and the corresponding SINR REM is the same as Figure 4.2.

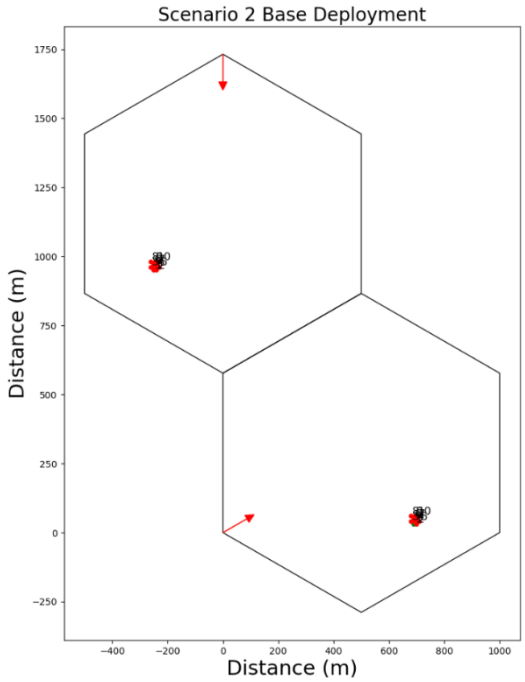

Figure 4.11 - Users clustering scenario: Base antennas positions

Table 4.11 and Table 4.12 present the scenario's base objective values and users SINRs.

Table 4.11 - Users clustering scenario: Initial objective values

	Objective Values [dB]
Main UE	15.5
Other UEs	14.4
Interfering UEs	7.3

Table 4.12 - Users clustering scenario: Initial UEs SINR values

	SINR values [dB]	
-	**Main Sector**	**Interfering Sector**
UE 1	15.5	8.0
UE 2	15.3	7.6
UE 3	15.2	4.3
UE 4	11.7	7.4
UE 5	15.3	11.5
UE 6	14.2	10.3
UE 7	11.7	13.7
UE 8	15.6	5.8
UE 9	15.7	5.4
UE 10	14.6	6.3

Has shown, the signal at the main site is evenly distributed among users with values close to 15 dB, whereas the signal quality in the interfering sector is generally poor, with the objective value falling in half comparing to the main site.

The algorithm's execution will follow the standards and conclusions taken from the previous scenario. Table 4.13 presents the algorithms parameters. The stopping conditions are put to allow a continuous run until all 30 iterations are completed, and the number of particles is placed at ten.

Table 4.13 - Users clustering scenario: Base parameters

Parameter	Value	Unit
n	10	-
W	0.7	%
C_1	0.35	-
C_2	0.65	-
$lwLmts$	[-30, -150, -15, -15]	Degrees
$upLmts$	[90, -30, 0, 0]	Degrees
$fitThr$	[10, 10]	dB
a	0.6	%
m	0.4	%
s	-0.2	%
I	30	-
T	10000	Seconds
S	30	-

The final results are 37.87 º and -133.02 º for the main and interfering bearing angles, and -0.17 º and -0.34 º for the main and interfering downtilt angles, Figure 4.12 and Figure 4.13.

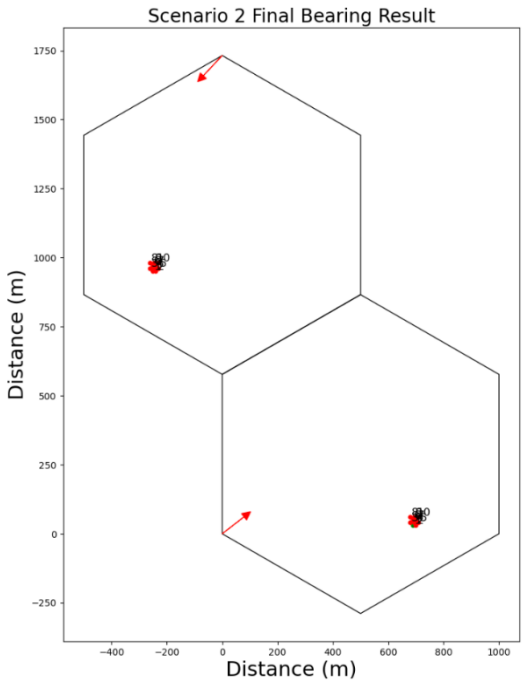

Figure 4.12 - Users clustering scenario: Final antennas positions

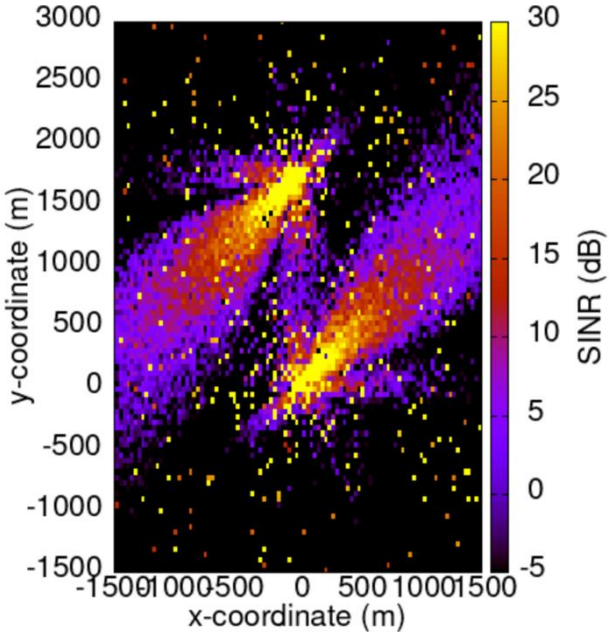

Figure 4.13 - Users clustering scenario: Final antennas REM

The final positions show good interference management between the sites; however, the main sector antenna should be facing the user group for better coherence. To determine why the algorithm avoided the direct path, a test was conducted where the main antenna was placed at around 10 degrees, and the interfering one around -130 degrees, resulting in Figure 4.14.

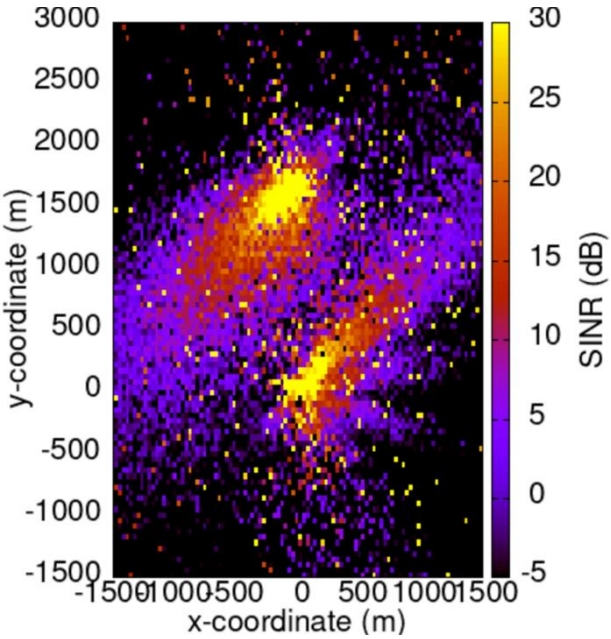

Figure 4.14 - Users clustering scenario: Direct path testing

As the REM map indicates, some antenna movements result in an altered/distorted propagation diagram. This happens because in many modern BS antenna systems, such as those used in 5G networks, the antenna is not physically moving in space as a traditional mechanical antenna. Instead, these antennas are using phased array technology to steer the radiation pattern in different directions. This technology utilizes a grid of individual antenna elements, each with adjustable phase shifters, to steer the beam electronically without the need for mechanical movement. So, when an antenna is moved in certain directions, resulting in a distorted propagation diagram, it's likely happening due to an inappropriate steering process in the electronic phased array. This means that the antenna's radiation pattern is being electronically manipulated to focus the energy on a specific direction but causing distortion or irregularities in the resulting propagation diagram.

Even though the direct path to the user group is compromised by the phased array steering, the algorithm was able to adapt and use a position where the secondary lobe gave a better signal than the base antenna deployment.

Table 4.14 - Users clustering scenario: Final objective values

	Objective Values [dB]		
-	Base	Result	Difference
Main UE	15.5	16.7	1.2
Other UEs	14.4	15.6	1.2
Interfering UEs	7.3	10.8	3.5

Table 4.15 - Users clustering scenario: Final UEs SINR values

	SINR Values [dB]					
	Main Sector			Interfering Sector		
-	Base	Result	Difference	Base	Result	Difference
UE 1	15.5	16.7	1.2	8.0	13.0	5.0
UE 2	15.3	16.5	1.2	7.6	12.4	4.8
UE 3	15.2	16.3	1.1	4.3	6.2	1.9
UE 4	11.7	13.1	1.4	7.4	11.6	4.2
UE 5	15.3	16.5	1.2	11.5	12.5	1.0
UE 6	14.2	15.5	1.3	10.3	13.1	2.8
UE 7	11.7	12.6	0.9	13.7	14.0	0.3
UE 8	15.6	16.8	1.2	5.8	8.4	2.6
UE 9	15.7	16.9	1.2	5.4	7.5	2.1
UE 10	14.6	16.0	1.4	6.3	9.3	3.0
Total	144.8	156.9	12.1	80.3	108.0	27.7

Table 4.16 - Users clustering scenario: Final UEs maximum throughput values

Maximum Throughput Values [Mbps]						
	Main Sector			Interfering Sector		
-	Base	Result	Difference	Base	Result	Difference
UE 1	518.9	557.8	**38.9**	287.0	438.9	**151.9**
UE 2	512.5	551.3	**38.9**	275.6	420.0	**144.4**
UE 3	509.2	544.8	**35.6**	188.4	237.0	**48.6**
UE 4	398.1	442.1	**44.0**	269.9	395.0	**125.1**
UE 5	512.5	551.3	**38.9**	391.9	423.1	**31.2**
UE 6	477.1	518.9	**41.8**	355.0	442.1	**87.0**
UE 7	398.1	426.3	**28.2**	461.1	470.7	**9.6**
UE 8	522.1	561.1	**38.9**	226.4	298.5	**72.2**
UE 9	525.4	564.3	**38.9**	215.9	272.8	**56.8**
UE 10	489.9	535.1	**45.2**	239.7	325.0	**85.3**
Total	**4863.8**	**5253.0**	**389.2**	**2910.9**	**3723.0**	**812.1**

The final results in Table 4.14, Table 4.15 and Table 4.16 reveal a network-wide improvement, but particularly in the interfering sector, where there were previously seven UEs with values below the threshold (10 dB), now there are only four, all with improved values. These outcomes prove that the algorithm doesn't need to sacrifice the interfering sector to improve the main one. It actually prioritizes the achievement of a stable network state, and then, even though it tries to improve the main user, it is also able to improve the interfering sector. The aforementioned claims are substantiated by the global best fitness values and positions graphs behaviours, Figure 4.15 and Figure 4.16.

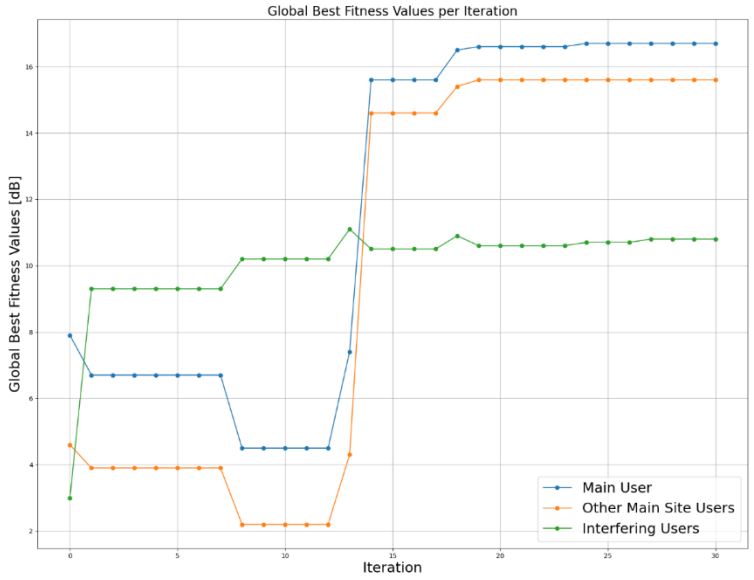

Figure 4.15 - Users clustering scenario: Global best fitness values per iteration

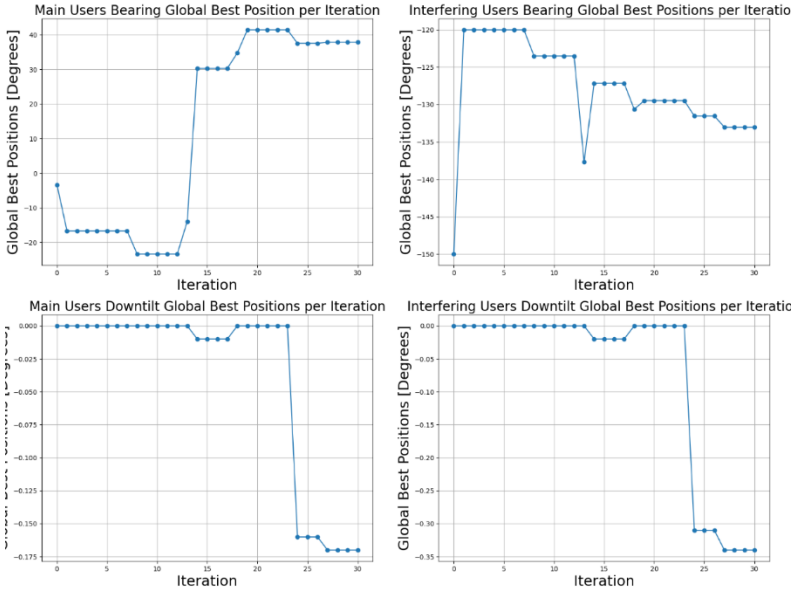

Figure 4.16 - Users clustering scenario: Global best positions per iteration

When comparing to the previous scenario, this user deployment took 14 iterations until an initial stable network state was found, instead of only one. This concludes that, for simpler user distributions, the proposed initialisation is enough to acquire a stable network state and perhaps even better than the base deployment. While for more complex scenarios, it requires a couple more iterations to adapt to the situation and then evolve.

As for the positions in each iteration, Appendix C - Figure C.1, it follows a similar behaviour to the previous executions.

4.3. USERS CLUSTERING INTERFERENCE SCENARIO

The third scenario will follow the basis establish in Section 4.2, where the user deployment will still simulate groups of users in a bus or train but placing them in a situation more susceptible to creating interference. In other words, the main sector users will maintain their positions, while the interfering ones will be positioned in closer proximity to the BS divider, as Figure 4.17 shows.

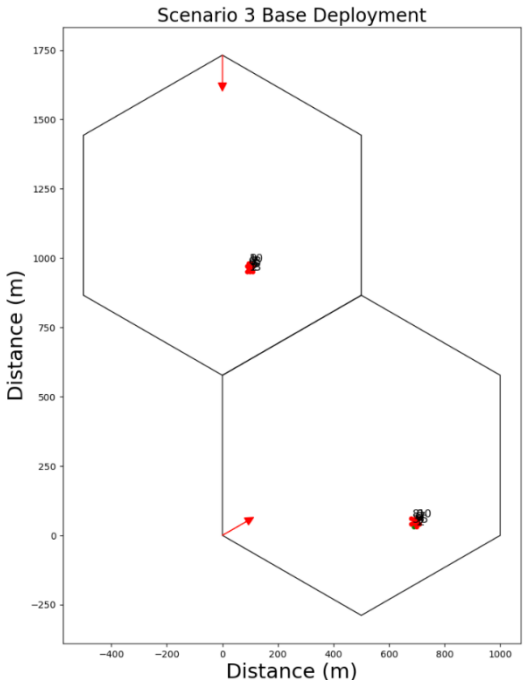

Figure 4.17 - Users clustering interference scenario: Base antennas positions

Table 4.17 and Table 4.18 display the scenario's base objective values and users SINRs.

Table 4.17 - Users clustering interference scenario: Initial objective values

	Objective Values [dB]
Main UE	14.6
Other UEs	13.3
Interfering UEs	9.4

Table 4.18 - Users clustering interference scenario: Initial UEs SINR values

	SINR values [dB]	
-	**Main Sector**	**Interfering Sector**
UE 1	14.6	6.9
UE 2	15.3	12.1
UE 3	13.6	13.1
UE 4	10.1	13.1
UE 5	13.1	8.3
UE 6	15.2	7.2
UE 7	15.4	4.9
UE 8	14.9	14.5
UE 9	13.1	14.2
UE 10	12.7	6.3

The base results for the main site are similar to the ones from Section 4.2, where they have good signal quality and distribution, but the interfering sector has better values than the previous base ones.

Table 4.13 contains the base parameters used in this scenario and it resulted in 37.5 º for the main sector antenna bearing and -130.79 º for the interfering one, Figure 4.18. As for the downtilt angles, both resulted in zero degrees.

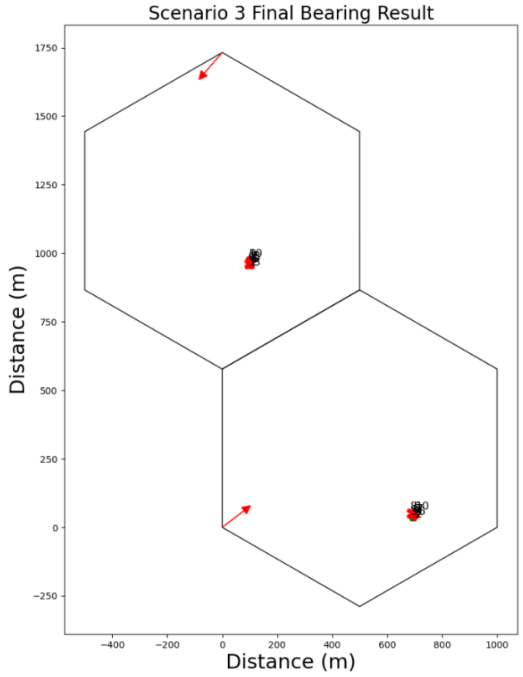

Figure 4.18 - Users clustering interference scenario: Final antennas positions

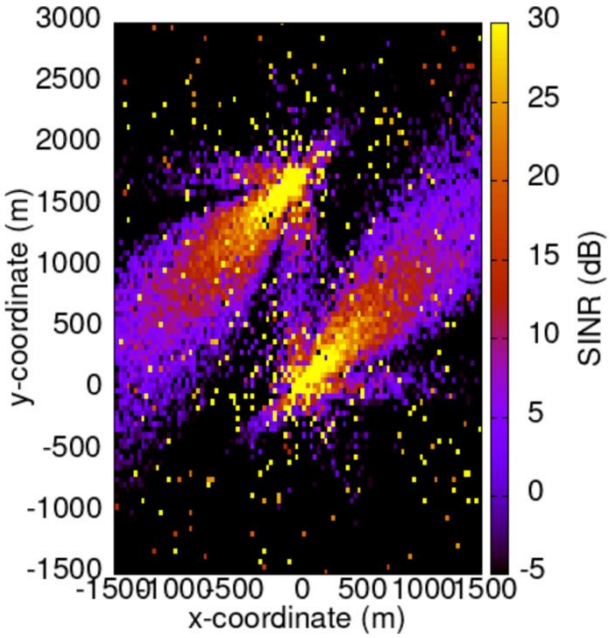

Figure 4.19 - Users clustering interference scenario: Final antennas REM

In the previous run, the main antenna adapted to the distortions in the propagation diagram by using the side lobes. Here the same adaptation was made, and the interfering sector also used its secondary lobe to provide signal and simultaneously avoid interference, as Figure 4.19 illustrates.

Table 4.19 - Users clustering interference scenario: Final objective values

	Objective Values [dB]		
-	Base	Result	Difference
Main UE	14.6	16.8	2.2
Other UEs	13.3	15.6	2.3
Interfering UEs	9.4	10.9	1.5

Table 4.20 - Users clustering interference scenario: Final UEs SINR values

	SINR Values [dB]					
	Main Sector			Interfering Sector		
-	Base	Result	Difference	Base	Result	Difference
UE 1	14.6	16.8	2.2	6.9	9.1	2.2
UE 2	15.3	16.6	1.3	12.1	12.5	0.4
UE 3	13.6	16.4	2.8	13.1	13.2	0.1
UE 4	10.1	12.6	2.5	13.1	11.6	-1.5
UE 5	13.1	16.5	3.4	8.3	12.7	4.4
UE 6	15.2	15.6	0.4	7.2	8.5	1.3
UE 7	15.4	16.1	0.7	4.9	7.8	2.9
UE 8	14.9	16.8	1.9	14.5	13.4	-1.1
UE 9	13.1	17.0	3.9	14.2	14.1	-0.1
UE 10	12.7	13.1	0.4	6.3	6.4	0.1
Total	-	-	19.5	-	-	8.7

Table 4.21 - Users clustering interference scenario: Final UEs maximum throughput values

	Maximum Throughput Values [Mbps]					
	Main Sector			Interfering Sector		
-	Base	Result	Difference	Base	Result	Difference
UE 1	489.9	561.1	71.1	256.0	319.0	63.0
UE 2	512.5	554.6	42.1	410.6	423.1	12.5
UE 3	457.9	548.1	90.1	442.1	445.2	3.2
UE 4	349.0	426.3	77.3	442.1	395.0	-47.1
UE 5	442.1	551.3	109.2	295.6	429.4	133.8
UE 6	509.2	522.1	12.9	264.3	301.4	37.1
UE 7	515.7	538.3	22.7	203.2	281.3	78.0
UE 8	499.6	561.1	61.5	486.7	451.6	-35.1
UE 9	442.1	567.6	125.5	477.1	473.9	-3.2
UE 10	429.4	442.1	12.6	239.7	242.4	2.7
Total	-	-	625.1	-	-	245.0

Table 4.19, Table 4.20 and Table 4.21 feature improvements in both sectors, with slightly higher values than the second scenario, meaning the algorithm is able to avoid interference in more extreme cases.

As illustrated in Figure 4.20 and Figure 4.21, one less iteration was required to attain a stable network state. This is a negligible point, as it could have occurred due to random constants like U_1 or U_2, and it has little to no impact on the overall results.

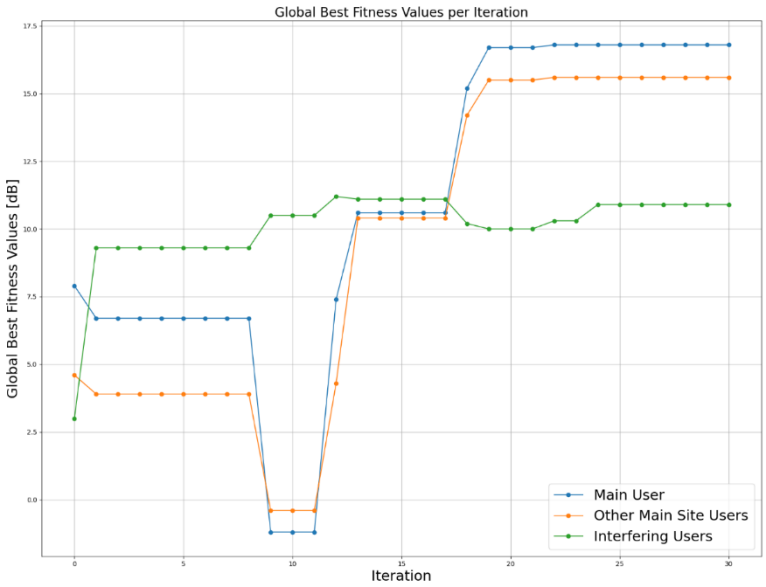

Figure 4.20 - Users clustering interference scenario: Global best fitness values per iteration

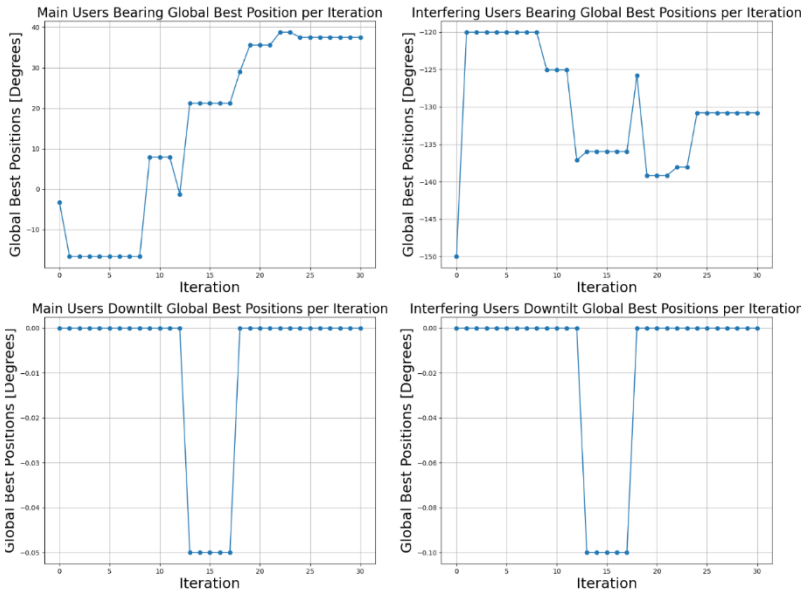

Figure 4.21 - Users clustering interference scenario: Global best positions per iteration

As present in Figure D.1, Appendix D, the particles positions in each iteration start by searching the space around them, and then converge towards the global best value.

4.4. USERS SPREADING AND CLUSTERING SCENARIO

Combining the first and second scenarios, this one simulates the deployment of a dispersed user group in the primary sector and a close group in the interfering sector, Figure 4.22. The developed algorithm will therefore be tested against an additional variation in this scenario.

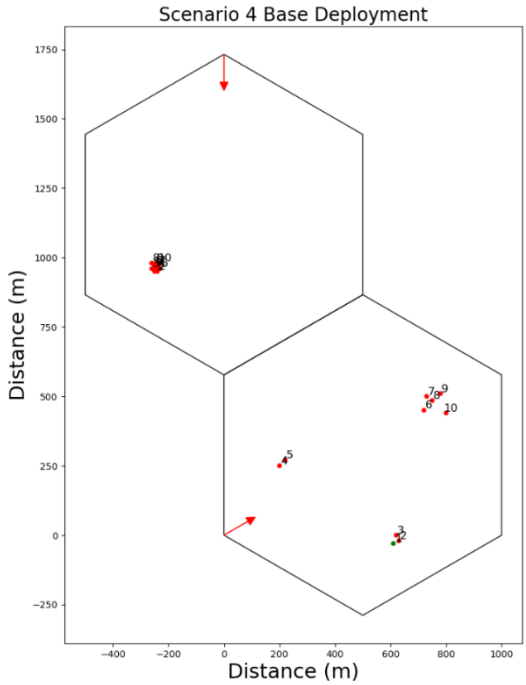

Figure 4.22 - Users spreading and clustering scenario: Base antennas positions

Table 4.22 and Table 4.23 present the scenario's base objective values and users SINRs.

Table 4.22 - Users spreading and clustering scenario: Initial objective values

	Objective Values [dB]
Main UE	9.7
Other UEs	13.8
Interfering UEs	8.5

Table 4.23 - Users spreading and clustering scenario: Initial UEs SINR values

	SINR values [dB]	
-	Main Sector	Interfering Sector
UE 1	9.7	3.3
UE 2	11.2	7.3
UE 3	11.3	7.8
UE 4	20.2	12.6
UE 5	21.1	12.3
UE 6	13.5	9.4
UE 7	12.3	8.9
UE 8	13.9	13.4
UE 9	14.3	3.4
UE 10	16.3	15.4

The base results indicate a favourable signal distribution throughout the main sector, except for the main user. On the other hand, the interfering users exhibit a poor signal distribution with values ranging from 3.3 dB to 15.4 dB.

As Table 4.24 presents, both fitness values thresholds were reduced to 9 dB.

Table 4.24 - Users spreading and clustering scenario: Base parameters

Parameter	Value	Unit
$\boldsymbol{n}$	10	-
$\boldsymbol{W}$	0.7	%
$\boldsymbol{C_1}$	0.35	-
$\boldsymbol{C_2}$	0.65	-
$\boldsymbol{lwLmts}$	[-30, -150, -15, -15]	Degrees
$\boldsymbol{upLmts}$	[90, -30, 0, 0]	Degrees
$\boldsymbol{fitThr}$	[9, 9]	dB
$\boldsymbol{a}$	0.6	%
$\boldsymbol{m}$	0.4	%
$\boldsymbol{s}$	-0.2	%
$\boldsymbol{I}$	30	-
$\boldsymbol{T}$	10000	Seconds
$\boldsymbol{S}$	30	-

This change was made because, in consecutive runs with 10 dB in each one, the algorithm was taking almost the thirty iterations until a base state was achieved. To prevent that and provide a faster convergence, both values were reduced, achieving better results.

The final positions obtained are 43.12 º and -127.93 º for the main and interfering bearing, and -0.14 º and -0.35 º for the downtilt angles, Figure 4.23.

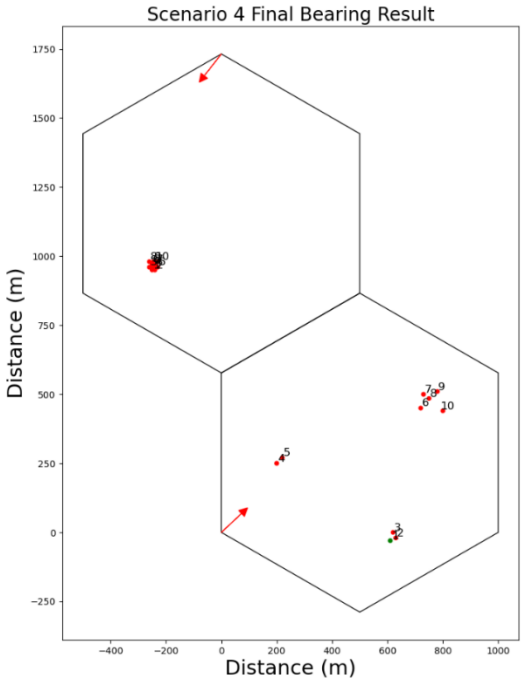

Figure 4.23 - Users spreading and clustering scenario: Final antennas positions

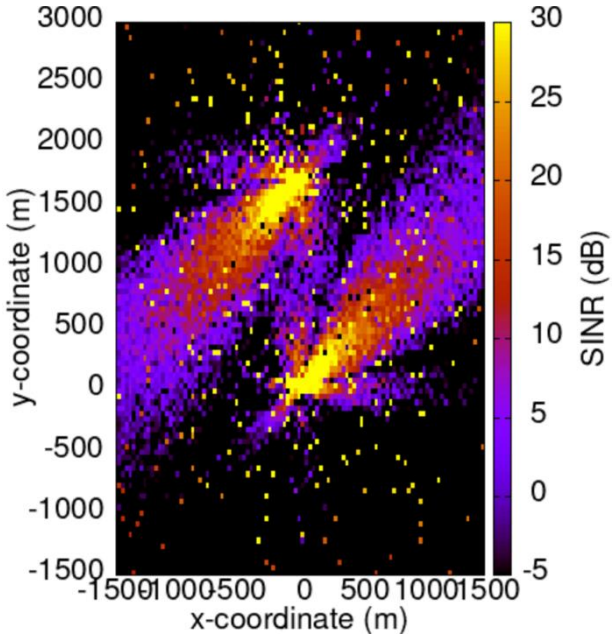

Figure 4.24 - Users spreading and clustering scenario: Final antennas REM

In Figure 4.24, both bearing angles exhibit the behaviours explained in the previous scenarios from where they were based on. The main antenna was led towards more users to keep the signal quality, while the interfering one was driven away to avoid interference.

Table 4.25 - Users spreading and clustering scenario: Final objective values

	Objective Values [dB]		
-	Base	Result	Difference
Main UE	9.7	12.5	2.8
Other UEs	13.8	15.2	1.4
Interfering UEs	8.5	10.0	1.5

Table 4.26 - Users spreading and clustering scenario: Final UEs SINR values

	SINR Values [dB]					
	Main Sector			Interfering Sector		
-	Base	Result	Difference	Base	Result	Difference
UE 1	9.7	12.5	2.8	3.3	6.5	3.2
UE 2	11.2	11.2	0.0	7.3	7.7	0.4
UE 3	11.3	12.8	1.5	7.8	11.0	3.2
UE 4	20.2	21.7	1.5	12.6	14.6	2.0
UE 5	21.1	29.3	8.2	12.3	11.3	-1.0
UE 6	13.5	14.7	1.2	9.4	10.3	0.9
UE 7	12.3	15.2	2.9	8.9	8.6	-0.3
UE 8	13.9	15.2	1.3	13.4	13.8	0.4
UE 9	14.3	14.3	0.0	3.4	6.5	3.1
UE 10	16.3	17.7	1.4	15.4	15.3	-0.1
Total	-	-	20.8	-	-	11.8

Table 4.27 - Users spreading and clustering scenario: Final UEs maximum throughput values

	Maximum Throughput Values [Mbps]					
	Main Sector			Interfering Sector		
-	Base	Result	Difference	Base	Result	Difference
UE 1	336.9	423.1	86.2	165.0	245.1	80.1
UE 2	382.6	382.6	0.0	267.1	278.4	11.3
UE 3	385.7	432.6	46.9	281.3	376.4	95.2
UE 4	672.4	721.8	49.4	426.3	489.9	63.6
UE 5	702.0	973.5	271.5	416.9	385.7	-31.2
UE 6	454.8	493.1	38.4	327.9	355.0	27.1
UE 7	416.9	509.2	92.4	313.1	304.3	-8.8
UE 8	467.5	509.2	41.7	451.6	464.3	12.7
UE 9	480.3	480.3	0.0	167.3	245.1	77.8
UE 10	544.8	590.4	45.6	515.7	512.5	-3.2
Total	-	-	672.0	-	-	324.6

Table 4.25 features an improvement in the interfering fitness value reaching 10 dB. This means that, even though the threshold was 9 dB, the algorithm was able to further improve the signal quality. In addition, is important to note that this example is the first one to contain a main user that was enhanced from bellow 10 dB to almost 13 dB. Table 4.26 and Table 4.27 show the detailed improvements for each user.

As demonstrated in Figure 4.25 and Figure 4.26, the algorithm required a total of 20 iterations to determine a stable network state; however, the outcomes would have likely been better had additional iterations been performed. Other note is that the behaviour continues to follow the logic explained in Chapter 3.3.

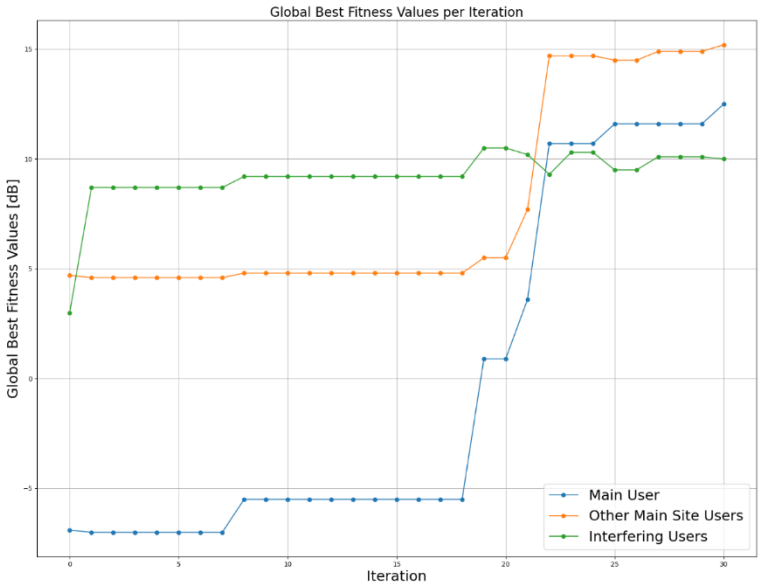

Figure 4.25 - Users spreading and clustering scenario: Global best fitness values per iteration

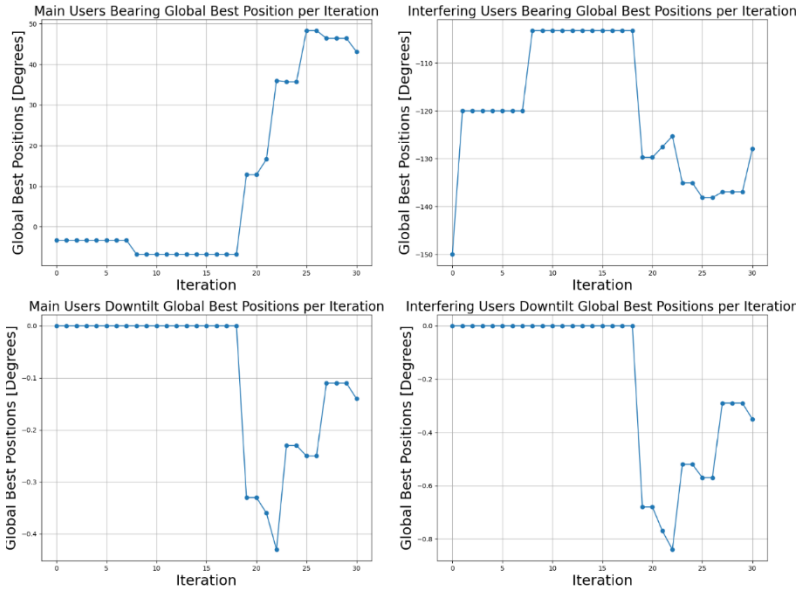

Figure 4.26 - Users spreading and clustering scenario: Global best positions per iteration

With regard to the positions in each iteration, (Appendix E, Figure E.1), their behaviour remains essentially the same from the preceding scenarios.

4.5. USERS CLUSTERING AND SPREADING SCENARIO

As a last scenario, this one will again combine both the first and second one, but spread the users in the interfering sector, and grouping them in the main one, Figure 4.27.

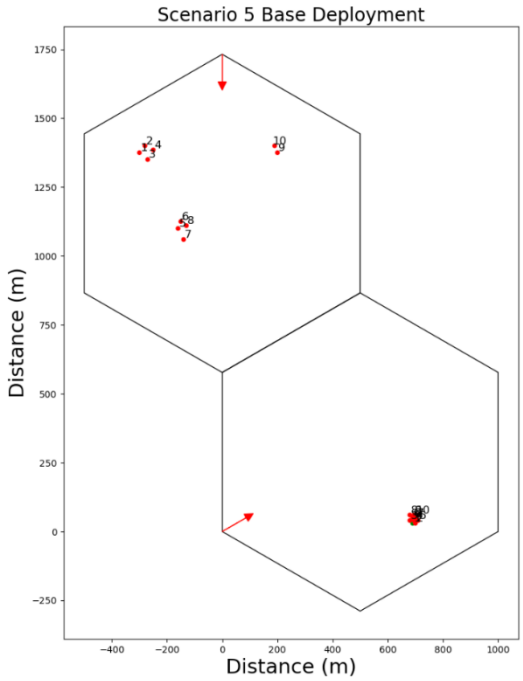

Figure 4.27 - User clustering and spreading scenario: Base antennas positions

Table 4.28 and Table 4.29 detail the base objective values and user SINRs for the scenario at hand.

Table 4.28 - User clustering and spreading scenario: Initial objective values

	Objective Values [dB]
Main UE	15.8
Other UEs	11.3
Interfering UEs	15.6

Table 4.29 - User clustering and spreading scenario: Initial UEs SINR values

	SINR values [dB]	
-	Main Sector	Interfering Sector
UE 1	15.8	19.4
UE 2	16.9	22.8
UE 3	11.0	19.1
UE 4	11.5	10.3
UE 5	9.2	15.2
UE 6	10.0	9.9
UE 7	15.1	21.8
UE 8	6.1	8.1
UE 9	14.9	16.1
UE 10	16.7	18.4

These values display an overall good network quality, except for three users with SINRs below 10 dB.

Table 4.24 represents the same base parameters used in this scenario, due to the same convergence logic explained. The outcome was 38.26 º for the main sector antenna bearing and -101.74 º for the interfering one, Figure 4.28 and Figure 4.29. As for the downtilt angles, -0.25 º for the main and -0.49 º for the interfering one.

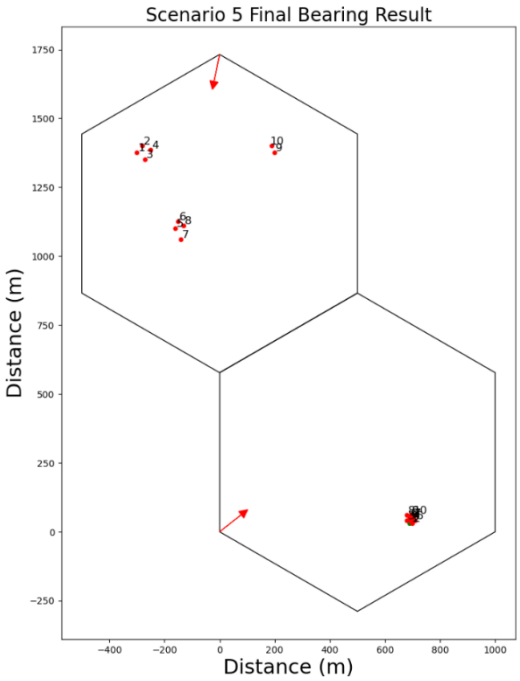

Figure 4.28 - User clustering and spreading scenario: Final antennas positions

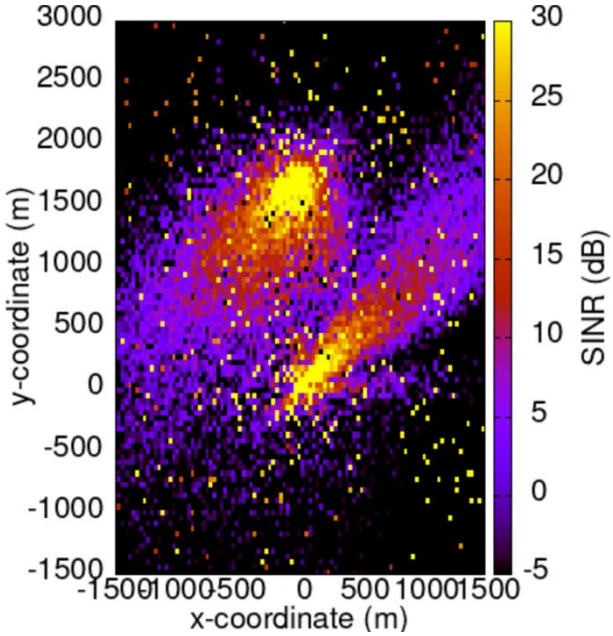

Figure 4.29 - User clustering and spreading scenario: Final antennas REM

Similarly to the previous one, the final bearing angles are close to their other scenarios counterparts. The primary bearing demonstrates a mere 0.39 º of deviation, whereas the interfering bearing exhibits 22.32 º of deviation. These changes pertain to the different distributions encountered in the user deployments. Additionally, as the interfering antenna approaches the outer limit and reduces all usable side lobes, it is expected that the values of UEs 9 and 10 will decrease.

Table 4.30 - User clustering and spreading scenario: Final objective values

	Objective Values [dB]		
-	**Base**	**Result**	**Difference**
Main UE	15.8	18.0	**2.2**
Other UEs	11.3	12.4	**1.1**
Interfering UEs	15.6	15.6	**0.0**

Table 4.31 - User clustering and spreading scenario: Final UEs SINR values

SINR Values [dB]						
	Main Sector			Interfering Sector		
-	Base	Result	Difference	Base	Result	Difference
UE 1	15.8	18.0	**2.2**	19.4	19.5	**0.1**
UE 2	16.9	17.9	**1.0**	22.8	21.1	**-1.7**
UE 3	11.0	12.6	**1.6**	19.1	17.5	**-1.6**
UE 4	11.5	12.1	**0.6**	10.3	18.8	**8.5**
UE 5	9.2	10.9	**1.7**	15.2	17.7	**2.5**
UE 6	10.0	10.8	**0.8**	9.9	10.5	**0.6**
UE 7	15.1	16.0	**0.9**	21.8	21.0	**-0.8**
UE 8	6.1	6.9	**0.8**	8.1	15.3	**7.2**
UE 9	14.9	16.3	**1.4**	16.1	8.7	**-7.4**
UE 10	16.7	16.7	**0.0**	18.4	8.0	**-10.4**
Total	-	-	**11.0**	-	-	**-3.0**

Table 4.32 - User clustering and spreading scenario: Final UEs maximum throughput values

Maximum Throughput Values [Mbps]						
	Main Sector			Interfering Sector		
-	Base	Result	Difference	Base	Result	Difference
UE 1	528.6	600.2	**71.6**	646.1	649.4	**3.3**
UE 2	564.3	596.9	**32.6**	758.2	702.0	**-56.1**
UE 3	376.4	426.3	**49.8**	636.3	583.9	**-52.4**
UE 4	391.9	410.6	**18.7**	355.0	626.4	**271.4**
UE 5	322.0	373.4	**51.4**	509.2	590.4	**81.2**
UE 6	345.9	370.3	**24.4**	342.9	361.1	**18.2**
UE 7	506.0	535.1	**29.1**	725.1	698.7	**-26.4**
UE 8	234.3	256.0	**21.7**	289.9	512.5	**222.6**
UE 9	499.6	544.8	**45.3**	538.3	307.3	**-231.1**
UE 10	557.8	557.8	**0.0**	613.3	287.0	**-326.3**
Total	-	-	**344.5**	-	-	**-95.6**

Through Table 4.30, Table 4.31 and Table 4.32, a unique occurrence emerged that had not occurred previously. Despite the interfering fitness value remaining unchanged, the SINR values of the actual UEs experienced an overall loss of 3 dB. This behaviour was anticipated based on Figure 4.28 and Figure 4.29, as UEs 9 and 10 were operating at the antennas signal limit. However, the fitness value remains representative of the samples due to significant enhancements observed in other UEs and the improved distribution of signal quality across UEs.

From iteration eight onward, the algorithm encountered difficulties in finding better solutions, as illustrated in Figure 4.30 and Figure 4.31. However, it was in iteration eight that a stable network state was achieved, and the results were already better than

the base deployment. This exemplifies a run that could have finished considerably earlier if the maximum number of iterations with the same result, S, had been set to four or five.

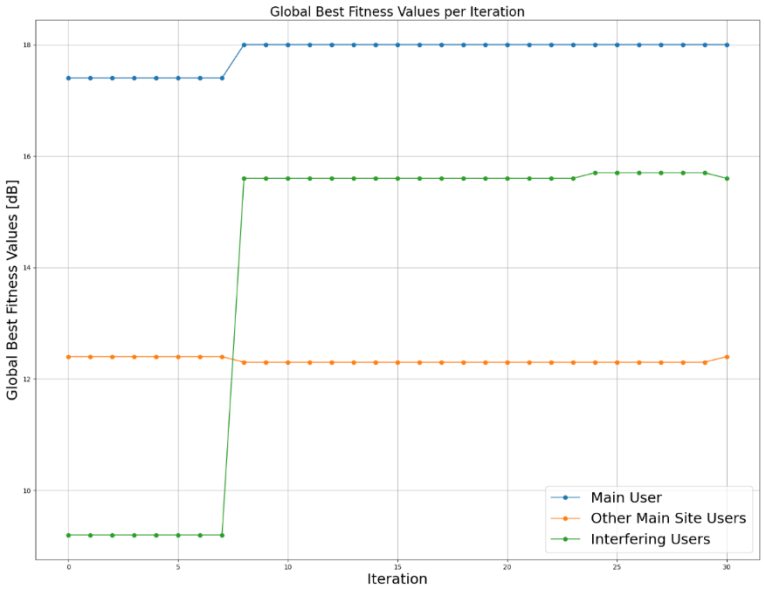

Figure 4.30 - User clustering and spreading scenario: Global best fitness values per iteration

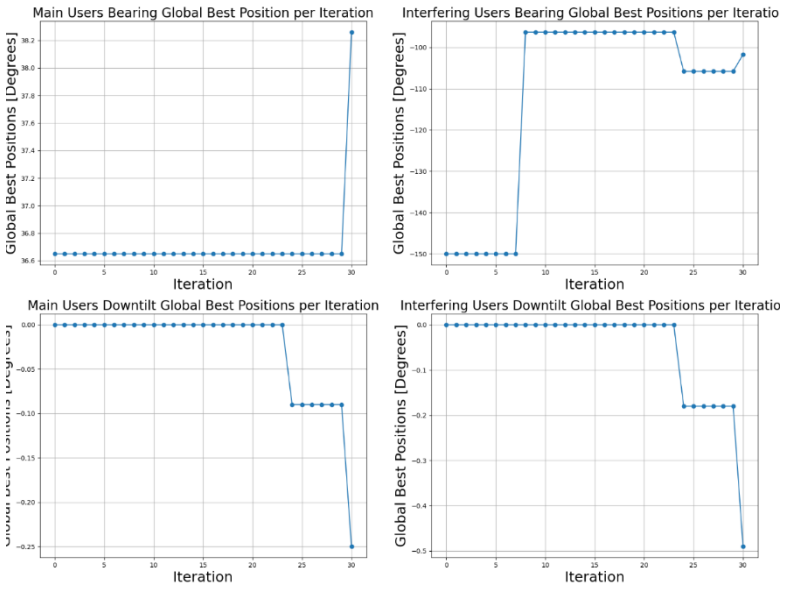

Figure 4.31 - User clustering and spreading scenario: Global best positions per iteration

Just like all the previous scenarios, the particles flow towards the optimal solution acquired, has shown by Figure F.1 (Appendix F).

4.6. BASE PSO

This section compares the previous results with the ones obtained from a base PSO algorithm, in order to ensure that the proposed initialisation establishes a correlation between the two sectors and provides a nearly optimal starting point. For this purpose, the chosen scenario was the third one, where the users are grouped and placed in a way that favours the creation of interference between both sectors. Here, the update logics remain the same as the ones explained in Section 3.3. Since the scenario will be the same as Section 4.3, Figure 4.17 represents the initial antennas positions and user distribution, and Figure 4.2 the base REM. Likewise, the base fitness values and the UEs SINR values are illustrated in Table 4.17 and Table 4.18. Table 4.33 contains the base parameters.

Table 4.33 - Base PSO: Base parameters

Parameter	Value	Unit
n	10	-
W	0.7	%
C_1	0.35	-
C_2	0.65	-
$lwLmts$	[-30, -150, -15, -15]	Degrees
$upLmts$	[90, -30, 0, 0]	Degrees
$fitThr$	[10, 10]	dB
a	0.6	%
m	0.4	%
s	-0.2	%
I	30	-
T	10000	Seconds
S	30	-

After running the algorithm, the final positions were -12.36 º and -131.57 º for the main and interfering bearing angles, as for the downtilt angles, -0.87 º and -0.56 º, Figure 4.32.

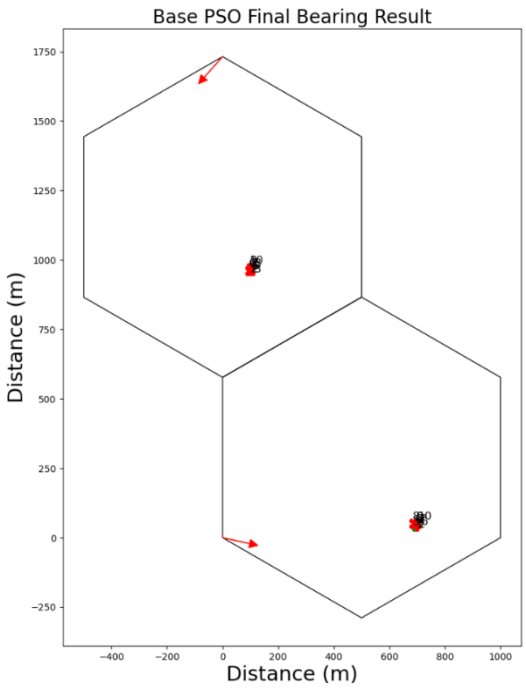

Figure 4.32 - Base PSO: Final antennas positions

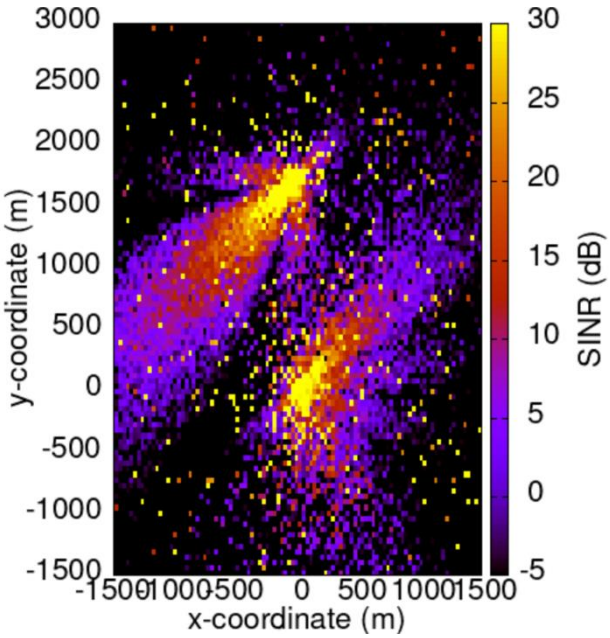

Figure 4.33 - Base PSO: Final antennas REM

By analysing these results, a difference of almost 50 degrees is present between the main bearing angles from proposed architecture and the base PSO. As Figure 4.33 shows, the base PSO wasn´t able to adapt to the antennas steering problems, leading to the results that follow.

Table 4.34 - Base PSO: Final objective values

	Objective Values [dB]		
-	Base	Result	Difference
Main UE	14.6	5.8	-8.8
Other UEs	13.3	3.3	-10.0
Interfering UEs	9.4	10.1	0.7

Table 4.35 - Base PSO: Final UEs SINR values

	SINR Values [dB]					
	Main Sector			Interfering Sector		
-	Base	Result	Difference	Base	Result	Difference
UE 1	14.6	5.8	-8.8	6.9	7.4	0.5
UE 2	15.3	6.7	-8.6	12.1	9.3	-2.8
UE 3	13.6	3.7	-9.9	13.1	8.2	-4.9
UE 4	10.1	2.0	-8.1	13.1	11.1	-2.0
UE 5	13.1	0.4	-12.7	8.3	10.8	2.5
UE 6	15.2	1.3	-13.9	7.2	12.3	5.1
UE 7	15.4	7.3	-8.1	4.9	10.7	5.8
UE 8	14.9	5.4	-9.5	14.5	11.0	-3.5
UE 9	13.1	6.5	-6.6	14.2	8.2	-6.0
UE 10	12.7	1.5	-11.2	6.3	12.8	6.5
Total	-	-	-97.4	-	-	1.2

Table 4.36 - Base PSO: Final UEs maximum throughput values

	Maximum Throughput Values [Mbps]					
	Main Sector			Interfering Sector		
-	Base	Result	Difference	Base	Result	Difference
UE 1	489.9	226.4	-263.6	256.0	269.9	13.9
UE 2	512.5	250.5	-261.9	410.6	325.0	-85.6
UE 3	457.9	174.2	-283.8	442.1	292.7	-149.3
UE 4	349.0	137.0	-212.0	442.1	379.5	-62.6
UE 5	442.1	106.8	-335.3	295.6	370.3	74.7
UE 6	509.2	123.2	-386.0	264.3	416.9	152.5
UE 7	515.7	267.1	-248.5	203.2	367.2	164.0
UE 8	499.6	215.9	-283.6	486.7	376.4	-110.3
UE 9	442.1	245.1	-197.0	477.1	292.7	-184.4
UE 10	429.4	127.1	-302.4	239.7	432.6	192.9
Total	-	-	-2774.1	-	-	5.9

Table 4.34, Table 4.35 and Table 4.36 feature major downgrades in the main sector, especially in the main user, and mixed results in the interfering site. As the main goal is to enhance the main user, while keeping the rest with satisfactory levels, the algorithm completely failed, not even being able to reach a stable network state.

This shows that, without the proposed initialisation, a base PSO algorithm isn't able to adapt to network issues, or even correlate the sectors to at least find a stable direction to move towards.

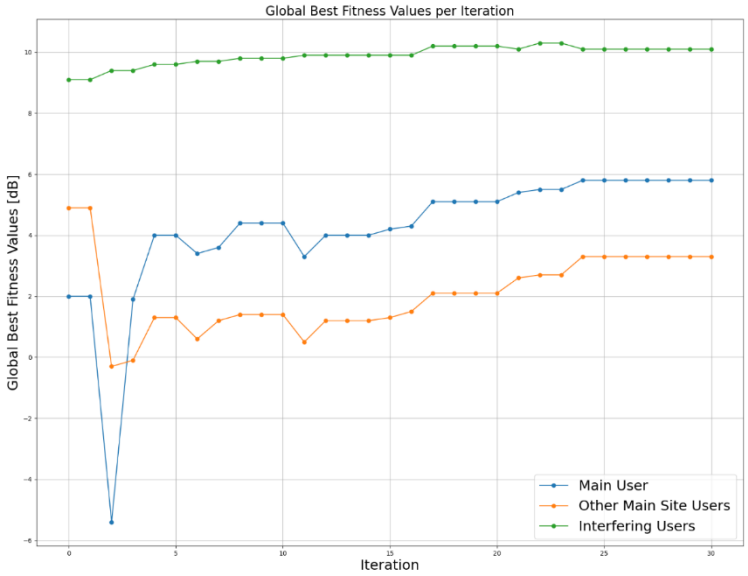

Figure 4.34 - Base PSO: Global best fitness values per iteration

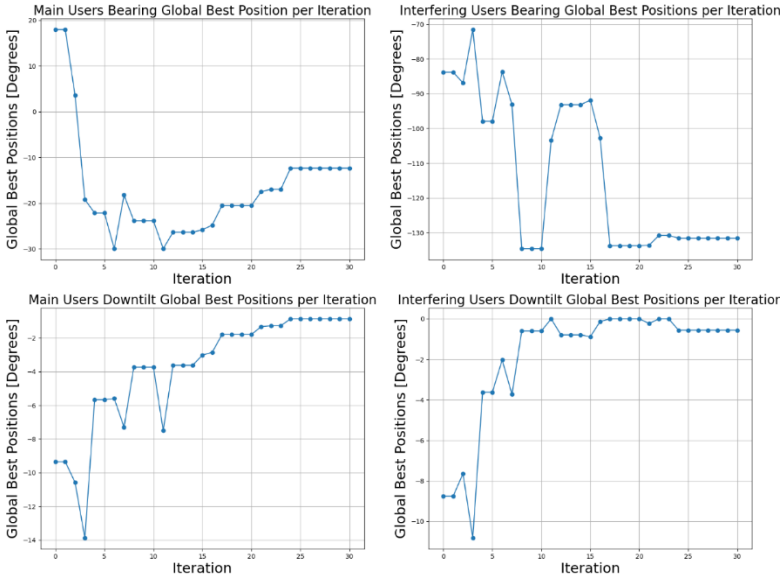

Figure 4.35 - Base PSO: Global best positions per iteration

Even though the acquired results aren't ideal, the algorithms progression in Figure 4.34 and Figure 4.35 show incrementing updates in the fitness values. This shows that a generic PSO requires a significantly greater number of iterations to achieve good results when comparing to the architecture that has been proposed.

At last, by analysing the positions in each iteration (Appendix G, Figure G.1), the particles movement was led to the global best to early, not giving enough time for them to search around the space. So, the base PSO algorithm would benefit from different weight distributions in C_1 and C_2. A more balanced distribution would lead to a broader search and consequently, better results. However, some executions were done where the initial random positions were placed in a small area, not allowing for a complete search.

4.7. RESULTS ASSESSMENT

The outcomes of testing and evaluating every scenario led to the formation of conclusions concerning the 5G network and the algorithm itself. Starting with an overall assessment, the algorithm showed very good interference management capabilities, as well as the expected behaviour based on the architecture described in Chapter 3.3.

In more specific results, the proposed initialisation has shown to be very useful. In simpler cases, it's enough to achieve a stable network state, or even improve from the base line deployment. When tackling more complex cases, it establishes a direction upon which the particles should be guided towards. This implies that the suggested initialisation is adequate for achieving a stable network state, or even superior, in the case of simple user distributions. However, in the case of more intricate scenarios, it requires additional iterations to adjust and then evolve.

In relation to the particle's movement, they start by exploring they're own vicinities around the solution space. It was apparent that, as the algorithm evolved, they were increasingly oriented towards the swarm's global best. This occurs as a result of the 0.35 and 0.65 weights assigned to the constants C_1 and C_2, respectively. The weight distribution outlined relies on the proposed initialisation in order to establish an initial correlation between the two search spaces and obtain a generally favourable path for the particles to follow. In the absence of this initialisation, the particles might be prematurely guided to a global best due to the accelerated convergence in an initial direction caused by the weight distribution; consequently, they might not have sufficient iterations to adjust their trajectory and reach the optimal solution.

With respect to the variation in the number of particles, it was determined that increasing this parameter led to the proposed initialisation acquiring a more optimal position to guide the particles. This increment will require additional computing resources, as well as simulation time. Therefore, certain factors must be taken into

account when determining the optimal quantity of particles, in addition to other fundamental parameters that impact these aspects as well.

The algorithm is also able to adapt to some challenges proposed by the network itself, like the user deployment in more interference favourable locations, and also the antennas steering disruptions. As the REM maps showed, some antenna movements resulted in an altered propagation diagram. This happened due to the antenna not being physically moved in space, but rather using phased array technologies to steer itself. So, when an antenna is moved to focus its energy in certain directions, it results in a distorted propagation with irregularities and, consequently, in bad signal throughput for the UEs. Despite these challenges, the algorithm was able to adapt and produce very good outcomes. Rather than following the direct path towards the UEs, the algorithm identified a trajectory in which the antennas could use their secondary lobes to provide the primary signal while simultaneously avoiding interference.

Concerning the primary objectives set, the algorithm developed should focus on enhancing the main user signal, but without sacrificing the other users or sectors. In retrospect, the algorithm architecture proposed demonstrated remarkable efficacy in enhancing the primary user signal and without the need to sacrifice the remaining users or the interfering sector. Additionally, the algorithm not only was able to improve the main user signal quality, but also the other main site users and interfering ones. The results show that the algorithm architecture actually prioritizes the achievement of a stable network state where all the defined thresholds are met, and only then, even though it tries to improve the main user, it is also able to improve the interfering sector and consequently the overall network.

To illustrate the benefits of the proposed architecture, a standard PSO algorithm was tested against it. The results showed major downgrades in the main sector, especially in the main user, and mixed results in the interfering site. Since the main goal is to enhance the main user, while keeping the rest with satisfactory levels, the base algorithm failed, not even being able to reach a stable network state. This proves that without the proposed initialisation a base PSO cannot adapt to network challenges or either correlate the sectors to get a stable direction to move towards. As previously mentioned, the results would be improved if certain parameters were altered or adapted; nevertheless, a significant number of additional iterations would be required in comparison to the proposed algorithm. So, through this comparison, the developed work was validated, given that the basic algorithm was unable to achieve the primary goals established, or even display any improvements.

One point worth detailing regarding the algorithm's development is its execution time. The code is in a serial loop, where each particle only executes its code when the previous one finishes, which causes the time per iteration to be high and consequently the total simulation time.

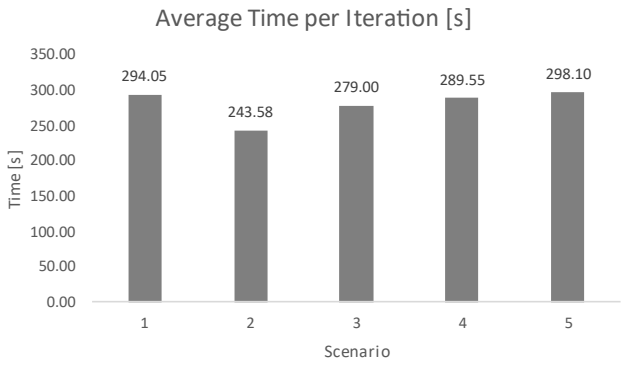

Figure 4.36 - Average time per iteration in seconds

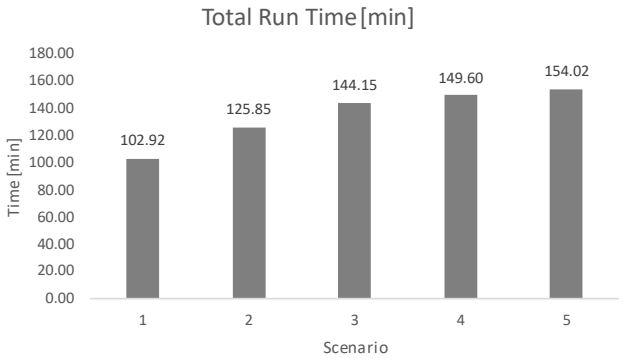

Figure 4.37 - Total run time in minutes

Figure 4.36 illustrates the average time per iteration, and the value is gathered after the algorithm goes through every particle and checks the stopping criteria. Additionally, in each particle, a network simulation is performed to acquire the necessary values for the algorithm to progress. This factor, in conjunction with the code being in a serial loop, makes the time per iteration around 290 seconds, which is very high. As for Figure 4.37, it represents the total execution time with 20 iterations for the first scenario and 30 for the rest, with 10 users. Each run took at least 2 hours to be completed in scenarios with 30 iterations.

These times, however, could be greatly reduced if a thread system was implemented. A thread would be created for each particle and, when they all finished simulating the network and calculate the fitness values, the best global variables would be updated, and the algorithm proceeded to the next iteration. With this, the average time per iteration

would be roughly divided by the number of particles and, consequently, the total run time. A recent study [26] examined this approach, in which it was suggested that threads could be used as particles to oversee local resources, while thread synchronisation and multithreading systems are implemented to manage global resources and facilitate data exchange among particles. An additional approach that can be employed to achieve even better efficiency is to streamline the network simulation. If the NS-3 code was further simplified to simulate only the strictly necessary, it could reduce a couple of seconds in each call. A few seconds per execution may not seem enough, but if only 5 seconds could be reduced per call, considering that a simulation is done for each particle in every iteration, an improvement of 50 seconds per iteration results in 1500 seconds (25 minutes) per run. Due to the intricate nature of a network simulation, this code reduction must be implemented with caution and only in areas where the results remain applicable to the current case study.

In summary, the developed work not only produced results that are precisely aligned with the proposed goals, but also yielded supplementary outcomes that showcased different capabilities for addressing network challenges and enhancing the network performance as a whole.

5. CONCLUSION AND FUTURE WORK

In cellular mobile networks, users' throughput should always be increased to carry out their intended network actions. This can arise from multiple reasons, whether a user is in a location that is hard to reach by the radio network, has high levels of interference, or even a special case in which a specific user needs this improvement. Any of these situations could lead to a call dropping, a reduction in the bit rate, or an incomplete data exchange, all of which could have a negative impact on the user experience. This thesis presented an AI solution that uses a PSO algorithm to make the required corrections and decisions to improve user throughput, while maintaining satisfactory service levels for the remaining users.

A chapter was devoted to providing a comprehensive outline of 5G technology, encompassing subjects like BS cooperation and different types of AI applications. Then, a detailed breakdown of every component in a base PSO algorithm was performed to facilitate its future implementation. Finally, an evaluation was conducted of the existing 5G network simulators, and the NS-3 was selected. The subsequent chapter documented the novel architecture that was suggested to maximise the throughput for a single user, while ensuring satisfactory levels for the remainder of the network. This sector encompassed both the conceptual design and practical implementation aspects, as well as the changes made relative to a base PSO algorithm. Finally, a multitude of test scenarios were designed and evaluated, encompassing both basic and complex user deployment configurations, to determine the effectiveness of the proposed approach. In these tests there were some limitations regarding the execution of the algorithm and network simulations, namely the number of particles, base stations and users. These restrictions arose due to the computational resources required to perform all the described tasks, in relation to the time required to complete each execution. Despite these limitations, the outcomes obtained through experiments and simulations have shown great promise. By implementing the suggested PSO-based optimisation method, the network throughput, QoS, and interference management were all significantly improved. In particular, the algorithm exhibited superior performance compared to baseline PSO approaches in various test scenarios, thereby demonstrating its efficacy in improving network performance and resource allocation.

As stated in the results assessment, the algorithm effectively mitigated interference and enhanced the overall network quality. The suggested initialisation method also demonstrated its utility, as it was enough to achieve a stable network state in simpler

scenarios and even achieve better results than the base deployment. When more intricate scenarios were used, the initialisation found a trajectory for the particles to follow towards an optimal solution. Furthermore, the algorithm demonstrated adaptability in the face of challenges introduced by the network simulation, such as disruptions caused by the antennas' steering and different user deployments. In such instances, the algorithm effectively adapted and, in some cases, even used the secondary lobes to maintain signal transmission and improve user throughput. When running a base PSO algorithm in the same intricate scenarios, results showed that the basic algorithm fails to achieve a stable network state even after thirty iterations. This demonstrated that the algorithm created in this thesis was more efficient, led to greater results, and ultimately better optimisation, as it was able to achieve SINR improvements up to 28.9 % and a throughput enhancement of 25.6 %.

With respect to its future implementation, the project exhibits numerous opportunities for extra development. With the objective of expanding and strengthening the proposed architecture, the intention is to continue with the work that has already been established. More specifically, reducing the execution time should be the first design goal. As mentioned earlier, the primary drawback of the developed work is the long period of time required to complete a simulation; this can be significantly mitigated through the implementation of a thread system. Inserting complexity in the simulation would constitute an additional future development. One possible approach is to incorporate obstacles such as terrain or buildings, increase the number of users, or simulate various environmental conditions such as rain, snow, or storms. It is crucial to recognise that execution of these modifications leads to an escalation of both the algorithm complexity and simulation time. A ML algorithm could be implemented in conjunction with the developed work as a crucial final future development, since these simulations/optimizations cannot be done in real time. In the beginning, the system would execute multiple benchmark tests to build datasets to create ML models that can be used in real time. Subsequently, in the event of a real-time scenario, the system would be equipped with historical data pertaining to the appropriate course of action. Moreover, the complexity of the algorithm could be increased even further by incorporating additional parameters, such as new network or antenna properties.

BIBLIOGRAPHY

[1] 5G Americas. "Becoming 5G Advanced: The 3GPP 2025 Roadmap" [Online]. (2022). Available: https://www.5gamericas.org/wp-content/uploads/2022/12/Becoming-5G-Advanced-the-3GPP-2025-Roadmap-InDesign.pdf

[2] X. Lin, "An Overview of 5G Advanced Evolution in 3GPP Release 18", in IEEE Communications Standards Magazine, vol. 6, no. 3, pp. 77-83, September 2022, doi: 10.1109/MCOMSTD.0001.2200001.

[3] Betanet. (n.d.). "The Role of Mobile Edge Computing in the 5G Era." [Online]. Available: https://betanet.net/view-post/the-role-of-mobile-edge-computing-in-the

[4] 3GPP. 3GPP TS 22.261: Service requirements for next generation new services and markets (Release 16). (2020). Retrieved from http://www.3gpp.org/

[5] 3GPP. 3GPP TR 21.917: Technical specification group services and system aspects; Release 17 work item description; (Release 17). (2021). Retrieved from http://www.3gpp.org/

[6] 3GPP. 3GPP TR 21.918: Technical specification group services and system aspects; Release 18 work item description; (Release 18). (2022). Retrieved from http://www.3gpp.org/

[7] Liu, Y., Zhou, S., Niu, Z., & Nallanathan, A. (2018). A survey of radio resource allocation in cognitive radio networks: approaches and challenges. IEEE Access, 6, 5754-5769.

[8] A. Mughees, M. Tahir, M. A. Sheikh and A. Ahad, "Towards Energy Efficient 5G Networks Using Machine Learning: Taxonomy, Research Challenges, and Future Research Directions", in IEEE Access, vol. 8, pp. 187498-187522, 2020, doi: 10.1109/ACCESS.2020.3029903.

[9] M. Osama, S. Ramly and B. Abdelhamid, “Binary PSO with Classification Trees Algorithm for Enhancing Power Efficiency in 5G Networks”, 2022, doi: 10.3390/s22218570.

[10] N. Zhao, Y. -C. Liang, D. Niyato, Y. Pei, M. Wu and Y. Jiang, "Deep Reinforcement Learning for User Association and Resource Allocation in Heterogeneous Cellular Networks", in IEEE Transactions on Wireless Communications, vol. 18, no. 11, pp. 5141-5152, Nov. 2019, doi: 10.1109/TWC.2019.2933417.

[11] S. Waleed, I. Ullah, W. Khan, A. Rehman, T. Rahman and S. Li, “Resource Allocation of 5G Network by Exploiting Particle Swarm Optimisation”, in Iran J Comput Sci 4, pp. 211–219, 2021, doi: 10.1007/s42044-021-00091-5.

[12] G. Du, L. Wang, Q. Liao and H. Hu, "Deep Neural Network Based Cell Sleeping Control and Beamforming Optimisation in Cloud-RAN", 2019 IEEE 90th Vehicular Technology Conference (VTC2019-Fall), Honolulu, HI, USA, 2019, pp. 1-5, doi: 10.1109/VTCFall.2019.8891410.

[13] K. Lu, S. Wu and H. Yang, "Optimized design pattern matrix of PDMA based on binary particle swarm optimisation for 5G", 2020 IEEE 19th International Conference on Cognitive Informatics & Cognitive Computing (ICCI*CC), Beijing, China, 2020, pp. 220-224, doi: 10.1109/ICCICC50026.2020.9450225.

[14] A. El-Hajj, W. Saad, and M. Debbah, "Particle Swarm Optimisation-based Resource Allocation in 5G Ultra-Dense Networks," IEEE Transactions on Wireless Communications, vol. 16, no. 3, pp. 1651-1665, 2017.

[15] Y. Liu, Z. Zhang, and K. Xu, "Joint Base Station Clustering and Beamforming Optimisation for Green 5G Networks Using Particle Swarm Optimisation," IEEE Transactions on Vehicular Technology, vol. 67, no. 8, pp. 7297-7310, 2018.

[16] S. R. Al-Rubaye, A. M. Al-Jumaili, and S. M. R. Iravani, "Energy-Aware Base Station Placement Optimisation for 5G Networks Using Particle Swarm Optimisation," IEEE Access, vol. 8, pp. 190780-190789, 2020.

[17] NS-3 Consortium. NS-3 Network Simulator. [Online]. (2022). Available: https://www.nsnam.org/
[18] OMNet++ Community. OMNet++ Discrete Event Simulation Framework. [Online]. (2022). Available: https://omnetpp.org/
[19] MathWorks. MATLAB Simulation Environment. [Online]. (2022). Available: https://www.mathworks.com/products/matlab.html
[20] M. Kowsalya, T. Srinivasan, K. Kim and I. -H. Ra, "Optimizing Network Slicing Through Neural Network and Particle Swarm Optimisation," 2023 Innovations in Power and Advanced Computing Technologies (i-PACT), Kuala Lumpur, Malaysia, 2023, pp. 1-6, doi: 10.1109/i-PACT58649.2023.10434782.
[21] O. Alluhaibi, M. Nair, A. Hazzaa, A. Mihbarey and J. Wang, "3D Beamforming for 5G Millimeter Wave Systems Using Singular Value Decomposition and Particle Swarm Optimisation Approaches," 2018 International Conference on Information and Communication Technology Convergence (ICTC), Jeju, Korea (South), 2018, pp. 15-19, doi: 10.1109/ICTC.2018.8539578.
[22] S. B. Behera and D. D. Seth, "Resource allocation for cognitive radio network using particle swarm optimisation," 2015 2nd International Conference on Electronics and Communication Systems (ICECS), Coimbatore, India, 2015, pp. 665-667, doi: 10.1109/ECS.2015.7124992.
[23] D. Ghosh and B. S. H, "Synergistic Optimisation of 5G Networks: Integrating Genetic Algorithms and Particle Swarm Optimisation for Enhanced Energy Efficiency and Network Performance," 2023 IEEE North Karnataka Subsection Flagship International Conference (NKCon), Belagavi, India, 2023, pp. 1-6, doi: 10.1109/NKCon59507.2023.10396185.
[24] M. F. Archi and D. Gunawan, "Initial Access in 5G mmWave Communication using Hybrid Genetic Algorithm and Particle Swarm Optimisation," 2020 3rd International Seminar on Research of Information Technology and Intelligent Systems (ISRITI), Yogyakarta, Indonesia, 2020, pp. 182-186, doi: 10.1109/ISRITI51436.2020.9315331.
[25] T. M. Shami, D. Grace and A. Burr, "Load Balancing and Control Using Particle Swarm Optimisation in 5G Heterogeneous Networks," 2018 European Conference on Networks and Communications (EuCNC), Ljubljana, Slovenia, 2018, pp. 1-9, doi: 10.1109/EuCNC.2018.8442519
[26] S. Thongkrairat and V. Chutchavong, "A Time Improvement PSO Base Algorithm Using Multithread Programming," 2019 4th International Conference on Communication and Information Systems (ICCIS), Wuhan, China, 2019, pp. 212-216, doi: 10.1109/ICCIS49662.2019.00044.
[27] S. Prabha. "An Introduction to Particle Swarm Optimisation Algorithm." Analytics Vidhya. [Online]. (2021, October 5). Available: https://www.analyticsvidhya.com/blog/2021/10/an-introduction-to-particle-swarm-optimisation-algorithm/
[28] GeeksforGeeks. (n.d.). "Shannon Capacity." GeeksforGeeks. [Online]. Available: https://www.geeksforgeeks.org/shannon-capacity/
[29] Ericsson. "5G evolution toward 5G advanced." Ericsson Technology Review, Ericsson, 25 Jan. 2023. Available: https://www.ericsson.com/en/reports-and-papers/ericsson-technology-review/articles/5g-evolution-toward-5g-advanced
[30] R. Eberhart and J. Kennedy, "A new optimizer using particle swarm theory," MHS'95. Proceedings of the Sixth International Symposium on Micro Machine and Human Science, Nagoya, Japan, 1995, pp. 39-43, doi: 10.1109/MHS.1995.494215.
[31] Y. Shi and R. Eberhart, "A modified particle swarm optimizer," 1998 IEEE International Conference on Evolutionary Computation Proceedings. IEEE World Congress on Computational Intelligence (Cat. No.98TH8360), Anchorage, AK, USA, 1998, pp. 69-73, doi: 10.1109/ICEC.1998.699146.

[32] J. Kennedy and R. Eberhart, "Particle swarm optimization," Proceedings of ICNN'95 - International Conference on Neural Networks, Perth, WA, Australia, 1995, pp. 1942-1948 vol.4, doi: 10.1109/ICNN.1995.488968.

[33] F. van den Bergh and A. P. Engelbrecht. 2001. Effects of swarm size on Cooperative Particle Swarm Optimisers. In Proceedings of the 3rd Annual Conference on Genetic and Evolutionary Computation (GECCO'01). Morgan Kaufmann Publishers Inc., San Francisco, CA, USA, 892–899.

[34] A. B. Author and C. D. Author, "Recent approaches to global optimization problems through Particle Swarm Optimization," Journal Name, vol. X, no. Y, pp. Z-Z, Month Year. [Online]. Available: https://www.researchgate.net/publication/228746170_Recent_approaches_to_global_optimization_problems_through_Particle_Swarm_Optimization

[35] Xiaohui Hu and R. C. Eberhart, "Adaptive particle swarm optimization: detection and response to dynamic systems," Proceedings of the 2002 Congress on Evolutionary Computation. CEC'02 (Cat. No.02TH8600), Honolulu, HI, USA, 2002, pp. 1666-1670 vol.2, doi: 10.1109/CEC.2002.1004492.

[36] M. Clerc and J. Kennedy, "The particle swarm - explosion, stability, and convergence in a multidimensional complex space," in IEEE Transactions on Evolutionary Computation, vol. 6, no. 1, pp. 58-73, Feb. 2002, doi: 10.1109/4235.985692.

APPENDIX

Appendix A - Base-Line Scenario First Test Results

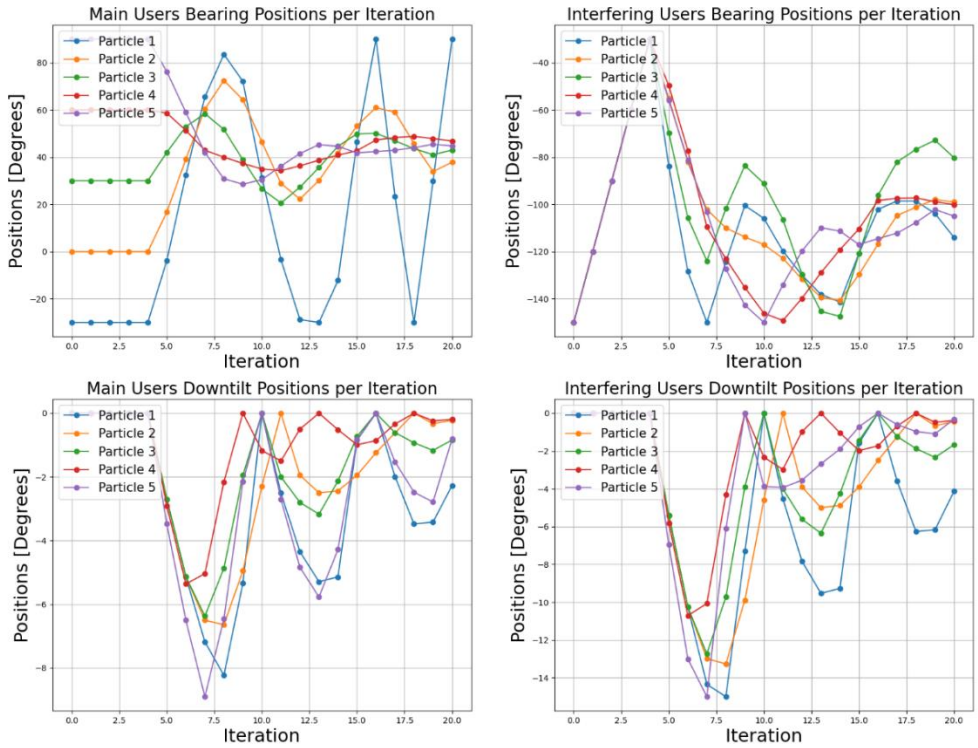

Figure A.1 - Section 4.1 base-line scenario (first test): Positions per iteration

Appendix B - Base-Line Scenario Second Test Results

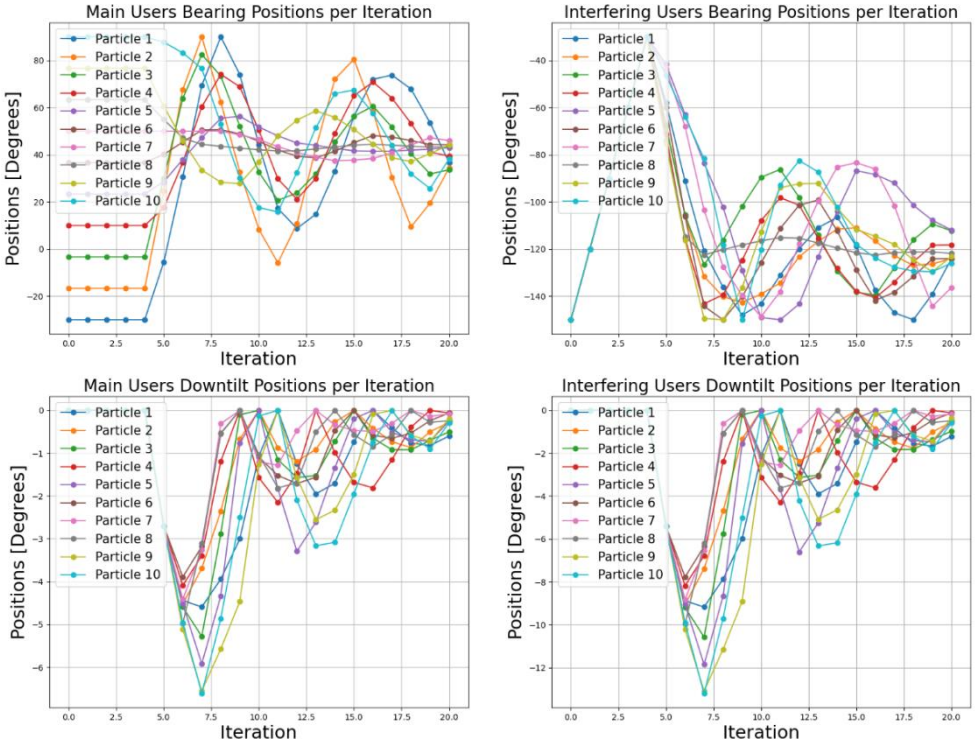

Figure B.1 - Section 4.1 base-line scenario (second test): Positions per iteration

Appendix C - Users Clustering Scenario Results

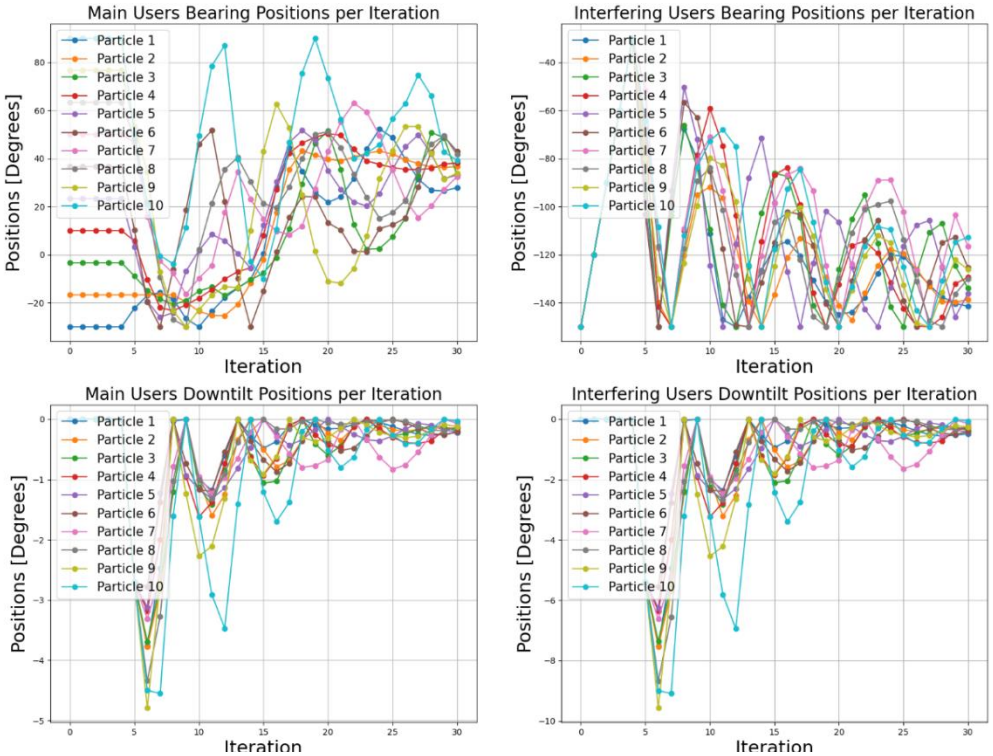

Figure C.1 - Section 4.2 users clustering scenario: Positions per iteration

Appendix D - Users Clustering Interference Scenario Results

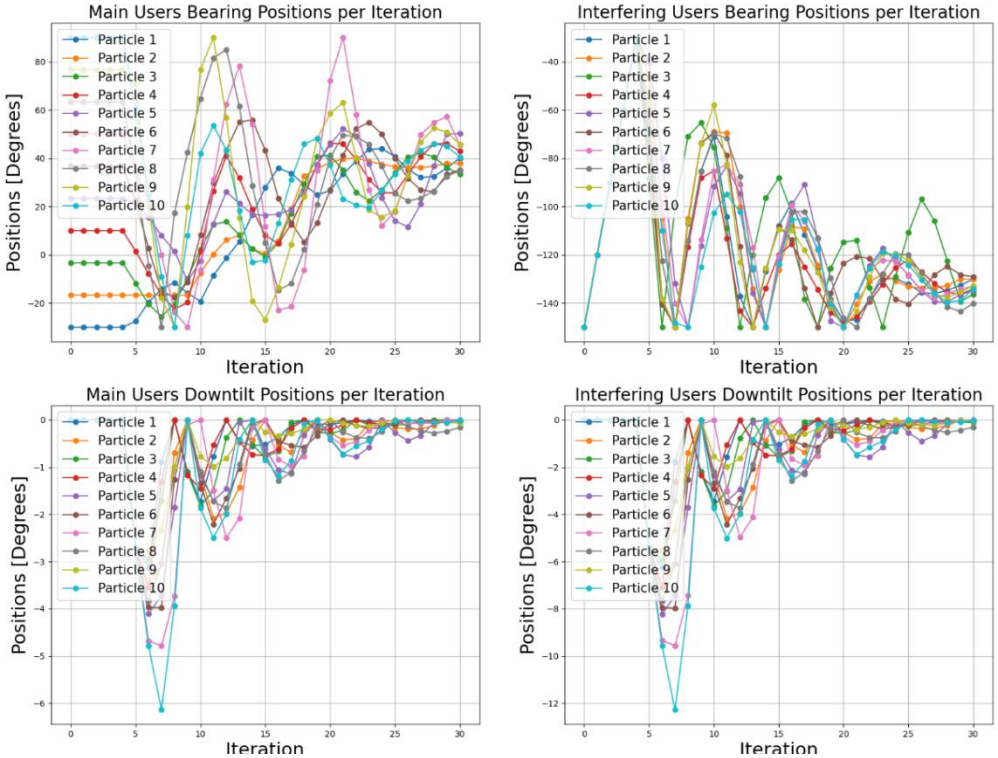

Figure D.1 - Section 4.3 users clustering interference scenario: Positions per iteration

Appendix E - Users Spreading and Clustering Scenario Results

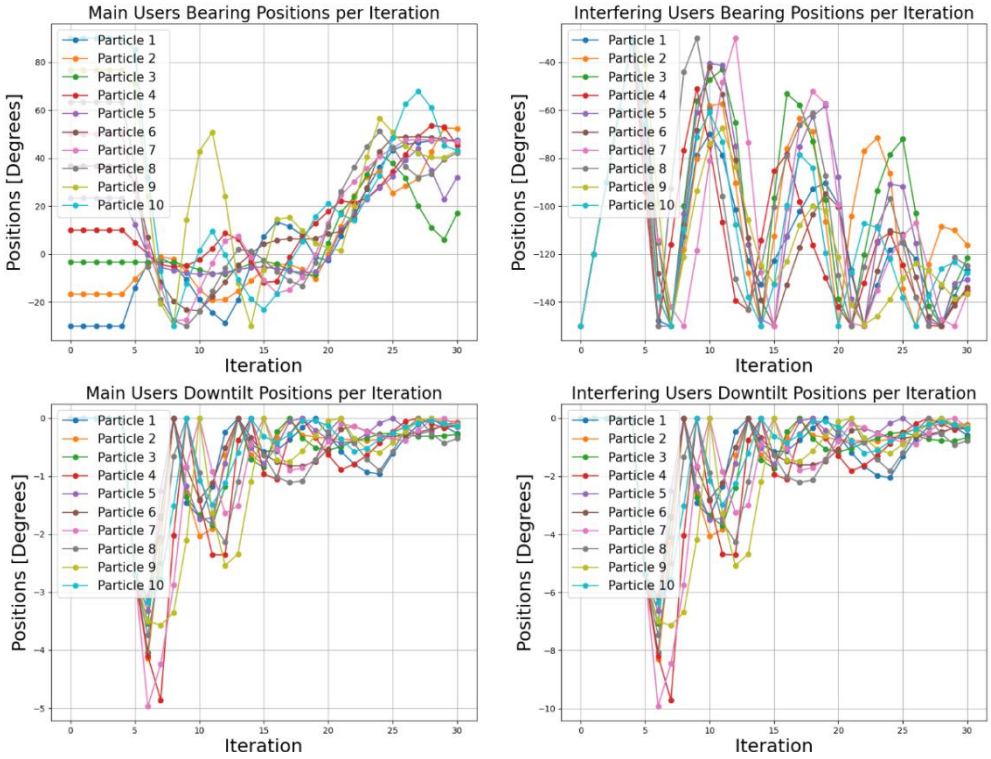

Figure E.1 - Section 4.4 users spreading and clustering scenario: Positions per iteration

Appendix F - Users Clustering and Spreading Scenario Results

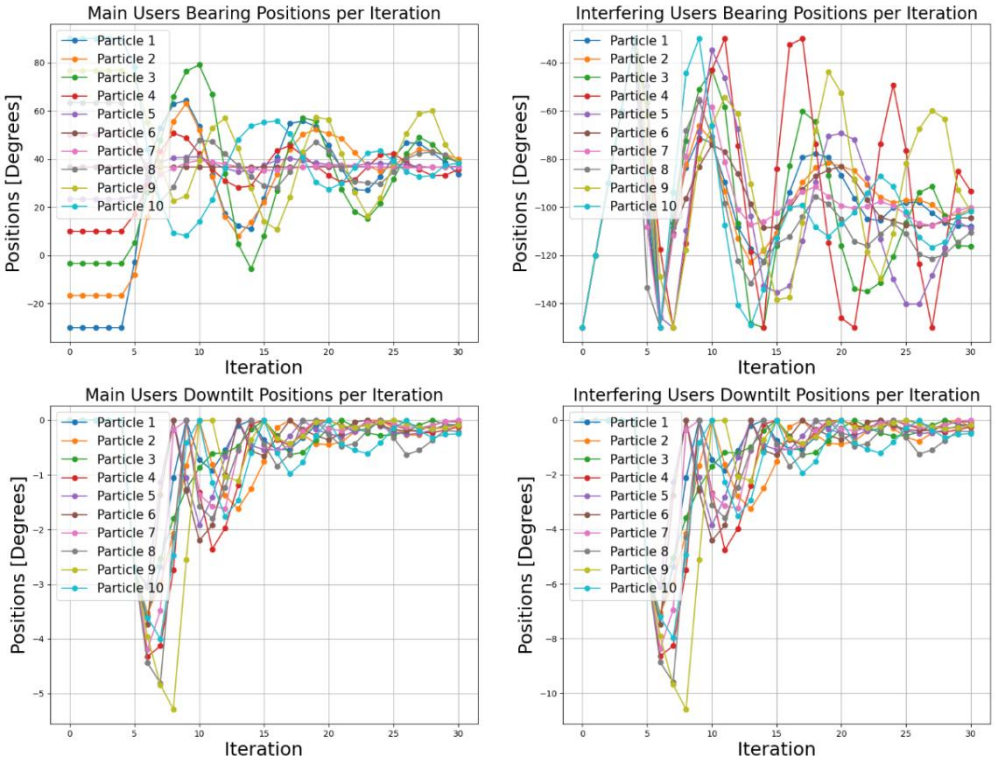

Figure F.1 - Section 4.5 users clustering and spreading scenario: Positions per iteration

Appendix G - Base PSO Results

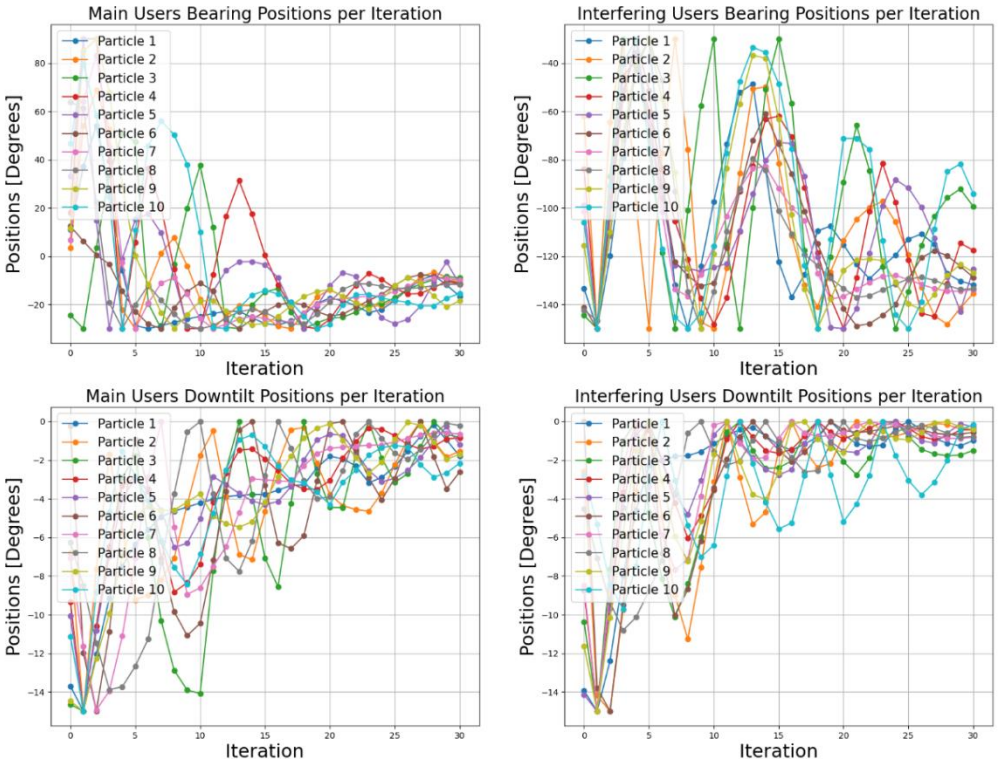

Figure G.1 - Section 4.6 base PSO scenario: Positions per iteration